Investigations of the role of the basolateral amygdala-nucleus accumbens circuit and endocannabinoid regulation of social interaction behavior in the *Shank3B*$^{-/-}$ model of autism spectrum disorder

By
Oakleigh Marie Folkes

Dissertation
Submitted to the Faculty of the
Graduate School of Vanderbilt University
in partial fulfillment of the requirements
for the degree of
DOCTOR OF PHILOSOPHY
in
Pharmacology

January 31st, 2020
Nashville, Tennessee

Approved by:
Danny G. Winder, Ph.D.
Fiona E. Harrison, Ph.D.
Jeffrey P. Conn, Ph.D.
Brad A. Grueter, Ph.D.
Sachin Patel, M.D., Ph.D.

This is dedicated to DML, for without her none of this would be possible.

ACKNOWLEDGEMENTS

I would like to first thank the funding sources that made this work possible, including the T32GM007628-38 Predoctoral Training Grant in Pharmaceutical Sciences, and Dr. Sachin Patel's RO1: 5R01MH107435-04 and his Simmons Foundation Autism Research Initiative Explorer Award.

I want to also thank my coauthors and collaborators for their time, energy, and intellectual input to help with this work. I am sincerely appreciative for all of the work and support from everyone in my lab and coauthors on my manuscript. Additionally, I want to thank my committee, Drs. Brad Grueter, Jeff Conn, Fiona Harrison, and my chair Dr. Danny Winder for being supportive, encouraging, and giving me great intellectual feedback throughout the completion of this work.

I also want to thank my mentor Sachin Patel. I am indebted to him for taking a risk on this project, and grateful for his support and mentorship. I am sincerely appreciative for his high expectations; I have achieved so much more and accomplished more than I thought possible under his guidance. Working in his lab has been a tremendous opportunity and I am thankful for all of the training and resources that were generously provided for me to complete this work.

I would also like to sincerely thank my former mentor Fiona Harrison. I am endlessly grateful for the opportunities that she provided me and for truly sparking a passion for neuroscience research. I have relied incredibly on the foundational training

and mentorship that Fiona has given me over the past 10 years, and am sincerely appreciative for all of her help and support.

In addition to my basic research, I was fortunate enough to train with the Vanderbilt program for molecular medicine (VPMM). I am grateful for the training and education provided to me by the program and the leadership of Dr. Mark de Caestecker. I am thankful for the research opportunities to shadow and learn in the laboratory of Dr. Blythe Corbett. Many of my ideas implemented in the lab were fostered from the opportunities to visit and work with patients. The time spent in the SENSE lab afforded me an outstanding education on my field of study that is invaluable. I am thankful to Dr. Corbett for opening her lab to me and for her mentorship.

Lastly want to acknowledge all of my family and friends whose support and encouragement made all of my success possible. I have the incredible fortune of having an immensely loving and wonderful family. I first want to thank my mother, who sacrifices enormously and did so to allow me the privilege to attend college and afford me the opportunity to get the training necessary to begin this work. Second I want to thank my dad and Maddy for their love and support, keeping me grounded in reality, and always reminding me first to take time for myself and to get outside. I also want to thank my sisters who always remind me of what is important in life and remind me how to stand up for myself; they are the strongest women I have ever met and truly my role models. Next, I want to thank my aunt and uncle, whose dining room table with their company is my favorite place in the world. I am grateful for their and my cousins never-ending love, encouragement, and unwavering faith in my ability to complete this dissertation. No

acknowledgement of my family would be complete without thanking my grandmother, whose love and friendship is my most prized possession; thank you for reminding me that forward is and was the only way to go, and that no matter what I faced I was tough and strong enough to overcome it.

Lastly, I want to thank my husband for his kindness, patience, and all of his editing of every single email and document I have ever sent. You have made this journey incredibly fun and exciting even when it was challenging and overwhelming. When the days are long you remind me why I love doing this work through your own enthusiasm. I am so thankful for all of your love and support and for a remarkable partner through this journey.

TABLE OF CONTENTS

Page

LIST OF FIGURES

CHAPTER 1:

CHAPTER 2:

APPENDIX:

LIST OF ABBREVIATIONS

2-AG- 2-arachidonoyl glycerol
AA- arachidonic acid
ACC- anterior cingulate cortex
ADHD- Attention Deficit Disorder
Autism Diagnostic Scale- ADI
ADOS- Autism Diagnostic Observation Schedule
AEA- anandamide
APs-action potentials
ASD- Autism Spectrum Disorder
BLA- basolateral amygdala
Ca2+- Calcium
CARS-Childhood Autism Rating Scale
CB1- cannabinoid receptor 1
CB2- cannabinoid receptor 2
CBD- cannabinodiol
CCK- cholecystokinin
ChR2- channelrhodopsin
CNO- Clozapine-N-Oxide
CNS- central nervous system
CNVs- Copy Number Variants
CPP- conditioned place preference
D1- dopamine receptor 1
D2- dopamine receptor 2
DAGL- diacylglycerol lipase
DSE- depolarization-induced suppression of excitation
DSI- depolarization-induced suppression of inhibition
DREADDs- designer receptors exclusively activated by designer drugs
DSM-V- Diagnostic and Statistical Manual of Mental Disorders V
eCB- endocannabinoid
eCB-LTD- CB1R-mediated long-term synaptic depression
EPM- elevated plus maze
EZM-elevated zero maze
FAAH- fatty acid amide hydrolyase
FF- Feed-forward
Fmr1- Fragile X Mental Retardation
FSI- fast-spiking interneurons
FXS- Fragile X Syndrome
GABA- gamma-aminobutyric acid
GIRKs- g-protein-coupled inwardly-rectifying potassium channels
GPCR- G-protein coupled receptors
LD- light-dark box
LPS- lipposacharide

LTP- Long term potentiation
MAGL- monoacylglycerol
mEPSC- mini excitatory post synaptic frequency
mGluR- metabotropic glutamate receptor
mPFC- medial prefrontal cortex
MSNs- Medium Spiny Neurons
NAc- nucleus accumbens
NAPE- N-arachidonoyl phosphatidyl ethanol
NAPE-PLC- Nape phospholipase
NpHR- *natronobacterium pharaonis, Halorhodopsin*
OA- oleamide
OEA- oleoylthanolamine
oEPSC- optically-evoked excitatory postsynaptic currents
P-MS- Phelan-McDermid Syndrome
PAMs- positive allosteric modulators
PEA- palmitoylethanolamide
PPR- paired pulse ratio
PSD- postsynaptic density proteins
RtPP- real-time place preference
SENSE- Social Emotional NeuroScience Endocrinology
sEPSC- spontaneous excitatory postsynaptic current
SHANK- Src-homology domain (*SH) and multiple ankyrin repeat domains*
SI- social interaction
sIPSC- spontaneous inhibitory post synaptic current
SNPs- single nucleotide polymorphisms
SSRI- Selective serotonin reuptake inhibitor
THC- delta-9-tetrahydrocannabinol
USVs- ultrasonic vocalizations
vHipp- Ventral Hippocampus
VPA- valproic acid
WT- wild type
YFP- yellow fluorescent protein

CHAPTER 1

INTRODUCTION

Autism Spectrum Disorders

Autism Spectrum Disorder (ASD) is a continuum of disorders comprised of impairment in social and language skills, and repetitive behaviors. Specifically, the Diagnostic and Statistical Manual of Mental Disorders V (DSM-V) defines an ASD patient as displaying symptoms of A) persistent deficits in social communication and social interaction across multiple contexts, and B) restricted, repetitive patterns of behavior, interests, or activities.[1] These symptoms are then assessed for a severity level ranging from 1-3. Patients with a severity level of 3 are marked as requiring very substantial support, display limited social interaction and social reciprocity, and have severe behavioral difficulty with flexibility and coping with change. Many of these patients are nonverbal and cannot use language to communicate. On the other hand, patients with a severity level 1 have noticeable but mild social impairments, such as difficulty initiating social interactions, some atypical responses to social interaction of others, and possible decreased motivation to engage in social interaction.[1]

Diagnosing ASD is compounded in difficulty, not only because of the wide range and presentation of symptoms, or heterogeneity, but also by the limitations of diagnostic tools. There are no biomarkers for ASD, and diagnosis is formed only by observed behavior. One such diagnostic tool is the Autism Diagnostic Observation Schedule (ADOS), an

assessment used clinically that measures naturally-occurring social communication patterns in patients with ASD. This diagnostic tool is useful for informing treatment options based on accurate measure of patients level of impairment in social communication.[2] This assessment has four modules for different developmental stages, such as children compared to adults, and for language skills ranging from nonverbal or verbally-fluent. Once the observer has chosen which module is appropriate for the participant, the assessment typically lasts 45 minutes to one hour and gives the participant a range of social cues in which the observer rates their response. These social cues may be in the form of a verbal question or in low verbal fluency modules, the observer will engage the participant in social play. For example, the observer may blow up a balloon and engage the participant to ask to continue blowing up a balloon, or the observer will attempt to engage the participant in exploring the room together.[2–4] Clinicians may also choose to use the Childhood Autism Rating Scale (CARS) or the Autism Diagnostic Interview (ADI), which are other commonly administered diagnostic tests.[5,6]

Children with ASD begin to show symptoms by 12- 18 months [7–9] however, in some cases, children may also develop typically and lose social skills between their first and second year.[10,11] Nevertheless, on average patients with ASD receive their diagnosis around 3 years old.

Although dependent on the patient and severity of diagnosis, the earliest recognized and most pronounced symptom of ASD are the social interaction and communication deficits.[12,13] These deficits lead to challenges in quality of life, such as difficulties in forming relationships and friendships, decreased participation in social interactions,

difficulty adapting in school or occupational-based social groups, and heightened stress when required to be in social situations. Moreover, patients have difficulties in regulating their own emotions and interpreting the emotions of others, emphasizing the effects poor social skills can have on quality of life of patients.

In patients diagnosed with ASD, the social deficits that can present as early as infancy include impairments in nonverbal communication such as impaired joint attention, inappropriate eye-gaze direction to caregivers, and inability to understand facial expression in caregivers.[12–15] Later in development, children with ASD are seen to have deficits in the use of symbols or finger-pointing to communicate, using inappropriate vocal-volume or tone, inappropriate non-verbal gestures, and understanding other perspectives or lack of make-believe play. Another common feature of ASD is the use of echolalia to repeat language and sound from others or television and movies rather than forming proper speech.[2]

There is no, one singular cause or neurobiological underpinning of Autism, however several twin studies indicate a strong heritability factor in developing ASD. The concordance for ASD in monozygotic twins is approximately 70-90% while dizygotic twins is 30%.[16–19] Additionally, there are high concordance rates in siblings (35%) and first-degree relatives of affected children (20%).[16,20] However, several genetic mutations that lead to ASD occur *de novo*. Because of the limited diagnostic tools and heterogeneity of the disorder, the genetic underpinnings have, until as recently as the late 1990s, been difficult to study.[21] Since the advent of new genetic tools, work in the field has culminated

in the development of several genetic underpinning and markers of ASD, such as defined mutations, genetic syndromes, and *de novo* copy number variations.

However, ASD-related genetic syndromes, defined mutations, and *de novo* copy number variations only result in about 10-20% of patients.[22] ASD syndromic disorders are well studied because of the relative ease of identification, and the ability to translate discrete genetic mutations to basic science and preclinical rodent research. Of these, the most commonly reported are Rett syndrome, which is a result of a loss-of-function of Mecp2; Angelmans syndrome, characterized by mutations of UBE3A; Fragile X syndrome (FXS), characterized by mutation in *FMR1*; Timothy syndrome, a mutation in CACNA1C a calcium channel integral to neuronal function; Cortical dysplasia-focal epilepsy syndrome a mutation in CNTNAP2; Smith-Lemli-Opitz syndrome, mutations in DHCR7 a cholesterol synthesis protein; and Phelan-McDermid Syndrome, characterized by a mutation in SHANK3 gene.

Current limitations of the treatment of ASD

Currently there are no FDA-approved pharmacological treatments for the social dysfunction and repetitive, restricted behaviors in ASD. Instead, behavior treatments are the leading intervention for the core symptoms of ASD, particularly in young children.[23,24] Unlike pharmacological treatments, behavioral therapies are tailored to fit the patient and the severity of the symptoms each patient displays. New groups and clinicians are taking novel approaches and expanding the tools used to enhance social function and decreased stress associated with entering social situations in patients with ASD. For example,

Marino F. et al has shown success in improving emotional recognition and comprehension with the use of a human-assisted social robot.[25] Additionally, groups like the Social Emotional NeuroScience Endocrinology (SENSE) lab expand upon commonly used behavioral therapy and used peer-mediation and musical theatre performance, as social competence interventions. Leading data from the SENSE lab show significant decreases in saliva cortisol levels in social situations following a regimented theatre games, rehearsal, and performance coupled with tailored peer-peer interactions.[26]

Nevertheless, one of the main limitations in treating ASD is the comorbidity of other medical conditions. For example, many patients with ASD also have gastrointestinal distress, sleep disturbances, seizures, as well as other neurological disorders like attention-deficit disorder (ADHD), and anxiety disorders.[27] In fact, it is estimated that up to 80% of patients with ASD meet the diagnostic criteria for an anxiety disorder, including obsessive-compulsive disorder, phobias, and social anxiety disorders, indicating a possible shared neurobehavioral or neural circuitry with anxiety disorders.[28–30]

Patients are often prescribed pharmacological treatments that largely treat the comorbidities in order to improve quality of life, although most have unwanted side effects, and only about 40% of patients respond to behavior and medical treatment.[31] Survey data indicates that an estimated 45% of patients take psychotropic medication, 12% antiepileptic medication and 6% vitamin supplements.[32,33] For instance, patients are prescribed typical and atypical antipsychotics as a way to decrease irritability; tricyclic antidepressants, selective serotonin reuptake inhibitors (SSRIs), and lithium to regulate

mood; a2-adrenergic agonists such as guanfacine to treat ADHD; and anti-convulsant to treat seizure disorders.

Moreover, clinical data indicates pharmacological interventions may have limited utility in treating the repetitive behaviors, such as Risperidone, an antipsychotic. However, approximately 47% of patients are nonresponsive to risperidone, and while clinicians report decreased aggression, self-injurious behaviors, hyperactivity and some repetitive behaviors, there is no effect on social behaviors and social communication.[34] Moreover, patients report sedation in half the population treated in a double blind clinical trial, as well as weight gain in 84 percent of patients. Similarly, fluvoxamine, an SSRI, also does not affect approximately 53% of patients, and does not affect social relationships. However, fluvoxamine does decrease aggression and some repetitive behaviors in patients with ASD.[32,35–37] Nevertheless, several clinical studies investigating drugs on behavioral outcomes in patients with ASD lack investigations in both adolescent and adult patients. These trials also fail to investigate sex effects of these compounds, and often are not considered in their disruptive properties to women's health. More research into novel therapeutic targets, more clinical studies on the lifespan of patients, and more inclusive studies are urgently needed.[24,32]

Although behavioral therapy is a well-researched treatment for ASD, it has limitations in accessibility, particularly to marginalized groups. Specifically, behavioral therapy requires multiple doctor visits, which are costly and time-consuming to those from low socio-economic statuses. Additionally, those who reside in rural areas are limited in the access to facilities or therapists, and service navigation induces significant sources of

stress onto the caretaker and patient. Behavioral therapies are also limited in their ability to address cultural barriers for both the patient and caretakers. For example, therapy may not address, and in some cases may induce language-barrier and race-related stress as a response to treatment. In other cases therapists fail to adapt to the cultural differences of each patient.[38]

Lower quality of life is predicted by ASD diagnosis, however characteristics that predict lower quality of life in patients include a female-identifying gender and severe symptoms, both of which are not treated by current behavioral therapy standards. First, for patients with Autism with severe language deficits or that are non-verbal, behavioral therapy options are very limited. Nevertheless, there is hope with new technology, such as use of eye gaze apparatuses, that there may be some new therapies available, however there is a large gap in resources available to these patients.

There is a similar unmet need in women with ASD. In fact, women with ASD go undiagnosed or misdiagnosed more often than male peers, which results in women missing critical windows for early life intervention.[39] When, later in life, women seek treatment and/or diagnosis to receive beneficial treatment or services, there are innumerable reports on the difficulties with professional therapists denying a diagnosis.[39] Moreover, women report that there is a lack of behavioral therapy targeted toward women, and health care professionals often dismiss the role of female identity in a patient's ASD phenotype. In particular, there is an immense, unmet need for treatment and therapy for women with ASD to include more direct teaching in self-advocacy and safety skills in order to improve quality of life.[24] This lack of behavioral therapy and intervention

puts women with ASD at risk for increased emotional, physical, and sexual abuse because of either passivity, or lack of social skills due to their ASD diagnosis.

Currently, women are at a heightened risk for depression when they conform to gender expectations.[40–42] In females with ASD there are not enough resources to intervene and assist females with ASD that have further psychiatric comorbidities, or as aforementioned specialized training to help women manage their diagnosis as it pertains to their gender and vulnerabilities. Women with ASD tend to display more internalizing disorders such as depression, anxiety, and eating disorders whereas male peers tend to display externalizing, such as hyperactivity and inattention. [24,43–45]

Given the vast limitations of behavioral therapy and unmet need of pharmacological treatment, novel therapeutic target research for the treatment of ASD is greatly needed.

Cannabinoids and endocannabinoids

One such novel target is the cannabinoid and endocannabinoid (eCB) system. Cannabis is a flowering plant that consists of both the psychoactive compound delta-9-tetrahydrocannabinol (THC) and cannabinodiol (CBD). THC has been investigated for its role in regulating mood, sensation, perception, tension, appetite and pain, and CBD for anxiolytic, antipsychotic, neuroprotective, anti-inflammatory and antiemetic properties.[46]

Cannabinoids act through two primary receptors: cannabinoid receptor 1 (CB1) and cannabinoid receptor 2 (CB2). The CB1 receptor is the most ubiquitously expressed receptor in the central nervous system (CNS) and is especially dense in expression in the

basal ganglia, hippocampus, cerebral cortex and cerebellum. The CB1 and CB2 receptors are G-protein coupled receptors (GPCRs) coupled to G_i/G_o G-proteins. Activation of these receptors inhibits adenylyl cyclase, and subtypes of voltage-dependent calcium channels while activating inward-rectifying potassium channels such as g-protein-coupled inwardly-rectifying potassium channels (GIRKS).[47]

Endocannabinoids regulate several CNS functions such as motor control, repetitive behaviors, feeding, pain perception, anxiety and stress, learning and memory, as well as social interaction behaviors. This system is comprised primarily of two key ligands 2-arachidonoyl glycerol (2-AG) and anandamide (AEA). AEA is synthesized from N-arachidonoyl phosphatidyl ethanol (NAPE), mores specifically in the CNS by NAPE-PLD and NAPE-PLC (Napephospholipase) and metabolized by fatty acid amide hydrolyase (FAAH) to ethanolamine and arachidonic acid (AA). On the other hand, 2-AG is synthesized by diacylglycerol lipase (DAGL) and metabolized by monoacylglycerol (MAGL) to glycerol and AA.[48] Additional eCB-related ligands include palmitoylethanolamide (PEA), which is evidenced to have anti-inflammatory and anti-nociceptive effects;[49] oleoylthanolamine (OEA), found to regulate food intake by reduction of ghrelin and neuropeptide [50,51] and oleamide (OA) which is involved in sleep regulation and sleep induction.[52]

In the CNS, post-synaptic 2-AG synthesis is prompted by neuronal activation on-demand. Activation of a post-synaptic neuron and subsequent calcium (Ca2+) release or Gq-GPCR activation stimulates DAGL activity and 2-AG production. 2-AG then traverses

the synapse in retrograde to bind to presynaptic CB1 receptors to suppress synaptic transmission and is degraded by presynaptic MAGL **(Figure 1.1)**.[53,54]

Activation of the CB1 receptor can lead to short and long-term plasticity. Short-term plasticity, or depolarization-induced suppression of inhibition (DSI) and depolarization-induced suppression of excitation (DSE), result from brief stimulation of the CB1R which prevents transmitter release by inhibition of Ca2+ channels or increasing K+ through GIRKs and can last for 10s of seconds. Additionally, CB1R-mediated long-term synaptic depression (eCB-LTD) is mediated by metabotropic glutamate receptor (mGluR) activation or synaptic stimulation.[53] Importantly, mGluR5, coupled to Gq/G11 G-proteins recruits phospholipase C-Beta as well as DAGL which stimulates 2-AG synthesis leading to LTD.[55]

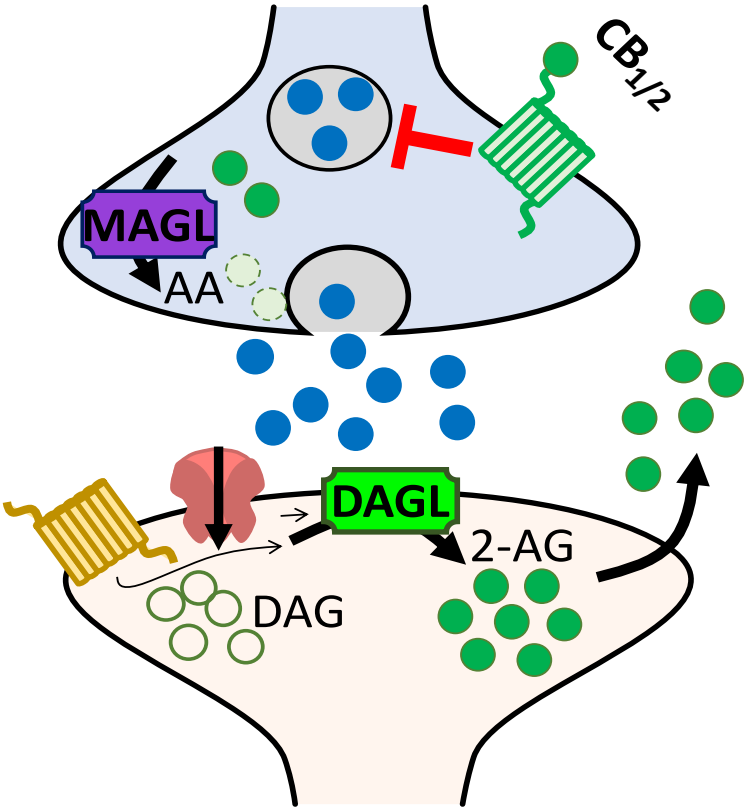

Figure 1.1: Endocannabinoid modulation of signaling transmission at a glutamatergic synapse.

Cannabinoid and endocannabinoid drugs have been in the clinic for several medical applications. CB1 and CB2 agonists such as THC, and synthetic agonist nabilone are used to treat nausea and vomiting side effects of chemotherapy and appetite stimulant

in AIDS patients. CBD, commercially available as Sativex, is prescribed for symptomatic neuropathic pain in cancer, multiple sclerosis, and seizures. Additionally, modulation of this system is being heavily investigated in preclinical studies for its role in Huntingtons disease, cocaine dependence, impulsivity, and anxiety-related disorders.[56] Specifically, our lab and others have demonstrated that pharmacological and genetic augmentation of 2-AG or AEA signaling decreases anxiety-like behavior.[57–62] These studies are paralleled by the clinical observation that agonism of the CB1 receptor by the primary psychoactive constituent in marijuana, THC, decreases anxiety in some patient populations.[63,64] Although activation of the CB1 receptor is anxiolytic, the mechanism by which eCBs regulate anxiety is not clearly determined. One possibility is that eCBs inhibit glutamate release from amygdala terminals.[65–67]

Moreover, eCBs play an important role in modulating social interaction. First, clinical studies show agonism of the CB1 and CB2 receptors through marijuana heightens social saliency, while enhancing interpersonal communication and decreasing hostility.[68] Additionally, enhancing 2-AG and AEA in the CNS increases social play and social reward in both genetic, ASD and wild-type mouse models, while decreasing 2-AG results in decreased social play.[68–76] CB1 signaling activation has also been shown to inhibit aggressive behavior through a 2-AG enhancement but not AEA enhancement in the CNS of rodent models.[77] Finally, pharmacological and genetic experiments further show that AEA mobilization, and resulting CB1 receptor activation, are both necessary and sufficient to express the rewarding properties of social interactions as assessed using a social conditioned place preference test.[68] More specifically, oxytocin, a neuropeptide crucial for

social behavior, regulates AEA release in the nucleus accumbens (NAc) which plays a key role on social behavior in a preclinical model.[68] In fact, further evidence supports both the NAc and amygdala are central regions for eCB regulation of social play in animal models.[78]

Current Understanding of Cannabinoids and Endocannabinoids in Patients with Autism

Currently, there are several anecdotal reports and newspaper headlines on the use of CBD and marijuana in ASD. However, there is very little clinical evidence reporting on the effects of cannabinoids or eCBs as a therapeutic treatment, and little is known about the safety of these drugs and compounds in ASD. Furthermore, there is little investigation on basal levels of eCBs in patients with ASD. Although several parents are self-reporting improvement, there is no FDA regulation on CBD, aside from one approved drug Epidolex, which further complicates studying the treatments parents are giving. Nevertheless, Epidolex is indicated for the treatment of pediatric seizure which is presented in over 20% of diagnosed ASD patients, and could significantly improve the quality of life of these patients.[79] More clinical research is urgently needed in the patients with ASD taking eCB or cannabinoid drugs, as the few clinical investigations report high efficacy in patients with mild side effects.

First, one recent clinical study in children 3-12 years old indicates that male and female ASD patients have significantly lower AEA in peripheral blood samples compared to typically developing subjects. However no other eCBs were measured in this study.[80] Next, patients with ASD or typically developing controls were given CBD treatment that

contained CBD and THC in a 20:1 ratio as an adjunct therapy. These subjects reported minimal side effects, such as aggregated sleep problems in 14%, restlessness in 9%, nervousness in 9%, and loss of appetite in 9% were among the highest reported. After treatment, behavioral problems were ranked as much improved or very much improved in 61% and slightly improved in an additional 10%. Interestingly, approximately 65% of patients also reported improvement in anxiety, and approximately 60% reported improvements in communication. Overall good quality of life was reported by 66.8% of parents after CBD treatment, indicating this system is a great candidate for novel therapeutic targets.[81,82] Further research is needed to find novel treatments that use this system, but minimize adverse side effects while enhancing efficacy, possibly by targeting specific brain regions of activity.

Because brain samples are difficult to obtain in patient populations, there is little evidence as to the brain regions responsible for the efficacy of CB1 agonism in ASD patients. However, a clinical study shows that single nucleotide polymorphisms (SNPs) in CNR1, the CB1 gene, are associated with activity in a striatal cluster in response to happy faces, not disgusted, suggesting that changes in CNR1 gene expression in the striatum are involved in perception and sensitivity to social reward.[83]

The Role of the Basolateral Amygdala and Nucleus Accumbens in ASD

Although the aforementioned genetic mutations resulting ASD-related syndromes are involved with various genes of various biological function, the current hypothesis is that each genetic mutation converges on common neurobiological underpinnings, or neural circuits.[84] Based on this hypothesis, there have been several studies in patients with ASD to determine what brain regions and circuits underlie the core symptoms of ASD. Because of the lack of treatments for the social interaction deficits, research in this field has been critical for developing novel therapeutic targets for treatment.

Autism is referred to as a developmental disconnection syndrome due to the gaining popularity of the connectivity theory of ASD. This theory comes from a wealth of studies from human and preclinical work indicating abnormal connectivity patterns underlie the core symptoms of ASD.[84,85] One region of particular interest is the amygdala because of its role in regulating social behavior and social perception. The amygdala is involved in regulating emotion, motivation, memories and is implicated in abnormal behaviors resulting from stress, post-traumatic stress disorder, and social behaviors. The amygdala functions to regulate eye gaze and face processing, and lesioning of the amygdala results in abnormal eye gaze when looking at human faces.[86]

In animal models, amygdala stimulation causes animals to become defensive and display fight or flight behavior while ablation of the amygdala in animals results in a gross disruption of social function, such as a loss of social communication skills, increased isolation, and abrupt changes in social hierarchy status.[87–89] As for human studies, subjects have increased amygdala activation when looking at socially salient stimuli such as gaze

or expression-recognition, whereas amygdala activation during social cue presentation is absent in patients with ASD.[90]

Furthermore, in ASD the amygdala is enlarged in patients, and inhibition of the amygdala heightens attention to social cues.[85,91,92] Lesion studies of the amygdala replicate several of the symptoms in ASD such as impairments in social judgement, and brain damage to this region often results in an acquired ASD diagnosis.[86] Additionally, there are functional connectivity abnormalities from the amygdala to several brain regions that regulate both repetitive behaviors and social function, such as the ventral striatum or NAc in patients with ASD.[85]

The NAc is another key structure in processing social reward response in patients with ASD. The NAc modulates processing of reward and pleasure, and activity in the ventral striatum is decreased in patients with ASD. The deficit in NAc activation is furthermore correlated to impairment in social reciprocity.[86] Preliminary deep brain stimulus studies have indicated that stimulation of the NAc results in substantial improvement in self-injurious repetitive behaviors and improvements in social communication behaviors in a single patient of ASD. However, more studies are needed in preclinical models to better understand how the amygdala and the NAc regulate social behaviors in ASD, and also what the role of the basolateral amygdala (BLA) to NAc circuit could play in directing social behaviors.[93]

Technological approaches and methods for studying neuronal circuitry on in vivo behavior

Given that these brain regions are critical for the core features of ASD, it is surprising that that little is known about the BLA, the NAc, or the connection between the two regions in ASD. Additionally, in wild type animals or typically developing patients, little is known about the BLA-NAc circuit in its role in ASD phenotypic behavior such as social interaction. One major barrier to understanding this circuit was the lack of technology available to study neuronal circuits in either preclinical animal models or in patients. With the recent invention of *in vivo* optogenetics we are now able to, in real time, activate or inhibit neuron terminals, or cell bodies, during *in vivo* behavior in order to understand what the effects of circuit mechanics are on real time behavior. It is now possible "to deliver causal and temporally precise gain or loss of function in one type of brain cell or in a defined projection from one brain region to another".[94]

In vivo optogenetics is a technique by which neurons are able to be activated or inhibited using light delivered via fiber optic probe to the brain region of interest. This tool is extremely powerful as it has a high speed and high accuracy, and causes less damage than electrical stimulation, or in some cases pharmacological interventions, such as muscimol delivery to kill cell populations in the brain. Using *in vivo* optogenetics, neurons fire time-locked to the delivery of light pulses to the millisecond.[94–100]

More explicitly, optogenetics relies on a combination of genetic expression of light-gated microbial opsins and light delivery to manipulate circuitry *in vivo* or *ex vivo*. Primarily, channelrhodopsin (ChR2) from *Chlamydomonas reinhardtii* is sensitive to blue

light (465nm) which triggers an opening of the ChR2 cation channel.[101–103] When cations stream into the neural cell through the membrane, neuronal firing occurs. When the light is removed, the pore returns to blocked in as little as milliseconds. In order to cause inhibition, halorhodopsin derived from halophilic bacterium *natronobacterium pharaonis* (NpHR, halorhodopsin), is delivered to brain tissue.[104] NpHR is a chloride pump sensitive to yellow/ orange light (580 nm). The chloride pump hyperpolarizes the neurons when light is delivered resulting in net inhibition of the cells.[95,97]

In addition to *in vivo* optogenetics, another tool to activate selective brain regions or circuitry in awake, behaving animals is designer receptors exclusively activated by designer drugs (DREADDs). In this approach, M3-mutant muscarinic receptors which are Gq GPCRs and M4-mutant muscarinic receptors which are and Gi GPCRs, are delivered to distinct brain regions of an animal and later selectively activated by Clozapine-N-oxide (CNO) which is delivered via IP injection.[105]

The restriction of this approach is that the activation is not real time as activation is not halted as quickly as the removal of light or initiated in the same capacity. Additionally, animals must receive an injection of CNO, which has been demonstrated to have off-target effects.[106] However, the benefit to this approach is that cables do not need to be used for light delivery, stimulation can occur over a longer time, and there is no risk of heat-induced changes in brain functioning.[107]

The role of the Basolateral Amygdala and Nucleus Accumbens in Preclinical Models

Currently, there are no studies on the role of the BLA-NAc circuit and the regulation of social behaviors in preclinical rodent models; however, the existing literature on this circuit indicates that the BLA-NAc regulates learned behavioral choice including reward seeking, risk-based decision making, fear, and depressive-like behavior; all of which may contribute to changes in social approach and social interaction behaviors.

The BLA regulates behavioral response to cues that predict aversive and rewarding events. It is hypothesized the BLA-NAc circuit underlies decision making in response to rewarding cues.[108,109] Thus far it is understood that the glutamatergic BLA input to the NAc is required concurrently with dopamine in order to promote reward seeking behavior in animals.[108] This was shown by first demonstrating that D1 (dopamine receptor 1) antagonist locally delivered to the NAc or GABA (gamma-aminobutyric acid) agonists baclofen and muscimol delivered to the BLA each reduce response to rewarding cues. Moreover, bilateral inhibition of the BLA (via GABAa/b agonism) reduces NAc firing and behavioral response to a rewarding cue, establishing a role of the circuit in cue response. This is further supported by evidence that the BLA responds to both rewarding and nonrewarding cues, while the NAc fires in response primarily to rewarding cues. As technology became more readily available and activation of the BLA-NAc could be manipulated by investigators, it was thus sought to understand the valence of the activation of the BLA-NAc circuit itself. In fact, activation of the BLA-NAc circuit reinforces behavioral responding to seek out stimulation of the BLA-NAc by nose-pokes

for self-inter-cranial stimulation.[109,110] Opposingly, inhibition of the BLA-NAc circuit may decrease reward seeking behaviors such as sucrose consumption if the BLA-NAc is inhibited during conditioning, but inhibition during reward consumption has no effect.[109,110]

The NAc regulates motivated behaviors via output from medium spiny neurons (MSNs) that express either D1 or D2 dopamine receptor (D1, D2). Stimulation of the BLA monosynaptically activates the NAc MSNs, but exposure to reward paired cues illicit activation of the BLA but not homogenous activation of the NAc MSNs. The BLA also synapses onto GABAergic fast-spiking interneurons (FSIs) within the NAc. The FSIs in the striatum are activated by excitatory input to serve as a time-contingent feedforward inhibition of circuit activation. During *in vivo* optogenetic activation, FSIs are thought to be predominantly the first cells activated, resulting in blunted MSN activation, while concurrent medial prefrontal cortex (mPFC) elicits NAc-MSN activation.[111]

It is hypothesized that while the majority of action potentials (APs) are gated by FSIs, some APs are elicited before FSI inhibition in as much as a 1ms time difference. The FSIs regulate the NAc via CB1 receptors, and act as a way to permit disinhibition of FSIs onto MSNs. CB1R is also expressed on excitatory terminals that project to the NAc, such as the BLA. In MSNs, eCBs have a higher probability of release during intensive activation, indicating a gating mechanism on these neurons. These mechanisms indicate there are many and vast regulatory mechanisms that go into regulating the excitatory drive onto NAc MSNs.[111]

Expectedly, the BLA-NAc circuit is well-evidenced in its role in motivated and reward-seeking behavior. Generally, BLA-NAc circuit has been shown to respond to reward-predictive cues, and reward conditioning enhances glutamatergic strength of the BLA-NAc circuit.[109,112,113] Exposure to cocaine and cocaine withdrawal alter excitatory synapses to both the FSIs and MSNs, indicating that this synapse can go under plasticity under specific conditions. Moreover, *in vivo* optogenetic-induced long term potentiation (LTP) at BLA-FSI NAc synapses results in faster acquisition of cocaine self-administration or enhances reward acquisition.[111]

In addition to cocaine-paired cues, activation of the BLA-NAc circuit disrupts alcohol drinking, and conditioned stimulus- cued alcohol seeking behavior.[114] Taken together, the BLA-NAc circuit is evidenced to have heavy influence on motivated behavior, and particularly reward seeking behavior. Previous studies further indicate that the BLA-has a role in assigning value to reward, and as such inactivation or lesion to either nucleus, or inhibition of the circuit using *in vivo* optogenetics, reduces the preference for a large, risky task. Instead, the inhibition of BLA-NAc shifts bias in animals to a small, certain reward as opposed to a riskier but more rewarding option.[113,115–120] More specifically, the BLA-NAc shell is hypothesized to be regulating punishment-induced inhibition of behavior, while the BLA-NAc core facilitates reward seeing behavior independent of risk, as shown in Piantadosi et al 2017, where the NAc shell or BLA is inhibited which reduces punished reward seeking, but NAc core inhibition reduces overall responding.[120,121]

Although the BLA-NAc circuit has been well-understood in terms of reward seeking behavior, little is known about the basal properties of BLA-NAc activity in social behavior and regulation of social reward, even though both regions are heavily involved in regulating social behavior. Of note, BLA-cholecystokinin (CCK) glutamatergic neurons terminating in D2-expressing NAc neurons have been shown to bidirectionally regulate social behavior after chronic social defeat stress, a preclinical model for depression.[122] Nevertheless, how BLA-NAc circuit activation regulates reward as it pertains to social reward-seeking behavior in mouse models of autism has yet to be explored.

Autism preclinical mouse models: Focus on Shankopathies and Shank deletion models

In order to study the effects of neural circuitry on ASD, preclinical studies rely heavily on genetic mouse models of the disorder. As previously mentioned, recent breakthroughs in genetic technology have led to the discovery of multiple genetic underpinnings and risk factors for ASD in patients. One such example is the *SHANK (*Src-homology domain (*SH) and multiple ankyrin repeat domains)* family of genes, located on chromosome 22q which codes for SHANK proteins.[123–129] *SHANK1*, *SHANK2*, and *SHANK3* have been identified in genetic studies and are mutated by both *de novo* and inherited mutations which result in ASD. Of these three genes, a meta-analysis in 5,657 patients with ASD and 19,163 controls, revealed copy number variants (CNV) and truncating mutations of *SHANK* genes are present in approximately 1% of patients with ASD. [124] *SHANK3* mutations are the most common, present in .69% of patients with ASD, and 2.12% of patients with intellectual disability.[124] Of note, *SHANK1* was the most rare of

SHANK mutations, present predominantly in males with ASD, and *SHANK2* the second most common but only present in 0.17% of patients with ASD.[124]

SHANK3 mutation is also commonly associated with 22q13 deletion syndrome, also known as Phelan-McDermid Syndrome (P-MS), caused by long arm of chromosome 22 deletion.[130–132] Although there are more than 90 genes that can be disrupted 22q13.3 deletion, clinical data indicates that the neurological features of P-MS are the result of haploinsufficiency of *SHANK3*, which is deleted in almost all cases of P-MS.[131,133–136] The majority of patients with P-MS are diagnosed with ASD, and it is thus that P-MS is recognized as a syndromic form of autism. Patients commonly present with developmental delay in speech, repetitive behavior, decreased pain perception, as well as distinct physical malformities.[131,137]

SHANK proteins code for postsynaptic density proteins (PSD) in excitatory, glutamatergic synapses. SHANK proteins are centrally located in the PSD and act as scaffolding which binds directly to critical neurotransmitter receptors in the synapse, actin cytoskeleton, or secondary scaffolding proteins **(Figure 1.2)**.[138,139] Of note, SHANK proteins bind directly to SAPAP and subsequently to PSD95 which interacts with NMDA receptors. PSD95, SAPAP, SHANK3, and Homer form a complex which localizes NMDAR and mGluR complexes within the PSD.[126,128,139–143] Deletion of *SHANK* genes results in changes to expression of Homer, SAPAP, NMDARs and AMPA receptors which alters molecular, morphological, and functional changes in excitatory synapse function.[143,144]

In brief, SHANK2 and SHANK3 have a prominent role in maturation of dendritic spines, where SHANK1 regulates size of spine heads. All three genes have alternate promoter sites which results in a large array of isoforms of each gene, and differential protein expression.[126]

Although investigations of *Shank1* and *Shank2* mutations are limited, *Shank1* and *Shank2* mutation preclinical mouse models have previously been behaviorally phenotyped. *Shank1* knockout (KO) animals display mild ASD phenotypes as characterized by mild anxiety-like phenotypes, impaired contextual memory, reduced pup ultrasonic vocalizations (USVs), reduced male scent marking, and increased repetitive behaviors.[145–147] Similarly, *Shank2* KO or knockdown animals display reduced social interaction behavior, reduced USVs, and increased repetitive jumping behavior.

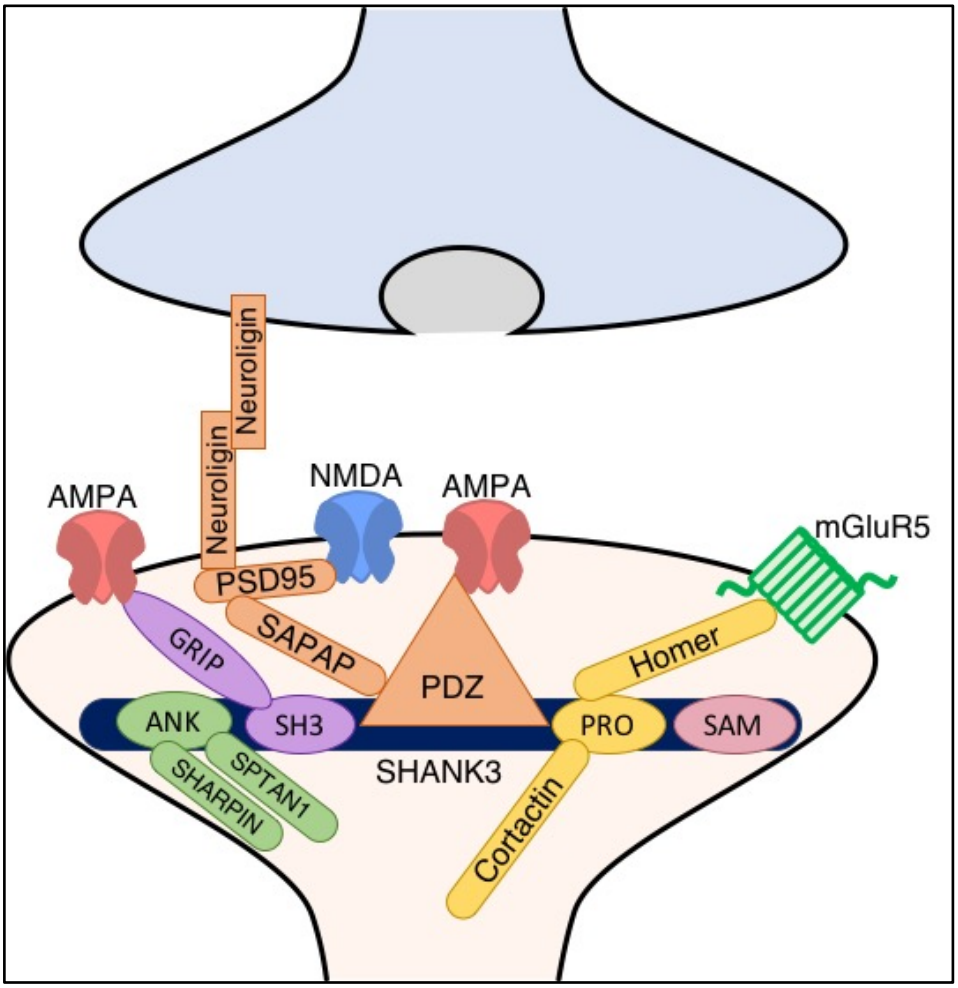

Figure 1.2: Postsynaptic density protein organization in glutamatergic synapse. Adapted from: (costales & kolevzon, 2015; monteiro & feng, 2017; sheng & kim, 2011).

On the other hand, *Shank3* mutation preclinical models and function at the protein level is the most extensively studied, primarily because of its heightened mutation levels in patients with ASD. *Shank3* has alternative splicing exons, alternative promoters, and is evidenced to be regulated by epigenetic mechanisms which leads to specific expression during development, in different cell

types, in different tissue types, and subcellular localization.[126,148–150] There are 10 transcripts produces by alternative splicing exons and 6 intragenic promoters of the *SHANK3* gene **(Figure 1.3)**. On the *SHANK3* gene there are 6 groupings of isoforms, *SHANK3A*-*SHANK3E*. SHANK3 A consists of isoforms 1-22, *SHANK3B* includes isoforms 3-20, *SHANK3*C 11-22, *SHANK3D* 13-22, *SHANK3E* 17-22, and finally *SHANK3F* 21-22. Each isoform grouping has a distinct expression pattern through the mouse brain. Notably, *Shank3A* and *Shank3E* are enriched in the striatum and present in the amygdala while others (3B-3D) have low expression in these regions.[126] Additionally, *Shank3B* isoform lacks PRO domains that bind to Homer [151,152] (and cortactin) and is involved in cytoskeletion regulation, plasticity, and synaptic transmission. The *Shank3B* isoform also lacks SAM domains which localizes SHANK to the PSD.[153] *Shank3A*, *Shank3C*, and Shank3E contain PRO and SAM regions.[154]

There are multiple mouse models of discrete *Shank3* mutations which result in different isoform expression. Of the 13 characterized models, there are 3 notable models. First, there are two Δex4-9 models which lack isoforms 1 and 2;[155–157] a *Shank3B* KO which is a Δex13-16 deletion that eliminates protein expression of the PDZ, SH3, PRO, SAM and ANK domains and lacks isoforms 1-7;[143] and a Δex4-22 deletion which disrupts all isoforms of the *Shank3* gene.[158] Behaviorally, all 3 models display abnormal, excessive repetitive

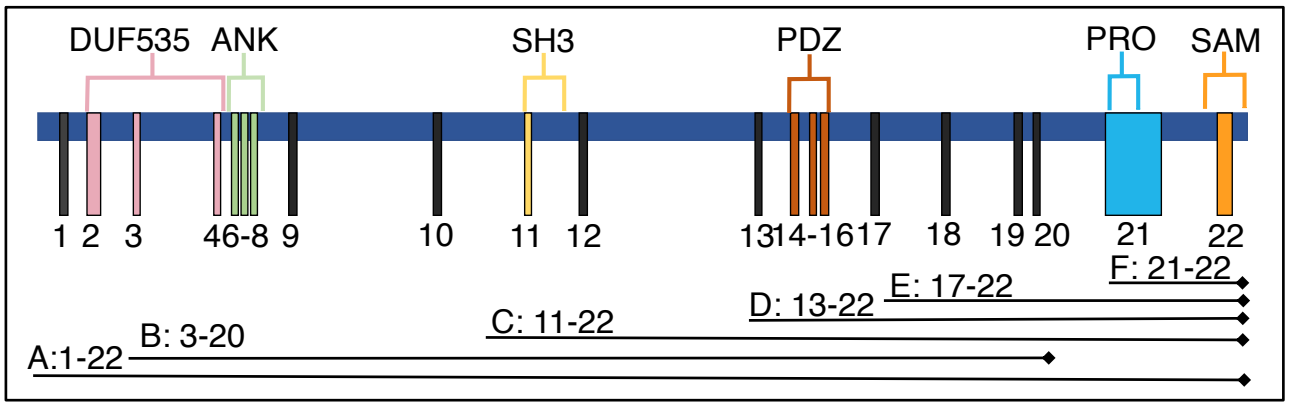

Figure 1.3: Shank3 gene including various isoforms. Note, not to scale. Formatted from (costales & kolevzon, 2015; monteiro & feng, 2017; sheng & kim, 2011).

behavior, however only the partial KO models (not including Δex4-22) show changes in social interaction behaviors.[143,156,159]

Shank3ex4-9 model

Two separate groups have reported on the Δex4-9 model, both of which found altered social behaviors in the KO animals. In Wang et al 2011, *Shank3*$^{e4-9}$ mice engage in fewer social interactions with wild type (WT) partners, and WT partners also initiate less social behavior with the *Shank3*$^{e4-9}$ animals. This group also found that ultrasonic vocalizations were disrupted in *Shank3*$^{e4-9}$ animals. Specifically, *Shank3*$^{e4-9}$ males make significantly more calls to a WT partners compared to a WT-WT pair and *Shank3*$^{e4-9}$ females made significantly less calls compared to WT-WT partner pairings. Furthermore, in *Shank3*$^{e4-9}$ males, calls were shorter in durations but had more modulation of frequencies in the calls relative to WT controls, whereas the *Shank3*$^{e4-9}$ females made one call that was absent of changes in frequency bands or any changes and complexities, which were present in WT

females.[159] Taken together these data indicate that the *Shank3*$^{e4-9}$ animals present with both abnormal social interaction behaviors as well as communication deficits.

Both groups also show the *Shank3*$^{e4-9}$ mouse self-grooms significantly more than wild type animals, and groom significantly more when in a social interaction test trial.[159]

Shank3e4-22 model

One of the groups that produced the *Shank3*$^{e4-9}$ also removed all *Shank3* isoforms using a two-step gene targeting and Cre/*lox*P strategy. Similar to the Shank3^{e4-9} model, the *Shank3*$^{e4-22}$ model expressed severe skin lesions from self-grooming, and groom significantly more compared to WT animals in a repetitive grooming assay.[158] Further testing of these mice show repetitive behavior extends beyond just grooming. In the hole board task, the *Shank3*$^{e4-22}$ model also shows increased re-investigation of the same hole in the hole board task and significantly fewer holes than WTs.

Additionally, the *Shank3*$^{e4-22}$ animals show complex changes in social behavior. In the three-chamber social interaction test the *Shank3*$^{e4-22}$ mice perform similar to their WT controls. However, in the dyadic social interaction test, *Shank3*$^{e4-22}$ mice engaged in longer and greater numbers of non-reciprocated behaviors, even though time spent socializing is the same. Finally, *Shank3*$^{e4-22}$ mice have shorter and fewer USVs as both juveniles and adults, and *Shank3*$^{e4-22}$ pups (p15) mice do not show a preference for their home nests in the nest-homing test.

One advantage of the *Shank3*$^{e4-22}$ model is that the underlying circuitry of social networks, and specific cell properties have previously been reported. In the striatum of the *Shank3*$^{e4-22}$ mice, authors report that animals have blunted striatal (NAc) long term

depression (LTD), increased neuronal excitability of NAc MSNs, but significantly diminished spontaneous postsynaptic current (sEPSC) frequency relative to control animals. Additionally, *Shank3*$^{e4\text{-}22}$ mice also have significant changes in Homer1b/c and mGluR5 proteins, decreased spine density, and attenuated PSD structures in the striatum. These data indicate that *Shank3*$^{e4\text{-}22}$ animals may have decreased number of excitatory synapses, which produces changes resulting in increased excitability of glutamatergic cells in the NAc. Striatal LTD impairment is hypothesized to be the result of impaired mGluR5-Homer1 scaffolding, which is pertinent to LTD in the striatum, and is supported by evidence that mGluR5 positive allosteric modulators (PAMs) rescue loss of LTD phenotype in *Shank3*$^{e4\text{-}22}$ animals.[158,160]

Moreover, *Shank3*$^{e4\text{-}22}$ mice display hyperactivity in the cortico-striatal-thalamic pathway, and enhanced functional connectivity between the cortex and striatum at baseline, which mimics deficiencies in patients with ASD.[161–165] Interestingly, the cortico-striatal functional connectivity is uncoupled during social interaction behavior. *Shank3*$^{e4\text{-}22}$ mice have lower NAc oscillatory power, recorded by local field potentials *in vivo*, both during and before social interaction. However activity in the NAc is higher before the introduction of a novel mouse compared to WT animals, which is perhaps the result of the aforementioned hyperactivation of NAc circuitry at baseline. The NAc is unable to dynamically change with the initiation of a social interaction as occurs in the WT controls. These data indicate that striatal circuitry may underlie the social interaction deficits and altered social approach behavior in ASD models. Because of the overwhelming similarities with ASD patients, this brain region warrants further investigation as the site of

dysregulation of social behavior, and as a potential target for treatment of social impairment.

Excitingly, this mouse model has provided significant utility in exploring novel treatments for ASD. Because the mGluR5 PAM normalized the LTD in the *Shank3*$^{e4\text{-}22}$ mice, the authors tested the ability of the compound to rescue behavioral phenotypes in the model. However, mGluR5 PAM significantly exacerbated repetitive grooming behavior in *Shank3*$^{e4\text{-}22}$, which although this may reveal mGluR5 activity as a site of aberrant repetitive behavior, this leaves the possibility of rescue within this system unknown. As previously mentioned, while mGluR5 protein levels are significantly increased the mGluR5-Homer scaffolds are decreased. Therefore, activity is anticipated to be increased in some brain regions or cell types while diminished in others. These disruptions are reminiscent of the mGluR5-Homer scaffold deficits apparent in fragile-x-syndrome, which may indicate a convergent pathophysiological mechanism of ASD. Further exploration of downstream effectors of mGluR5, such as the eCB system, may provide a novel therapeutic target for social interaction and repetitive behavior deficits in ASD.[166,167]

Shank3B$^{-/-}$ model

Finally, as stated previously *SHANK3* mutation is found in a relatively high percentage of ASD patients, these mouse models, and the *Shank3B*$^{-/-}$ in particular have remarkable translatability to patients. First, *Shank3B*$^{-/-}$ mice demonstrate increased repetitive behavior and robust, consistent, decreased social behavior, especially compared to the *Shank3*$^{e4\text{-}22}$ model. Additionally, findings in patients with *SHANK3* mutations show that the PRO,

SH3, and ANK domain mutations lead to ASD diagnosis, all of which are disrupted in the *Shank3B*$^{-/-}$ animal.[123,124,126,127,168–170]

The social interaction behavior in the *Shank3B*$^{-/-}$ mouse model differs from that of the *Shank3*$^{e4\text{-}22}$ mouse in that there is a marked deficit across several social behavior assays, whereas the *Shank3*$^{e4\text{-}22}$ mouse had mild reductions in the amount of time partner mice spent reciprocating social behavior. *Shank3B*$^{-/-}$ mice spend significantly less time in the social chamber of the three-chamber social interaction task as well as less time close to the target mouse location in this task. *Shank3B*$^{-/-}$ animals also present with a loss of reciprocal social interactions, anogenital sniffing, and nose-to-nose sniffing as assessed in a dyadic social interaction task.[143] Finally social novelty, measured in the three-chamber apparatus, is also deficient in the *Shank3B*$^{-/-}$ model.[143]

Additionally, similar to patients with ASD who present with increased anxiety, the *Shank3B*$^{-/-}$ mouse model also has elevated anxiety-like behavior. Time in the open arms is increased in the elevated zero maze (EZM) as well as increased latency to cross to light side of the light dark box in *Shank3B*$^{-/-}$ mice relative to WT controls. Also Shank3B$^{-/-}$ animals spend more time rearing in the open field task. Interestingly these behaviors are also replicated in the *Shank3*$^{e4\text{-}22}$ mice.[143,158]

Nevertheless, there are similarities between both models in striatal properties. First, the striatal volume of the *Shank3B*$^{-/-}$ mouse is significantly increased compared to WT controls. Additionally, Homer protein expression in the PSD is significantly decreased in the striatum and the PSDs are thinner, and shorter compared to WT controls. This finding is coupled to altered binding potential of mGluR5 in the striatum and amygdala in

Shank3B$^{-/-}$ animals, and decreased mGluR5 expression in the stratum and increased mGluR5 protein expression in the amygdala.[171]

Interestingly, cortico-striatal signaling is also dysfunctional in the *Shank3B*$^{-/-}$ mouse model. Cortico-stiatal pop spike amplitude is decreased in *Shank3B*$^{-/-}$, as measured by extracellular field recordings, while mini excitatory post synaptic frequency (mEPSC) and amplitude of striatal MSNs is significantly decreased in *Shank3B*$^{-/-}$ mice compared to WTs; there are additional reports of cortico-striatal circuitry having increased striatal mEPSC frequency during development (p14) of pups. Nevertheless, although there is a reduction of basal excitatory synaptic transmission in the striatum, similar to the *Shank3*$^{e4\text{-}22}$ mouse, there is increased *in vivo* activity in the striatum of the *Shank3B*$^{-/-}$ mouse model which may be the result of increased cortical activity.[172] These data collectively indicate that the *Shank3B*$^{-/-}$ mouse model presents a model for mimicking the genetic deletion found in patients with PMS and ASD, while also providing a tool to study underlying striatal circuitry and validating novel therapeutic targets that lead to prominent phenotypes in the model.

Endocannabinoid signaling in preclinical mouse models of Autism Spectrum Disorder

As previously stated, the eCB system has been shown to be a potential target for treating ASD; however little preclinical data exists validating the target in ASD mouse models. Nevertheless, there does exist some data to indicate that the eCB system could be a likely target to treat abnormalities in ASD.

Studies have been conducted in Fragile X Mental Retardation (*Fmr1*) Knock out Mice, the BTBR mouse model, prenatal valproic acid (VPA) rat models, and postnatal lipposacharide (LPS) administration rat models.

First, the Fmr1 mouse models Fragile X Syndrome (FXS), a monogenetic cause of ASD. Approximately 10-30 percent of patients with FXS are also diagnosed with ASD, and commonly present with anxiety, repetitive behaviors, intellectual disabilities, developmental abnormalizes, and physical malformations.[173,174] Similarly, the *Fmr1* mouse model is characterized by working memory deficits, hyperactivity, repetitive behaviors, anxiety-like behavior, social interaction deficits, and audiogenic seizures are increased compared to WT controls.[175]

Fmr1 KO mice have a loss of forebrain 2-AG retrograde signaling in excitatory synapses. mGluR5-dependent 2-AG release is deficient in *Fmr1* KO mice relative to WT controls, and functionally eCB-LTD in excitatory, forebrain synapses is diminished. This result arises from a lack of mGluR5-DAGLα coupling in *Fmr1* KO mice due to incorrect targeting of DAGLα to dendritic spines.[55] In conjunction, enhancement of 2-AG by acute JZL184 administration corrects the eCB-LTD, hyperlocomotion, and anxiety-like behavior in the *Fmr1* KO model.[55] Additionally, pharmacological antagonism or genetic removal of *CB1* restored cognitive deficits and decreased seizures. Pharmacological antagonism of *CB2* normalized anxiety-like behavior.[70,176] Finally, AEA enhancement via acute administration of a FAAH inhibitor improves working memory, anxiety-like behavior, and social impairment in the *Fmr1* KO mouse.[72,177]

In addition to the *Fmr1* model, eCB enhancement is shown to enhance social interaction behavior in the BTBR mouse model. The BTBR mouse is an inbred mouse strain with high face validity for idiopathic autism because there are no specific genetic causes for the phenotype in this model. This model is characterized by reduced social play and social approach behavior, increased restricted and repetitive behaviors, cognitive deficits, and heightened stress susceptibility.[174,178–180] mGluR5 antagonism of the BTBR mouse significantly decreases repetitive grooming behavior but had no effect on social behavior.[179] Nevertheless, increased levels of AEA by FAAH inhibition significantly increased social interaction behavior via a CB1-mediated mechanism.[72]

Finally, eCB alterations were found in environmental-based models of ASD, specifically the prenatal VPA exposure and LPS injection models. First, VPA is an antiepileptic drug which leads to decreased social interaction and increased repetitive behavior in offspring after injection at 12.5 day of gestation in rats. Male VPA-exposed pups treated with an acute dose of FAAH inhibitor displayed increased social behavior compared to VEH treated animals; social behavior was enhanced in the three-chamber social test, increased social play, and normalized communication deficits compared to vehicle treatment alone.[71,181,182]

Infection or influenza in mothers while pregnant heightens risk for ASD in children.[183] Modelling this, dams given LPS results in offspring that have impaired social behavior, deficits in social communication, and increased stereotyped behavior.[184,185] FAAH inhibition systemically or directly to the BLA improves social behavior in postnatal LPS injection mouse model of ASD.[186]

Although there is precedent for using each of these models, none of them have the high genetic predictability for ASD combined with high face validity like the *Shank3* models. Currently, little is known about the role of eCBs in the *Shank3B*$^{-/-}$ mouse mode, however in *Shank3B*$^{-/-}$ mice, there is defective striatal eCB-LTD in D2 MSNs which is not resultant from alterations in CB1R-mediated signaling in the SHANK3BKO, but instead from altered eCB signaling activity.[187]

Conclusions

The goal of this research is to first explore the underlying circuitry of social interaction behaviors as it pertains to ASD, and subsequently validate novel therapeutic targets within the circuit to ameliorate abnormalities in mouse models. Indeed, here myself and colleagues first validated the importance of a novel social circuit, the BLA-NAc, and its regulation of social interaction behavior in WT mice. Although the BLA and NAc brain regions are well established in their contributors to social behavior in both mouse models and humans, we here show that activation of the circuit is sufficient to disrupt social interaction behavior *in vivo* in a mouse model.

Second, we show that the BLA-NAc circuit is also involved in the disruption of social behavior in the SHANK3BKO mouse model of ASD, as inhibition of the circuit restores social interaction behavior *in vivo* during social tasks. Finally, we show that the BLA-NAc circuit is regulated by eCBs, specifically 2-AG, and that acute, systemic administration of JZL184, a MAGL inhibitor, significantly increases social interaction behavior, and significantly reduces grooming behavior in the SHANK3BKO mouse. This data demonstrates that regulation of the eCB system

is able to treat both of the core features of ASD and has the potential to also manipulate several of the ASD comorbidities. Further exploration of the BLA-NAc circuit and the eCB system in ASD is necessary to fully understand the role of these components in maladaptive social behavior, and the potential of the eCB system to treat these behaviors.

CHAPTER 2

An Endocannabinoid-Regulated Basolateral Amygdala-Nucleus Accumbens Circuit Modulates Sociability

Oakleigh M. Folkes[1,2], Rita Báldi[1], Veronika Kondev[1,3], David J. Marcus[1,3], Nolan D. Hartley[1,3], Brandon D. Turner[3,4], Jade K. Ayers[1], Jordan J. Baechle[1], Maya P. Misra[1], Megan Altemus[1], Carrie A. Grueter[4], Brad A. Grueter[3,4], Sachin Patel[1,2,3,5*]

Department of [1]Psychiatry and Behavioral Sciences, Vanderbilt University Medical Center, Nashville, TN USA 37232
Departments of [2]Pharmacology and [3]The Vanderbilt Brain Institute, Vanderbilt University School of Medicine, Nashville, TN USA 37232
Department of [4] Anesthesiology, Vanderbilt University Medical Center, Nashville, TN USA 37232
Departments of [5] Molecular Physiology & Biophysics, Vanderbilt University School of Medicine, Nashville, TN USA 37232

ABSTRACT

Deficits in social interaction (SI) are a core symptom of Autism Spectrum Disorders (ASD), however treatments for social deficits are notably lacking. Elucidating brain circuits and neuromodulatory signaling systems that regulate sociability could facilitate a deeper understanding of ASD pathophysiology and reveal novel treatments for ASD. Here we found that in vivo optogenetic activation of the basolateral amygdala-nucleus accumbens (BLA-NAc) glutamatergic circuit reduced SI and increased social avoidance in mice. Furthermore, we found that 2-arachidonoylglycerol (2-AG) endocannabinoid (eCB) signaling reduced BLA-NAc glutamatergic activity, and that pharmacological 2-AG

augmentation via administration of JZL184 blocked SI deficits associated with in vivo BLA-NAc stimulation. Additionally, optogenetic inhibition of the BLA-NAc circuit significantly increased SI in the *Shank3B*$^{-/-}$, an ASD model with substantial SI impairment, without affecting SI in wild-type mice. Finally, we demonstrated that JZL184 delivered systemically or directly to the NAc also normalized SI deficits in *Shank3B*$^{-/-}$ mice, while ex vivo JZL184 application corrected aberrant excitatory and inhibitory neurotransmission and reduced BLA-NAc-elicited feedforward inhibition of NAc neurons in *Shank3B*$^{-/-}$ mice. These data reveal circuit-level and neuromodulatory mechanisms regulating social function relevant to ASD and suggest 2-AG augmentation could reduce social deficits via modulation of excitatory and inhibitory neurotransmission in the NAc.

INTRODUCTION

Autism Spectrum Disorders (ASD) are neurodevelopmental disorders characterized by two core symptom domains, repetitive behaviors and abnormal social communication and social behaviors.[1] Currently, there are no FDA-approved pharmacological treatments for the core symptoms of ASD. Therefore, elucidation of new therapeutic approaches is urgently needed. In particular, there is an unmet need for pharmacological treatment of social interaction and social communication deficits in ASD.[32,34–37]

One such novel target could be the endocannabinoid (eCB) system. eCBs regulate several central nervous system (CNS) functions including motor control, repetitive behaviors, pain perception, anxiety, stress, learning and memory, and social behaviors[46,188] all of which are implicated in ASD.[1] Regarding social behaviors, the eCB 2-

arachidonoylglycerol (2-AG) has a demonstrably significant role in regulating social behavior, as increasing levels of 2-AG increases social play in juvenile rats, while decreasing 2-AG results in decreased acquisition of social conditioned place preference (CPP)[68,182] in mice. Despite these data, the neural circuit and synaptic mechanisms by which eCB signaling affect social function are not well understood.

In animal models, the nucleus accumbens (NAc) and amygdala are two central regions for eCB regulation of sociability.[68,76,78] Canonically, the NAc enhances motivated behavior and social function via a dopamine-dependent mechanism.[78,189–192] Although disruptions in amygdala and NAc function have been demonstrated in ASD,[193–195] how amygdala-NAc circuit activity relates to sociability deficits in ASD is not well understood. Existing literature on the amygdala, specifically the basolateral amygdala (BLA), indicates that the BLA-NAc circuit regulates learned behavioral choice including reward seeking, risk-based decision making, fear, and depressive-like behavior, all of which may contribute to changes in social approach and social behaviors.[108,109,111,113–115,122,196] Because the BLA-NAc circuit underlies decision making in response to rewarding cues and subsequent behavioral responses,[108,109] we hypothesize that activity in the BLA-NAc circuit may regulate multiple aspects of sociability under physiological conditions, and perhaps under conditions of impaired social function.

ASD is a highly heritable neuropsychiatric disorder, as evidenced by twin and familial studies, and one of the most common genetic findings in ASD patients are mutations in Src-homology domain 3 (SH3) and multiple ankyrin repeat domains 3 (SHANK3) encoding genes.[130,132,197,198] SHANK3 is a postsynaptic density protein expressed in

glutamatergic neurons that serves as a scaffold for key glutamatergic receptors.[126,199] The *Shank3B*$^{-/-}$ mouse model is characterized by an excision of exons 13-16 that causes removal of two major *Shank3* isoforms, and replicates the genetic findings commonly presented in patients.[123,124,126,127,170] This excision results in a loss-of-function of the SHANK3 protein. *Shank3B*$^{-/-}$ mice demonstrate excessive, repetitive grooming and deficits in social behavior, making the model a good candidate for exploring novel ASD therapeutic targets and circuit dysfunction.[143,200] Previous studies suggest that the significant changes in social behavior in the *Shank3* loss-of-function models may be mediated by signaling changes in the NAc,[158] warranting further investigation of the NAc and NAc-associated circuitry, in the regulation of social function and pathophysiology of ASD.

Here we utilized optogenetic circuit mapping to demonstrate that activation of the BLA-NAc circuit disrupted physiological social function and that inhibition of this circuit reversed social deficits in *Shank3B*$^{-/-}$ mice. We further demonstrated that 2-AG signaling is a negative regulator of BLA-NAc glutamatergic transmission and that pharmacological augmentation of 2-AG levels mitigated social avoidance induced by BLA-NAc circuit activation and those observed in *Shank3B*$^{-/-}$ mice, possibly via decreasing BLA-NAc-elicited feed-forward inhibition.

RESULTS

Optogenetic activation of the BLA-NAc circuit disrupts social behavior

To examine the role of the BLA-NAc circuit in social function, we utilized an in vivo optogenetic approach in which we injected a ChR2 (AAV5-CaMKIIa-hChR2(H134)-EYFP) viral vector into the BLA and delivered blue-light stimulation into the NAc via fiber optic cannulas. First, we tested the effects of 20Hz blue light stimulation (5ms light pulses, 10-13mW, 5s on 5s off) on social function using the 3-chamber social interaction (SI) task in male and female C57BL/6J mice. We found that blue light delivery into the NAc impaired sociability in ChR2-expressing compared to YFP-expressing (AAV5-CaMKIIa-EYFP) control animals **(Figure 2.1, see Figure 2.16 for placement)**. This light stimulation pattern did affect distance traveled in this apparatus **(Figure 2.1 C)**, but significantly decreased time ChR2-expressing mice spent in the social chamber relative to YFP-expressing mice **(Figure 2.1 D)**. We also found that ChR2-expressing mice, relative to YFP controls, spent significantly less time in close proximity (5cm) to the target animals **(Figure 2.1 E)** and spent less time sniffing or investigating the cup in which the target mouse was contained **(Figure 2.1 F)**. Importantly, BLA-NAc stimulation for 5 minutes prior to the 3-chamber SI task did not alter sociability **(Figure 2.2 A-B)**, suggesting that the sociability-impairing effects of BLA-NAc activation required ongoing circuit stimulation. We next validated our optogenetic stimulation protocol using ex vivo whole-cell electrophysiological recordings.

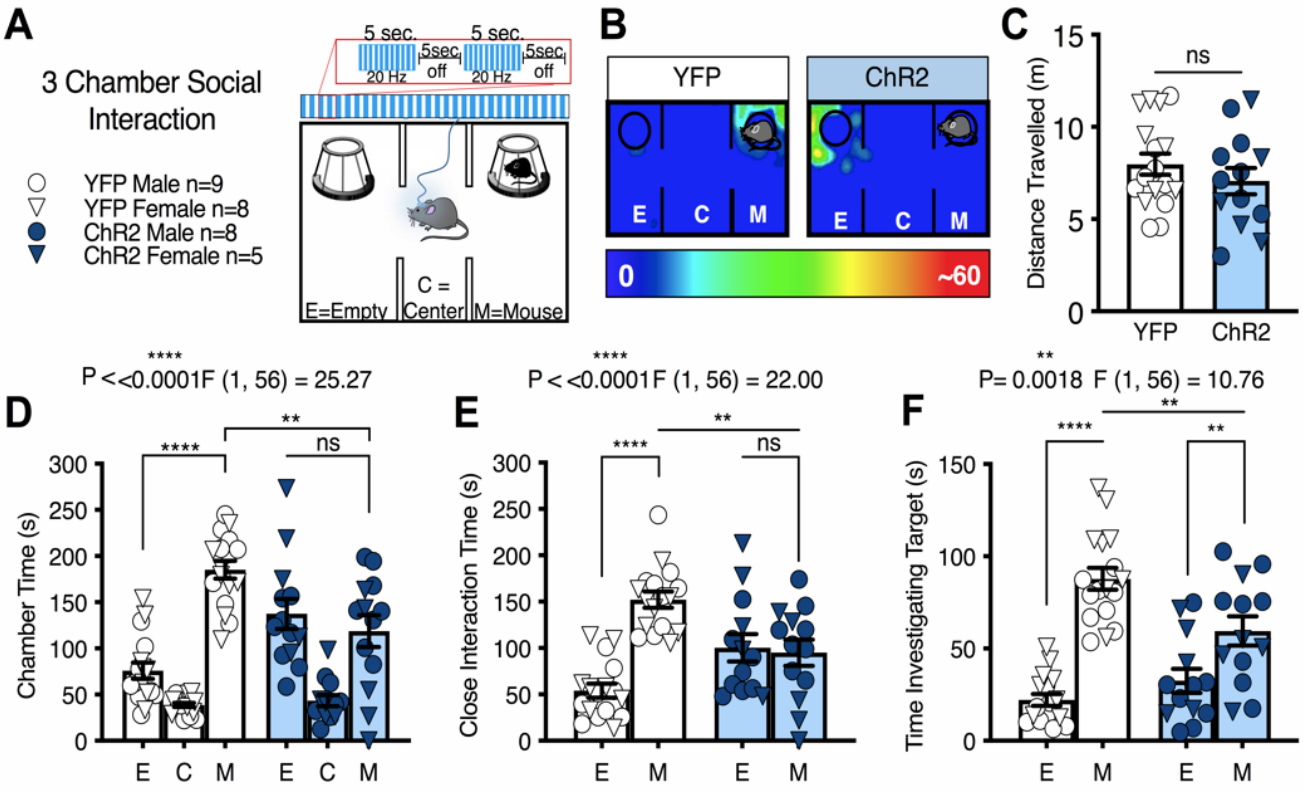

Figure 2.1: Activation of BLA terminals in the NAc decreases sociability A) 3-chamber SI task and optogenetic stimulation protocol. Animals were continuously stimulated during the 5-minute test using a 20Hz pattern (10mW, 5s on 5s off). **B)** Representative heat maps of chamber time in a ChR2 and YFP control mouse. **C)** Optogenetic stimulation of the BLA-NAc circuit did not affect distance traveled (ns p = 0.3224). **D)** Animals that express ChR2 showed reduced social preference (**p = 0.0010, ****p < 0.0001, ns p = 0.5565), **E)** decreased close interaction time (**p = 0.0011, ****p < 0.0001, ns p = 0.9353) and **F)** reduced time investigating, or sniffing, the target mouse compared to animals that express YFP (M-M **p = 0.0026, E-M **** p < 0.001, **p = 0.0071). YFP n= 17, ChR2 n=13 (C-F). Data analyzed via Two-Way Mixed-Effects ANOVA followed by Sidak's multiple comparisons test (D-F) and unpaired two-tailed t-test (C). P and F values for Chamber x Virus interaction shown in D-F.

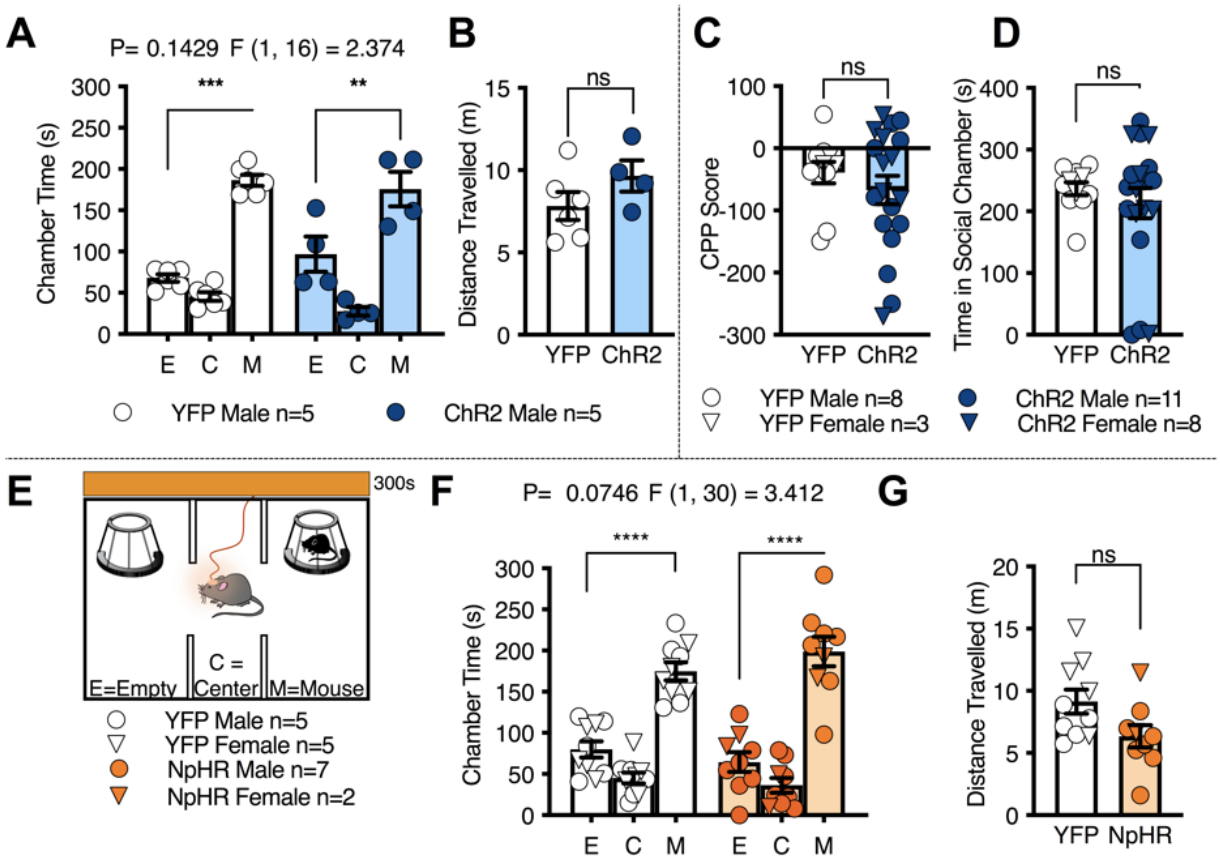

Figure 2.2 Prestimulation and inhibition of the BLA-NAc circuit do not alter Social Behavior. A-B) Pre-stimulation of blue light does not disrupt social interaction behavior in the three-chamber social interaction task. A) After 5-minute blue light pre-stimulation, mice expressing YFP and ChR2 both display significant preference for mouse-containing chamber (***p = 0.0002, **p = 0.0086). **B)** There was no effect of pre-stimulation on distance travelled (ns p = 0.1983); YFP n=5, ChR2 n=5 (A, B). **C-D) Unilateral stimulation during the Social CPP testing**. **C)** Unilateral blue light stimulation in the NAc does not cause any changes in CPP score (ns p = 0.3974) or **(D)** time in social-paired side (ns p = 0.4872) in the CPP task in ChR2-expressing animals compared to YFP-expressing animals; YFP n=11, ChR2 n=19 (C, D). **E-G) Inhibition of BLA-NAc circuit does not affect social preference. E)** Animals received constant orange light stimulation (10-13mW) for the duration of the 3-chamber social interaction task. **F)** Mice expressing YFP and NpHR both have a preference for the social chamber (YFP: ***p = 0.0002, NpHR: ***p < 0.0001) **G)** while distance travelled is not changed by NpHR or YFP expression (ns p = 0.0500); YFP n=10, NpHR n=9 (F, G). Data analyzed via Two-Way Mixed-Effects ANOVA with Sidak's multiple comparisons test (A, F) or unpaired two-tailed t-test (B-D, G). P and F values for Chamber x Virus Interaction shown in (A, F).

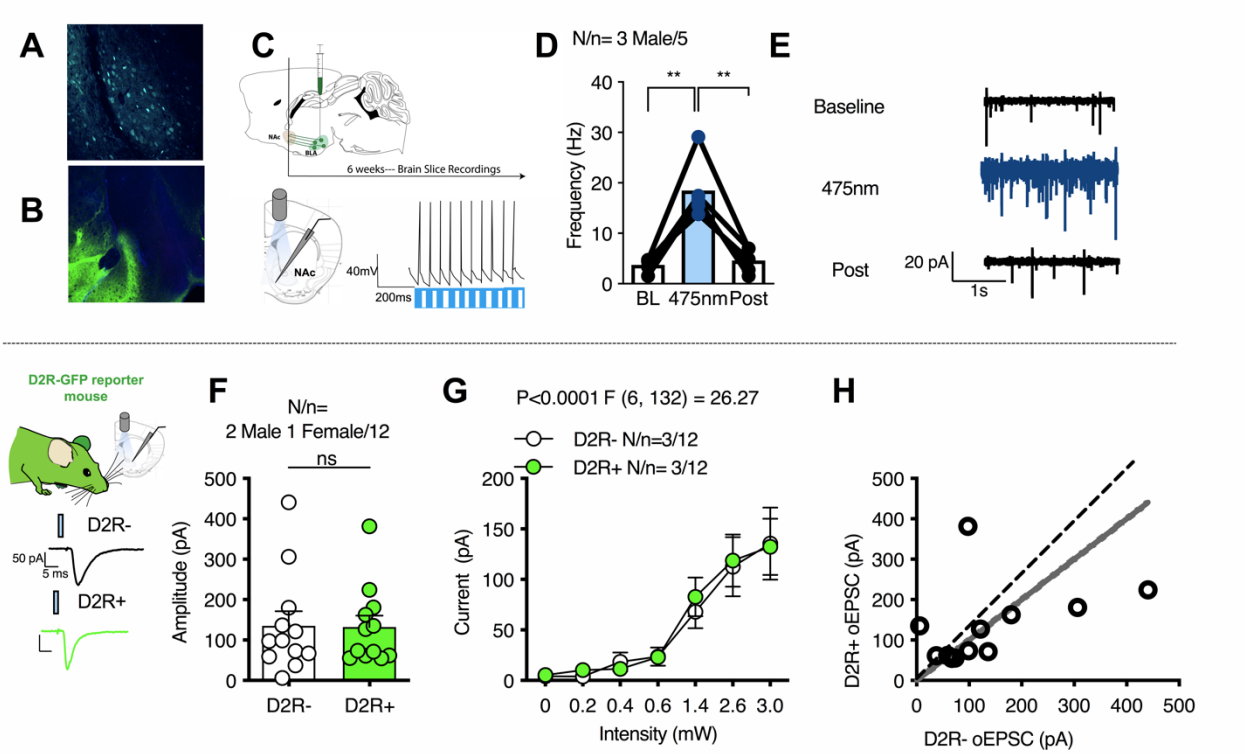

Figure 2.3: Blue light reliably stimulates BLA-NAc terminals projecting to dopamine D2 receptor positive (D2R+) and D2R negative (-) cell populations A) ChR2 (green) was delivered to BLA. **B)** Viral expression of the BLA terminals in the NAc. **C)** Schematic of whole-cell recording approach in the NAc while blue light (475nm) was delivered to stimulate BLA terminals. Blue light stimulation causes action potential firing in NAc neurons. **D**) Optogenetic stimulation of BLA terminals increases frequency of sEPSCs recorded from NAc neurons. (Baseline (BL)-475nm: ** p = 0.0051, 475nm-post-stimulation (Post): ** p = 0.0038); N=3. **E)** Sample current traces before, during, and after blue-light stimulation. **F-H**) D2R-GFP reporter mice were injected with ChR2 in the BLA, and whole-cell recordings were performed in the NAc in GFP+ (D2R+) or GFP- (D2R-) cells. There is no difference in **(F)** amplitude (ns p = 0.9492, N=3) or **(G)** optical EPSC input-output curves between BLA projections onto D2R- and D2R+ cells in the NAc. **H**) There was no bias of BLA inputs to D2+ or D2- neurons; D2+ N=3, D2- N=3 (G, H). Data analyzed data analyzed via unpaired, two-tailed t-test.

These studies revealed 20Hz blue light stimulation within the NAc triggered high-fidelity neuronal firing, confirming that this frequency of stimulation increased NAc neuronal activity and increased spontaneous glutamate release onto NAc medium spiny neurons (MSNs) (**Figure 2.3 A-E**). Optogenetic stimulation of BLA afferents to the NAc also resulted in optically-evoked excitatory postsynaptic currents (oEPSCs) onto D2 dopamine receptor

expressing MSNs (D2+ MSNs), and D2-(presumptive D1) MSNs, indicating BLA glutamatergic afferents to the NAc target both subtypes equally **(Figure 2.3 F-H)**.

Lastly, we sought to determine whether BLA-NAc activity could bi-directionally modulate sociability. Thus, we repeated the 3-chamber SI task in animals that bilaterally expressed either NpHR (AAV5-CaMKIIa-eNpHR3.0-EYFP) or YFP in order to inhibit BLA-NAc activity in vivo **(Figure 2.2 E)**. However, we found no effects of constant orange-light (620 nm, 10-13mW) inhibition of the BLA-NAc circuit on sociability in the 3-chamber SI test **(Figure 2.2 F-G)**, suggesting BLA-NAc activity is not necessary for physiological expression of SI.

To extend upon the observation that BLA-NAc activation disrupts sociability, we next analyzed the effects of BLA-NAc activation in a juvenile reciprocal SI test using a wireless in vivo optogenetic system **(Figure 2.4)**. In this task, we found that unilateral 20 Hz blue light stimulation significantly increased time fleeing or withdrawing from the social target **(Figure 2.4 A)** and decreased time spent social sniffing **(Figure 2.4 B)** in mice that expressed ChR2 relative to YFP controls. In contrast, we found no effects of blue light stimulation in ChR2-expressing compared to YFP-expressing controls on the time the test animals spent following the social target **(Figure 2.4 C)** or engaged in passive social behavior **(Figure 2.4 D)**. Lastly, immobility time was increased **(Figure 2.4 E)** while exploration time **(Figure 2.4 F)** and self-grooming **(Figure 2.4 G)** were decreased in ChR2 animals compared to YFP-expressing controls. These data are consistent with our 3-chamber SI data and indicate that BLA-NAc pathway activation reduces social behavior and induces social avoidance in a more naturalistic setting.

We next tested the effects of BLA-NAc activation on motivational aspects of SI seeking using a social CPP task **(Figure 2.4 H)**. After conditioning, we found that bilateral (but not unilateral, **Figure 2.2 C-D**) blue light delivery during social CPP testing resulted in decreased time spent in the social-paired chamber and lower CPP scores (post-test chamber time minus pre-test chamber time) **(Figure 2.4 I-K)**, in ChR2-expressing animals compared to YFP controls. Of note, virus expression did not alter pre-test chamber preference **(Figure 2.4 L)**. Taken together, data from these three assays indicate BLA-NAc activation impairs motivational aspects of SI seeking, reduces social preference, and induces social avoidance, in male and female mice.

Optogenetic activation of the BLA-NAc circuit is rewarding but not anxiogenic

The NAc is well-known to regulate reward-related processes[196,201] suggesting BLA-NAc stimulation could reduce sociability via an occlusion of the rewarding aspects of SI. To examine this possibility, we first tested the reinforcing effects of BLA-NAc stimulation using a real-time place preference (RtPP) assay. Consistent with previous studies,[122] we found animals expressing ChR2 spend more time in the ON chamber, in which blue light stimulation was delivered, versus the OFF, chamber in the RtPP task **(Figure 2.5 A-B)**, without significantly affecting locomotor activity **(Figure 2.5 C)**. Taken together with our previous data above, these results indicated BLA-NAc glutamatergic circuits can support RtPP and social avoidance in parallel. These data also suggest BLA-NAc stimulation could indeed impair social function via occlusion of the rewarding aspects of social behavior. If this were the case, one would also predict occlusion of natural reward seeking, such as

food seeking, behavior by BLA-NAc stimulation. To test this hypothesis more explicitly, we measured time in a chamber containing a highly palatable food (vanilla Ensure) in lieu of a social target in a modified 3-chamber task design **(Figure 2.5 D)**. In this task we observed BLA-NAc stimulation did not disrupt chamber preference **(Figure 2.5 E)**, alter time spent in close proximity to the Ensure-containing cup **(Figure 2.5 F)**, or affect time spent drinking Ensure **(Figure 2.5 G)**. Overall these data suggest BLA-NAc activation does not reduce sociability via occlusion of the rewarding aspects of SI. Additionally, because changes in anxiety and anxiety-like behavior can affect social behavior,[1,202,203] we next tested the effects of BLA-NAc stimulation on anxiety-like behavior and found activation did not alter behavior in the light-dark box (**Figure 2.6 A-D)** and neither activation nor inhibition affected anxiety-like behavior in the elevated-plus maze **(Figure 2.6 E-L)**. Taken together that these data indicate social avoidance observed during BLA-NAc stimulation was not secondary to increased anxiety-like behavior.

eCB signaling broadly regulates BLA-NAc glutamatergic transmission

Given the prominent role of eCB signaling in the regulation of central glutamatergic transmission,[204] and the role of eCB signaling in social function,[72,76,78] we next examined the possibility that eCB signaling regulates BLA-NAc glutamatergic activity. Indeed, the cannabinoid receptor agonist CP55940 significantly decreased oEPSC amplitude at BLA-

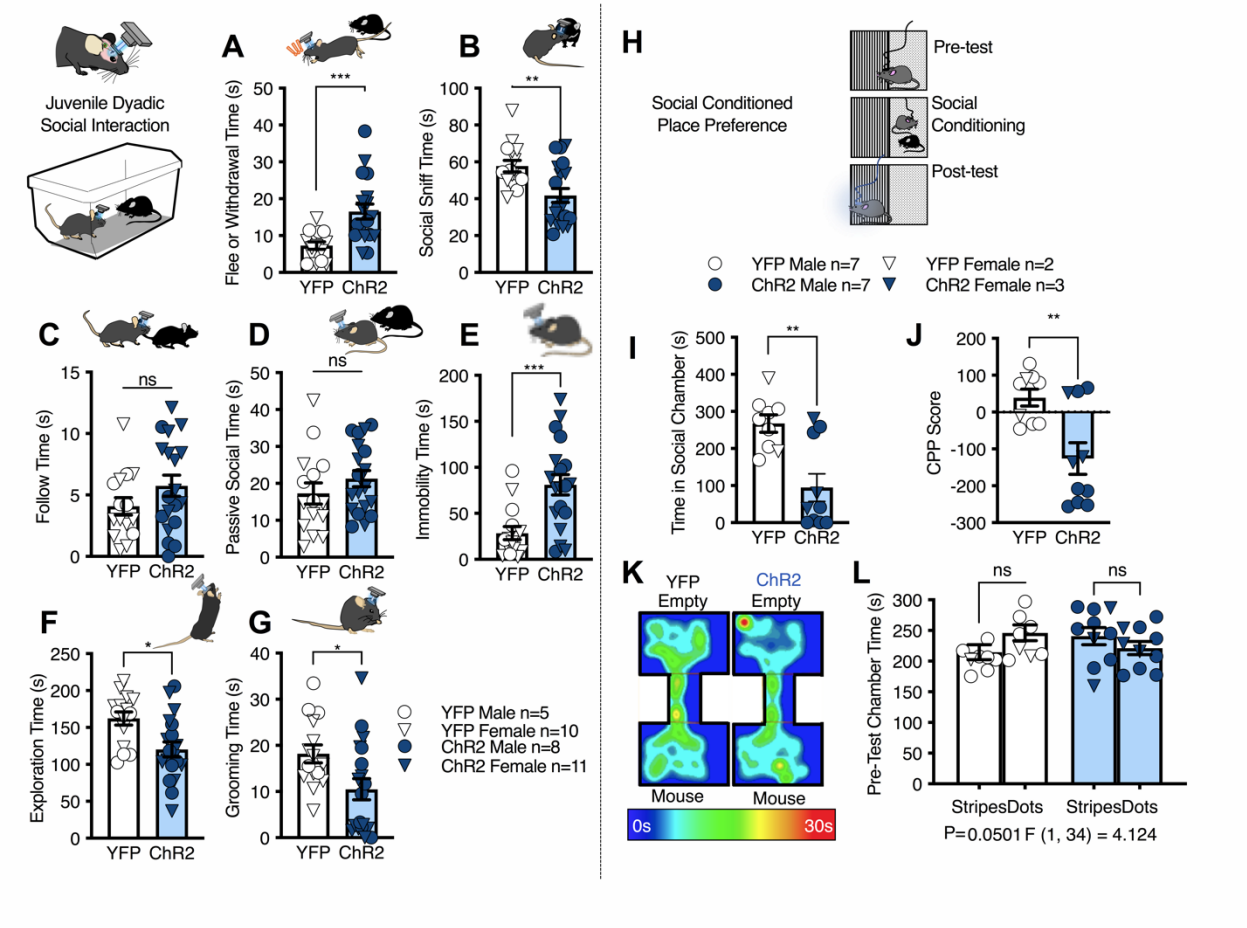

Figure 2.4 Activation of BLA terminals in the NAc increases social avoidance and reduces social interaction seeking A) Optogenetic stimulation of the BLA-NAc circuit increased fleeing and withdrawal behaviors (***p = 0.0007) and **(B)** decreased social sniffing behaviors (**p = 0.0041) compared to YFP expressing controls. There was no effect of BLA-NAc activation on **C)** following (p = 0.1573) or **D)** passive social behavior (p = 0.2604). Animals expressing ChR2 were significantly more **E)** immobile (***p = 0.0007) and **F)** explored less (*p = 0.0049) than YFP controls. **G)** Animals that expressed ChR2 self-groomed significantly less than YFP-expressing controls (*p = 0.0184) YFP n=15, ChR2 n=19 (A-G). **H)** Social CPP paradigm. **I)** Bilateral activation of BLA-NAc circuit significantly decreased time in social-paired chamber during the post-test (**p = 0.0013) **J)** and reduced CPP score relative to YFP controls (**p = 0.0041). **K)** Representative heat maps for social CPP experiment. **L)** No pre-test preference to either chamber was detected (YFP dots vs stripes, p = 0.1777, ChR2 dots vs stripes, p = 0.4619. YFP n=9, ChR2 n=10 (I, J, L). Data analyzed via unpaired, two-tailed t-test (A-G and I-J) and Two-Way Mixed Effects ANOVA with Sidak's multiple comparisons post-hoc test (L), with P and F values for Chamber x Virus interaction shown in L.

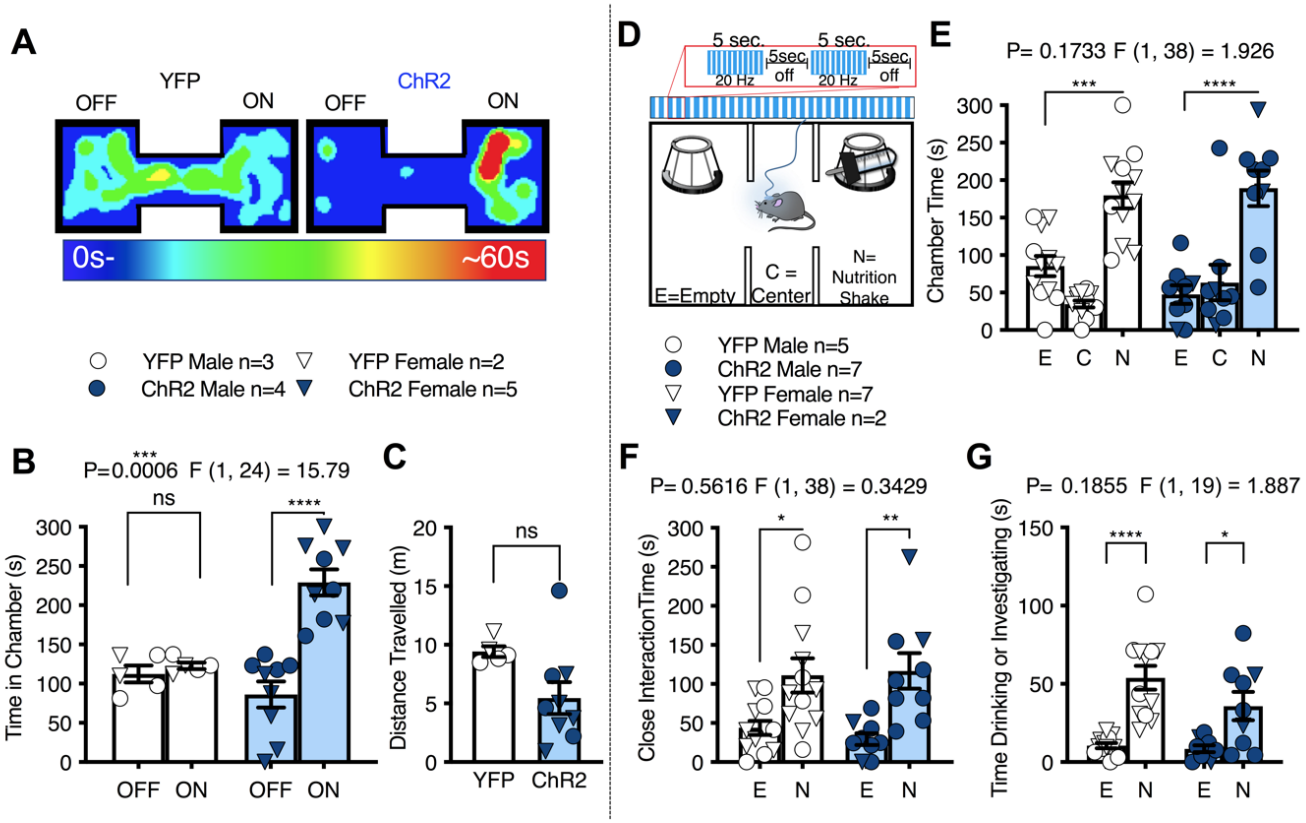

Figure 2.5 Activation of BLA terminals in the NAc is rewarding but does not reduce palatable food-seeking. A-C) Effects of BLA-NAc stimulation in the RtPP assay **A)** Representative heat maps of RtPP results. **B-C)** Animals expressing ChR2 spent significantly more time in the stimulation-paired (ON) compared to non-paired (OFF) side in RtPP assay (ns $p = 0.9083$, ****$p < 0.0001$) without any effect on total distance travelled (unpaired t-test, $p = 0.0568$). YFP n=5, ChR2 n=9 (B, C). **D-G)** Effects of BLA-NAc stimulation on Ensure seeking behavior. **D)** In a modified 3-chamber task a sipper bottle of Ensure was added to one chamber while stimulation was delivered to animals. **E)** Activation of the BLA-NAc circuit did not alter time spent in in the chamber with (***$p = 0.0003$, ****$p < 0.0001$) **(F)** close to (*$p = 0.0102$, **$p = 0.0037$), or **G)** time spent drinking (****$p < 0.0001$, *$p = 0.0128$) the nutrition shake in ChR2-expressing animals compared to YFP-expressing animals. YFP n=12, ChR2 n=9 (E-G). Data analyzed via unpaired, two-tailed t-test (C), and Two-Way Mixed-Effects ANOVA with Sidak's multiple comparison post-hoc tests (B, E-G), with P and F values for Chamber x Virus interaction shown in (B, E-G).

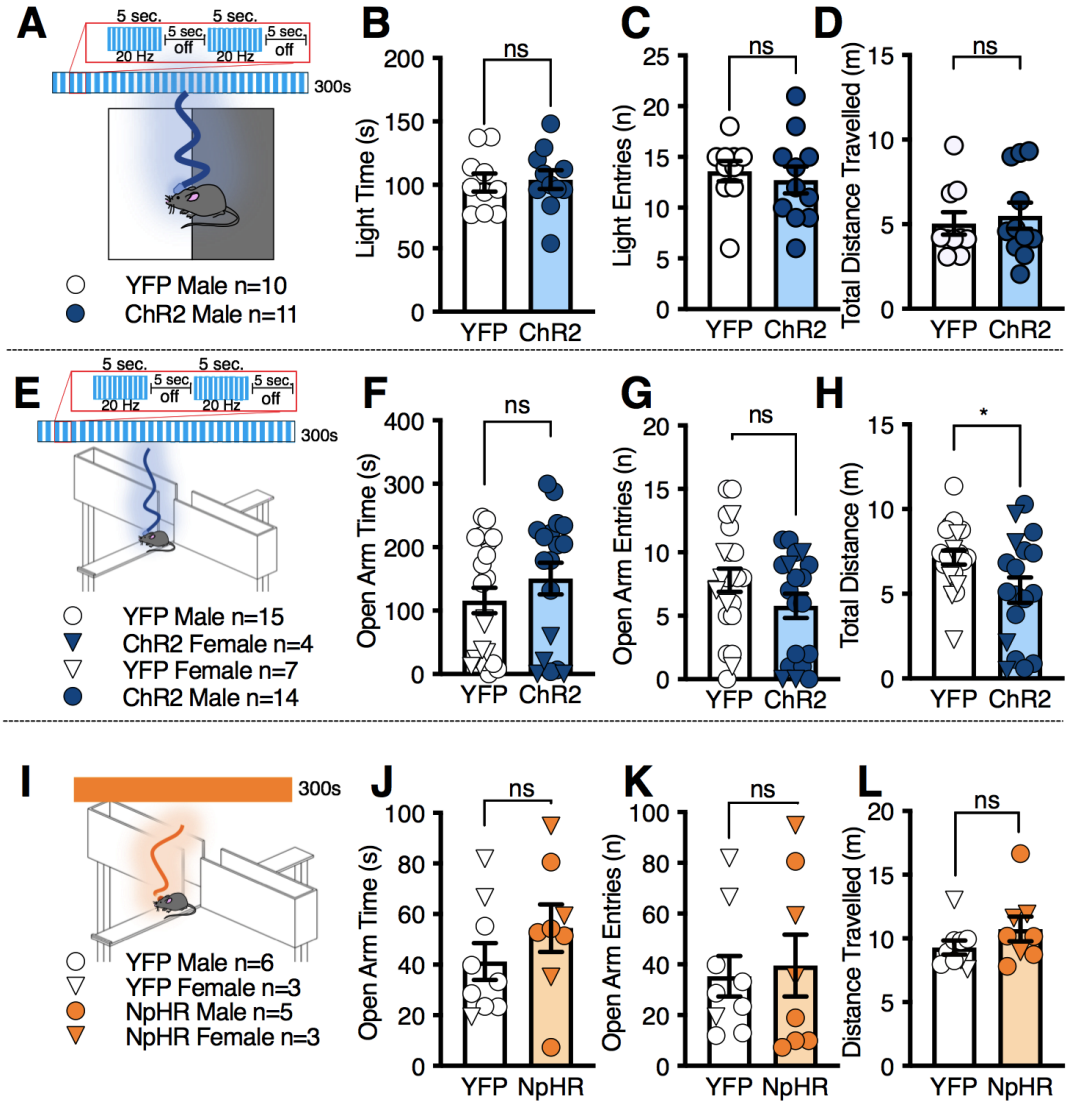

Figure 2.6 Activation and inhibition of BLA terminals in the NAc does not alter anxiety-like behavior. A) Schematic representing stimulation during light-dark box testing. **B)** ChR2-expression did not alter time in light chamber (ns p = 0.8346), **C)** number of light entries (ns p = 0.6105), or **D)** total distance travelled (ns p = 0.6598); YFP n= 10, ChR2 n=11 (B-D). **E)** Schematic of stimulation during elevated plus maze. **F)** Animals expressing ChR2 spent similar time in open-arms (ns p = 0.2779) and **G)** entered open arms a similar number of times compared to YFP-expressing animals (ns p = 0.1328). **H)** ChR2-expressing animals travelled less distance than YFP-expressing animals (*p = 0.0238); YFP n=22, ChR2 n=18 (F-H). **I)** Schematic showing optogenetic inhibition during elevated plus maze. **J)** Virus expression did not change open arm time (ns p = 0.2802), **K)** open arm entries (ns p = 0.7736), **L)** and did not alter distance traveled in the elevated plus maze (ns p = 0.2025); YFP n=9, NpHR n=8 (J-L). Data analyzed via unpaired two-tailed t-test.

NAc synapses, confirming the presence of functional cannabinoid receptors in this pathway **(Figure 2.7 A)**. Because previous investigations have shown differential eCB signaling at glutamatergic synapses onto distinct striatal MSN subtypes and within distinct BLA-NAc subcircuits,[122,205–207] we further examined the effect of 2-AG signaling and CB1 function at BLA-NAc D1+ and D1- (presumptive D2) MSNs glutamatergic synapses. We first found that increasing 2-AG levels via inhibition of monoacylglycerol lipase (MAGL) with JZL184 significantly reduced the frequency, but not amplitude, of asynchronous EPSCs onto both D1+ and D1- NAc MSNs (**Figure 2.7 B-C)** and that WIN55212-2, another direct cannabinoid receptor agonist, resulted in suppression of oEPSC amplitude and long-term depression onto both D1+ and D1- MSNs **(Figure 2.7 D)**. We next investigated the expression of depolarization-induced suppression of excitation (DSE), a protocol used to measure endogenous retrograde synaptic 2-AG signaling, and found DSE was present at both BLA to D1+ and D1- MSN synapses **(Figure 2.7 E)**, although the suppression was more robust in D1+ relative to D1- MSNs **(Figure 2.7 F)**. Lastly, we examined the role of JZL184 on spontaneous synaptic activity in the NAc. JZL184 did not alter spontaneous EPSC (sEPSC) frequency onto either D1+ or D1- MSNs **(Figure 2.7 G)** but significantly decreased spontaneous inhibitory post synaptic current (sIPSC) frequency, which was statistically significant, via post hoc analysis for D1+ MSNs **(Figure 2.7 H)**. There was no effect of JZL184 on D1+ or D1- sIPSC amplitude **(Figure 2.7 I)**. These data suggest that eCB regulation of BLA-NAc glutamatergic transmission is present on both primary MSN

cell types in the NAc and that 2-AG signaling can also affect NAc local GABAergic neurotransmission.

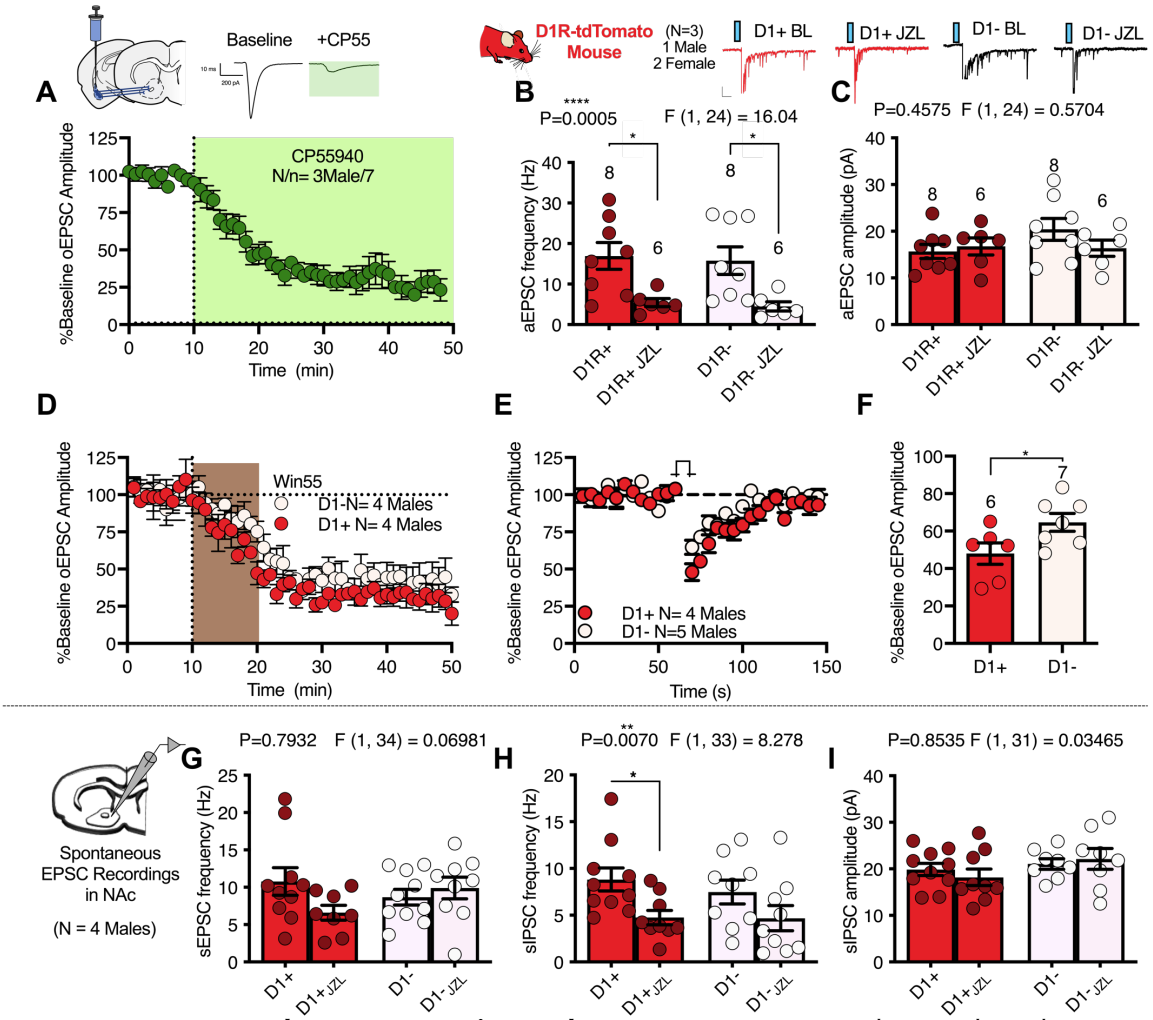

Figure 2.7 CB1 receptors and 2-AG augmentation regulate BLA-NAc synapses. A) The cannabinoid receptor agonist CP55940 decreased oEPSC amplitude in NAc; N= 3. **B)** JZL184 reduced aEPSC frequency in D1R+ (*p = 0.0171) and D1R- cells (*p = 0.0197), **(C)** but did not affect aEPSC amplitude after BLA-NAc optogenetic stimulation; D1+ N=3, D1- N=3 (B, C). **(D)** WIN55212-2 (Win55), a cannabinoid receptor agonist, uniformly decreased oEPSC amplitude in D1+ and D1- NAc cell types; D1+ N=4, D1- N= 4. **E)** DSE was present in both D1+ and D1- NAc cells, **F)** although DSE magnitude was increased in D1+ compared to D1- cells (*p = 0.0450); D1+ N=4, D1- N= 5 (E, F). **G)** sEPSC frequency in NAc recordings were unaffected by JZL184, **H)** but there was a significant effect of JZL184 on sIPSC frequency (*p = 0.0400). **I)** There are no effects of JZL184 on sIPSC amplitude; D1+ N=4, D1- N= 4 Data analyzed via Two-Way Mixed-Effects ANOVA followed by Sidak's multiple comparisons test (B-C, G-I) and unpaired two-tailed t-test (F). P and F values for Drug Effect shown in (B-C and G-I).

2-AG augmentation prevents BLA-NAc activation-induced social impairment

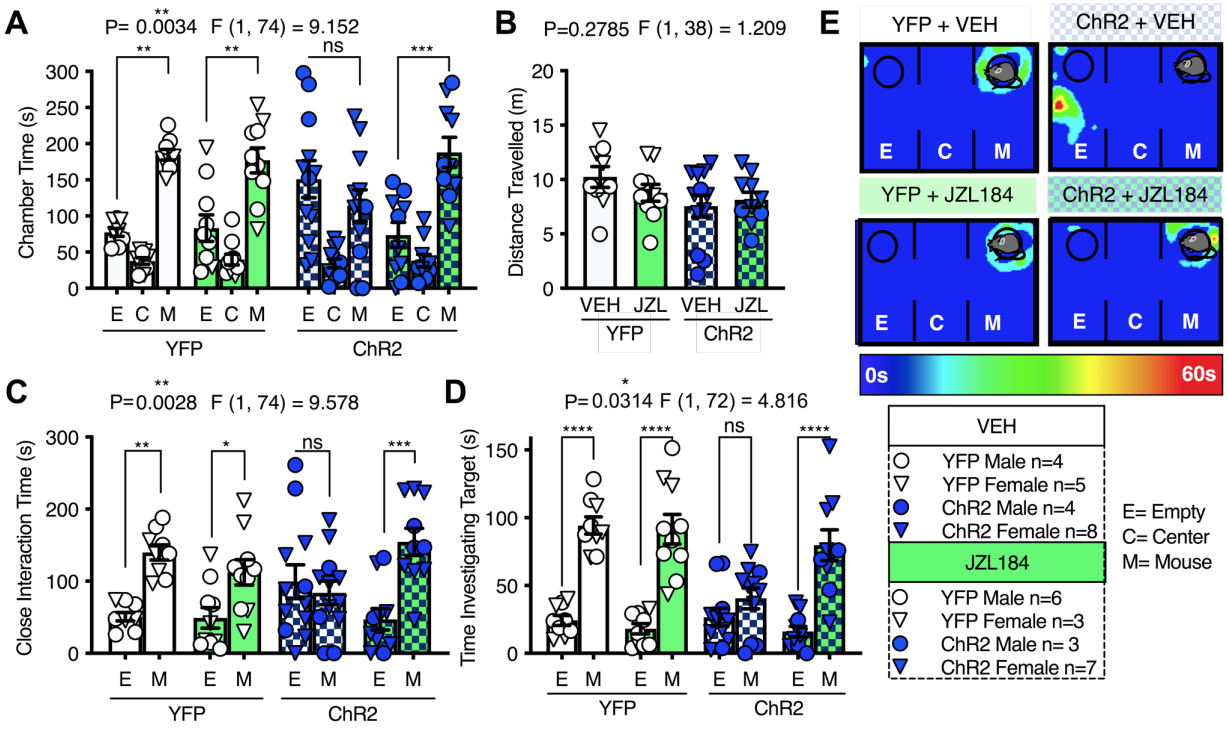

Figure 2.8 JZL184 pretreatment blocks BLA-NAc activation-induced decreases in sociability A) YFP-expressing animals that received JZL184 or VEH treatment showed a social preference (Veh: **p = 0.0015, JZL: **p = 0.0041), **(C)** spent more time in close interaction zone (Veh: **p = 0.0032, JZL:*p = 0.0429), and **(D)** and increased time investigating mouse, relative to empty, target (Veh: **** p <0.0001, JZL **** p <0.0001). ChR2 animals pre-treated with VEH had no **A)** social chamber preference (ns p = 0.4699), **C)** preference for time spent near the target (ns p =0.9302), or **D)** increased time investigating mouse, relative to empty, target (ns p = 0.5315). ChR2 animals treated with JZL184 have a significant preference for the **A)** mouse chamber (***p = 0.0003), **C)** and spend increased time in close interaction (***p = 0.0001) and **D)** investigating the mouse, relative to empty, target (****p < 0.0001). **B)** There was no effect of virus or drug treatment on distance traveled. **E)** Representative heat maps of each treatment condition. YFP + VEH n=9, YFP + JZL184 n=9, ChR2 + VEH n=12, ChR2 + JZL184 n=10 (A-D). Data analyzed via Three-Way Mixed-Effects ANOVA followed by Sidak's multiple comparisons test (A, C-D) or Two-Way ANOVA with Sidak's multiple comparisons test (B). P and F values for Chamber x Virus x Drug Interaction shown in (A, C-D) or Virus x Drug (B).

Our data thus far suggest 2-AG signaling can reduce presynaptic glutamate release at BLA-NAc synapses, suggesting that pharmacological 2-AG augmentation could counteract the social impairment observed after BLA-NAc circuit activation. To test this hypothesis, we administered JZL184 (8mg/kg IP) 1 hour prior to BLA-NAc stimulation in the 3-chamber SI task. We found that JZL184 prevented blue light delivery-dependent

suppression of sociability in the 3-chamber SI test in ChR2-expressing animals but did not affect SI in YFP-expressing controls (**Figure 2.8 A)**; JZL184 did not affect distance travelled in this assay **(Figure 2.8 B)**. ChR2-expressing JZL184-treated mice also spent more time in the close interaction zone of the 3-chamber apparatus **(Figure 2.8 C)** and more time investigating the mouse-containing cup relative to the empty cup **(Figure 2.8 D)** compared to vehicle-treated ChR2-expressing mice. Lastly, neither pharmacologically increasing (JZL184 8mg/kg IP) nor decreasing (DO34 50 mg/kg IP) 2-AG levels affected SI in naive, non-surgical animals **(Figure 2.9 A-D)**. These data indicate that, while pharmacological

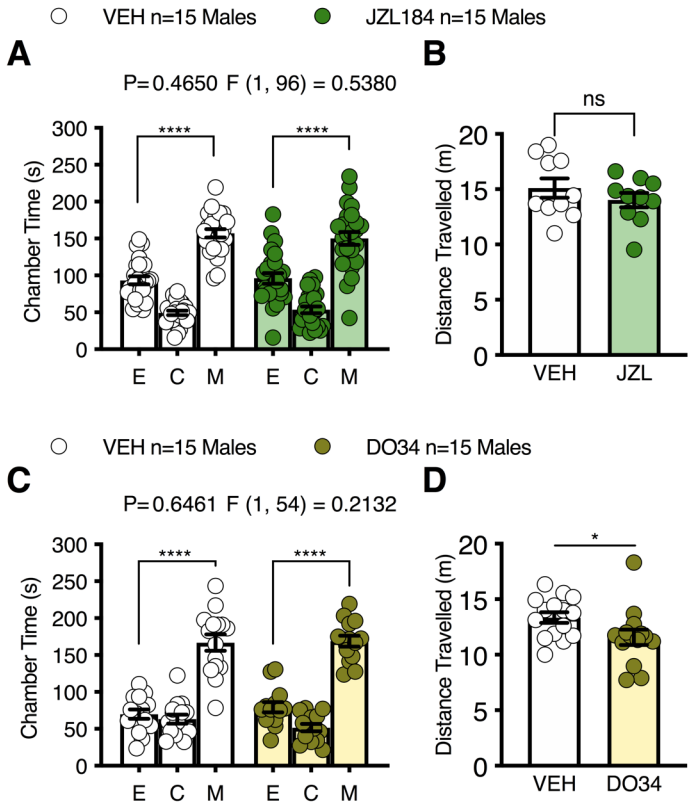

Figure 2.9 Pharmacologically modulating 2-AG levels does not impair SI in naïve mice. **A-B)** JZL184 (8mg/kg) was given 2 hours before the 3-chamber social interaction task. **A)** Both VEH and JZL184-treated animals have a preference for mouse chamber (****p < 0.0001) (VEH n= 15, JZL184 n=15) and **B)** do not exhibit differences in distance travelled (ns p = 0.3314). Distance travelled only collected from cohort 1 (VEH n=10, JZL184 n=10). **C-D)** DO34 50mg/kg was given 2 hours before the 3-chamber social interaction task. **C)** VEH and DO-34 treated animals have a preference for the social chamber (**** p < 0.0001). **D)** DO-34 pretreatment significantly decreases distance traveled relative to VEH treatment alone (*p = 0.0404); VEH n= 15, DO34 n=15 (C, D). Data analyzed via Two-Way Mixed-Effects ANOVA with Sidak's multiple comparisons test (A, C) or unpaired two-tailed t-test (B, D). P and F values for Chamber x Drug Interaction shown in (A, C).

modulation of 2-AG levels has little effect on physiological expression of sociability, 2-AG augmentation is able to attenuate the social avoidance behavior induced by BLA-NAc circuit activation.

Optogenetic BLA-NAc circuit inhibition reduces social deficits in *Shank3B*$^{-/-}$ mice

That BLA-NAc inhibition did not affect social behavior in wild-type (WT) mice (see **Figure 2.16 for placement**) suggests that the BLA-NAc circuit does not physiologically regulate sociability under basal conditions. However, it is possible that BLA-NAc activity could contribute to social impairment under pathological conditions, such as those observed in the *Shank3B*$^{-/-}$ model of syndromic ASD. Indeed, we found, using a counterbalanced cross-over design, that bilateral orange-light stimulation of NpHR, and thus inhibition of the BLA-NAc circuit, normalized time in the mouse chamber during orange light-ON relative to light-OFF testing in *Shank3B*$^{-/-}$ mice **(Figure 2.10 A** and see **Figure 2.16 C-D** for cannula placements**)**. Consistent with previous data, YFP-expressing *Shank3B*$^{-/-}$ controls showed a lack of sociability[143,144,208] under both light-ON and light-OFF conditions in the 3-chamber test, while NpHR-expressing *Shank3B*$^{-/-}$ mice exhibited social-chamber preference only under light-ON conditions **(Figure 2.10 B, F)**. There were no changes in the distance travelled between groups **(Figure 2.10 C, G)**. Orange light inhibition of the BLA-NAc circuit in *Shank3B*$^{-/-}$ mice also resulted in a significant preference for time investigating the mouse-containing cup in NpHR-expressing mice under light ON, but not light OFF, conditions, while YFP-expressing mice show no preference under either condition **(Figure 2.10 D, H)**. These data support the hypothesis that reducing BLA-NAc

activity can enhance sociability under pathological conditions associated with reduced SI, such as those observed in the *Shank3B*$^{-/-}$ model.

2-AG augmentation reduces social deficits and feed-forward GABAergic signaling in *Shank3B*$^{-/-}$ mice

Finally, because acute treatment with JZL184 was able to reverse the sociability deficits resulting from overactivation of the BLA-NAc circuit, and inhibiting the BLA-NAc circuit reverses social deficits in *Shank3B*$^{-/-}$ mice, we hypothesized that acute treatment with JZL184 (8mg/kg IP) would increase social behavior in *Shank3B*$^{-/-}$ mice **(Figure 2.11 A)**. While vehicle treatment did not increase SI in *Shank3B*$^{-/-}$ animals, JZL184 pretreatment resulted in significant social preference in *Shank3B*$^{-/-}$ animals in the 3-chamber SI task **(Figure 2.11 B-E)** but had no effect on distance travelled **(Figure 2.11 C)**. JZL184 treatment also resulted in a preference for investigating the target mouse relative to the empty cup in *Shank3B*$^{-/-}$ mice **(Figure 2.11 D)**. In addition to social deficits, *Shank3B*$^{-/-}$ animals display aberrant repetitive grooming behavior,[143,144,208] modeling the second core feature of ASD: restricted and repetitive behaviors. We subsequently demonstrated that the amount of time grooming is significantly reduced by JZL184 (8mg/kg IP) treatment in *Shank3B*$^{-/-}$ animals but did not affect grooming behavior in WT mice **(Figure 2.11 F)**.

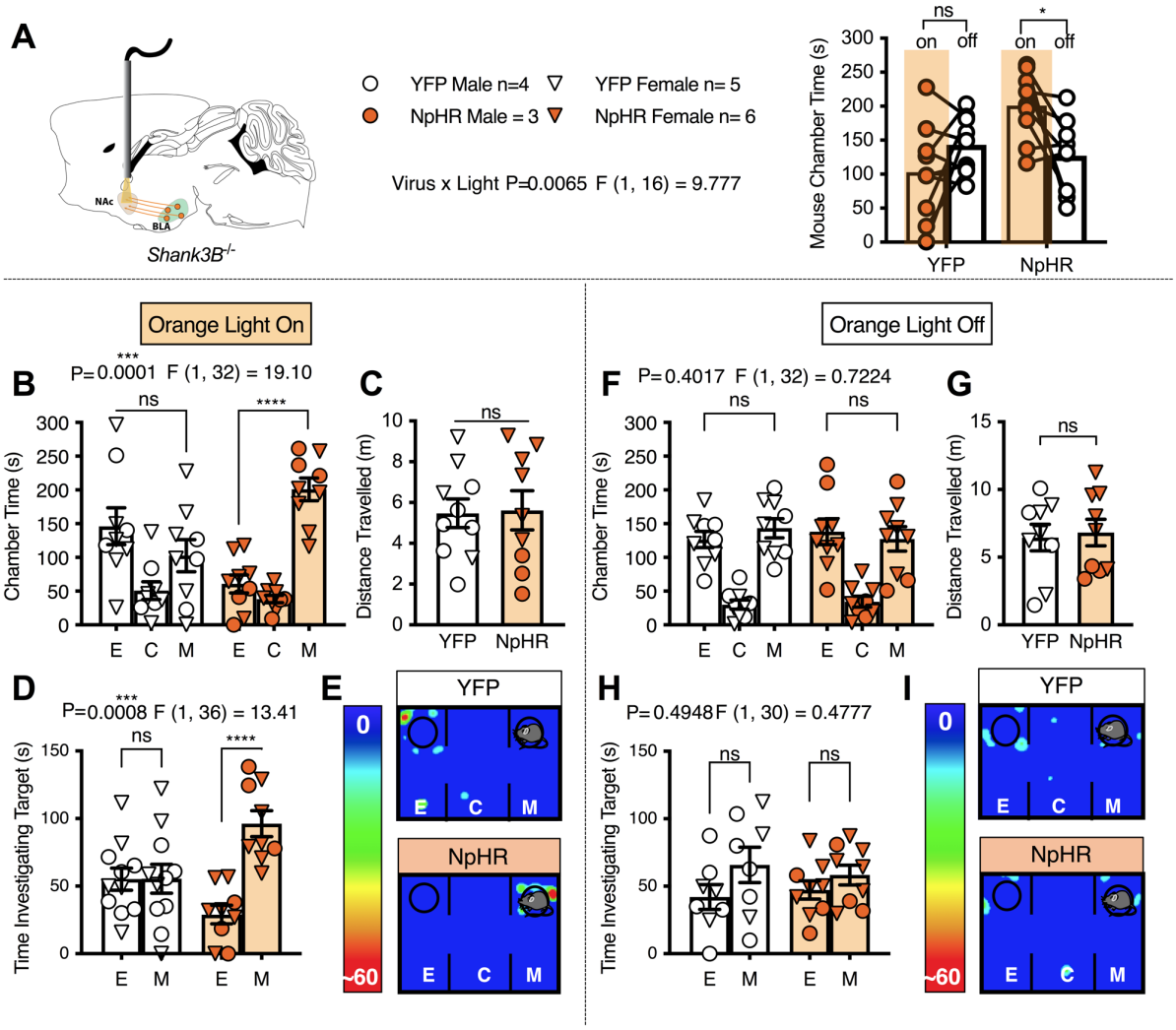

Figure 2.10 Inhibition of the BLA-NAc circuit normalized SI deficits in *Shank3B*$^{-/-}$ mice. A) *Shank3B*$^{-/-}$ mice expressing NpHR in the BLA with bilateral orange light stimulation delivered to the NAc spend significantly more time in the mouse chamber during orange light delivery (ON) compared to light-OFF conditions (*p = 0.0230). YFP animals do not show a preference for the mouse chamber (ns p = 0.2529). **B)** *Shank3B*$^{-/-}$ mice expressing YFP under light ON conditions do not exhibit social preference (ns p = 0.2831), while animals that express NpHR have a preference for the mouse chamber (****p < 0.0001). **D)** Mice that express NpHR have a significant increase in time investigating the mouse cup under light ON conditions (****p < 0.0001). **C)** No effect on distance traveled was observed (ns p = 0.9057) in light ON paradigm. **E)** Representative heat maps under light ON conditions. **F)** Neither YFP (ns p = 0.7166) nor NpHR (ns p = 0.8731)-expressing *Shank3B*$^{-/-}$ showed mouse-chamber preference **H)** or preference for time investigating mouse target (YFP ns p = 0.1617, NpHR ns p = 0.6193) under light OFF conditions. **G)** There are no effects on distance travelled under light OFF conditions (p = 0.7959). **I)** Representative heat maps under light OFF conditions. YFP n=9, NpHR n=9 (B-D, F-H). Data analyzed via Two-Way Mixed effects ANOVA with Sidak's multiple comparisons test (A, B, D, F, H) or unpaired, two-tailed t-test (C, G). P and F values for Light x Virus interaction shown in (A) and Chamber x Virus interaction shown in (B, D, F, H).

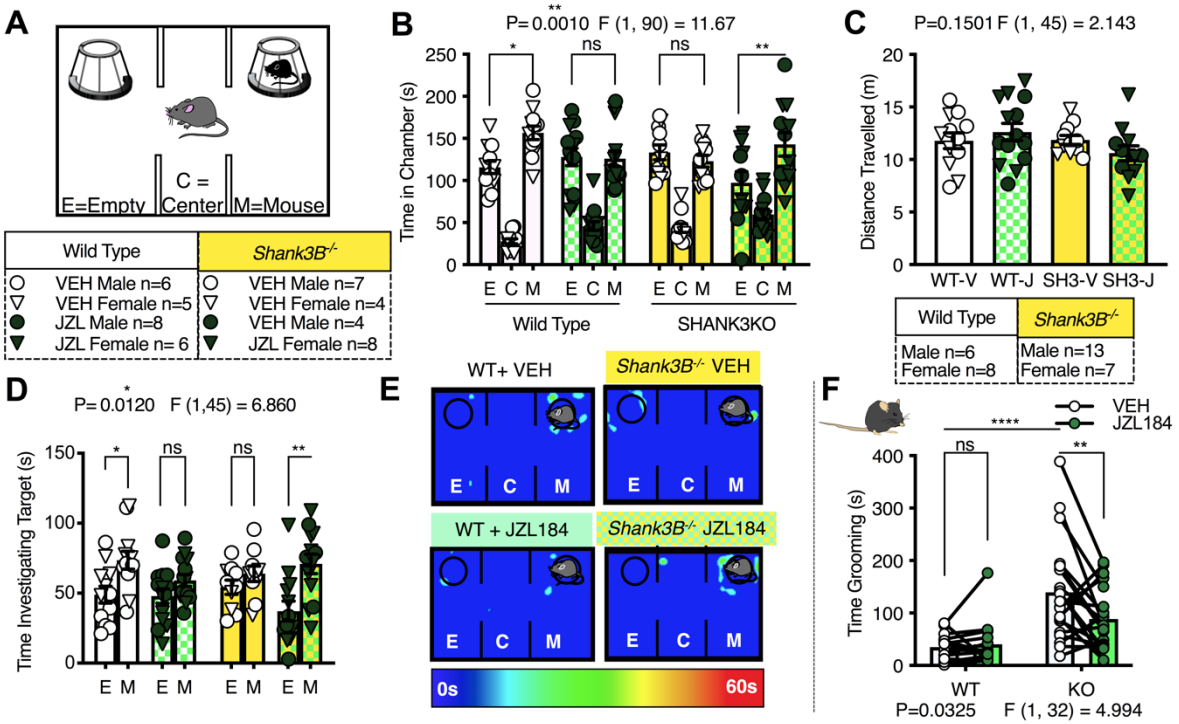

Figure 2.11 Systemic JZL184 treatment reverses the core behavioral abnormalities in *Shank3B*$^{-/-}$ animals: A) Diagram of 3-chamber SI task. **B)** VEH treatment did not affect SI in WT mice (**p = 0.0242), and did not induce a preference in *Shank3B*$^{-/-}$ (ns p = 0.9360), while JZL184 eliminated social preference in WT mice (ns p = 0.9998) but resulted in significant social preference in *Shank3B*$^{-/-}$animals (**p = 0.0094). **C)** There is no difference in distance travelled between groups. **D)** JZL184 treated *Shank3B*$^{-/-}$ animals (***p = 0.0002) and VEH treated WT mice (*p = 0.0155) had preference for investigating the mouse, over empty, target while JZL184 WT (ns p = 0.7103) and VEH *Shank3B*$^{-/-}$ mice (ns p = 0.0.9529) did not; WT + VEH n=11, WT + JZL n=14, KO + VEH n=11, KO + JZL n=12 (B-D). **E)** Representative heat maps of 3-chamber SI task. **F)** *Shank3B*$^{-/-}$ mice treated with VEH spend significantly more time grooming compared to WT VEH animals (****p < 0.0001). *Shank3B*$^{-/-}$ mice treated with JZL184 spent significantly less time grooming compared to VEH treatment (**p = 0.0069) and WT VEH treatment, while JZL184 had no effect in WT mice (ns p = 0.9548); WT n=14, KO n=20. Data analyzed via Three-Way Mixed effects ANOVA with Sidak's multiple comparisons test (B, D), Two-Way ANOVA with Sidak's multiple comparisons test (C), or Two-way RM ANOVA with Sidak's Multiple Comparisons (F). P and F values for Chamber x Genotype x Drug interaction shown in (B, D) or Genotype x Drug interaction (C, F).

While our data clearly show systemic pharmacological augmentation of 2-AG reduced social impairment upon BLA-NAc stimulation, and in *Shank3B*$^{-/-}$ mice, these data do not conclusively link the two findings in a manner that supports the site of action of JZL184 as being within the BLA-NAc circuit. To directly test the hypothesis that systemic

JZL184 administration effectively reduces social impairment via NAc-mediated mechanisms, we administered JZL184 (5μg/μL) or vehicle directly into the NAc using a microinfusion approach prior to conducting the 3-chamber SI task in *Shank3B*$^{-/-}$ mice **(Figure 2.12 A**, and **Figure 2.16 E** for cannula placements**)**. JZL184 microinfusion did not affect distance traveled in this task (**Figure 2.12 B)**; however, it increased time *Shank3B*$^{-/-}$ mice spent in the mouse chamber and time investigating the target mouse under the cup **(Figure 2.12 C-E)**. Vehicle microinfusion did not result in increased time spent in the mouse

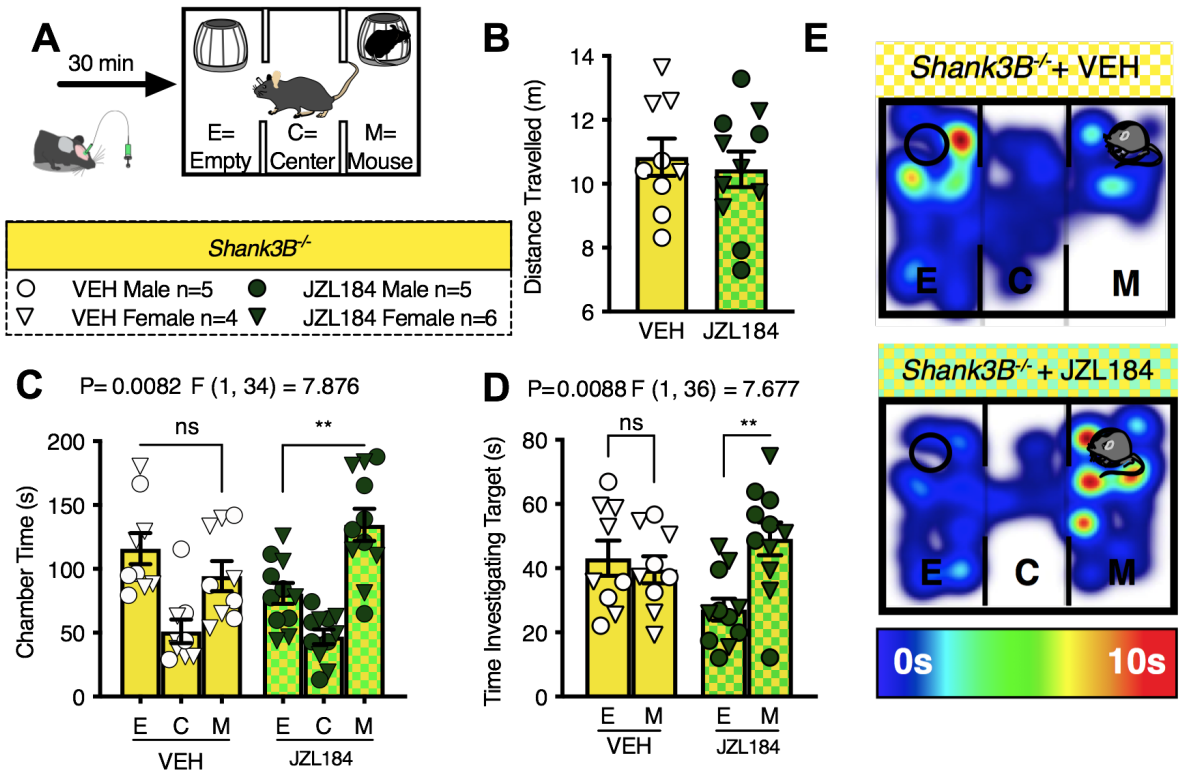

Figure 2.12 JZL184 microinfused into the NAc reverses the sociability deficit in *Shank3B*$^{-/-}$ animals: A) Diagram of microinfusion experimental design. **B)** JZL184 administered to the NAc does not alter distance traveled. **C)** VEH-treated *Shank3B*$^{-/-}$ animals did not exhibit a preference for the mouse chamber (ns p = 0.8566), while JZL184 increased social chamber preference (**p = 0.0014). **D)** Additionally, VEH -treated *Shank3B*$^{-/-}$ did not have a preference for investigating the mouse cup while JZL184 increased investigation time (**p = 0.0022); VEH n=9, JZL184 n=11 (B-D). **E)** Representative heat maps of 3-chamber SI task. Data analyzed via unpaired, two-tailed t-test (B) or Two-Way ANOVA with Sidak's multiple comparisons test (C, D). P and F values for Chamber x Drug interaction shown in (C, D).

containing chamber or increase time in social investigation of mouse relative to empty cup. These data indicate local actions of JZL184 within the NAc are sufficient to normalize SI deficits in *Shank3B*$^{-/-}$ mice. Given that elevating 2-AG selectively within the NAc is sufficient to increase social behavior in the *Shank3B*$^{-/-}$ mouse, we investigated the effects of JZL184 on the synaptic signaling in the NAc as well as specifically after BLA-NAc optogenetic stimulation to gain insight into the potential mechanisms by which JZL184 may affect sociability in *Shank3B*$^{-/-}$ mice. Firstly, we found no changes in the intrinsic excitability of NAc MSNs as measured by the number of action potentials generated per current injection, action potential threshold, resting potential, or input resistance between WT and *Shank3B*$^{-/-}$ mice **(Figure 2.13 A-D)**. However, we found that *Shank3B*$^{-/-}$ animals display a robust increase in sIPSC frequency **(Figure 2.14 A)** but not amplitude **(Figure 2.14 B)**, as well as

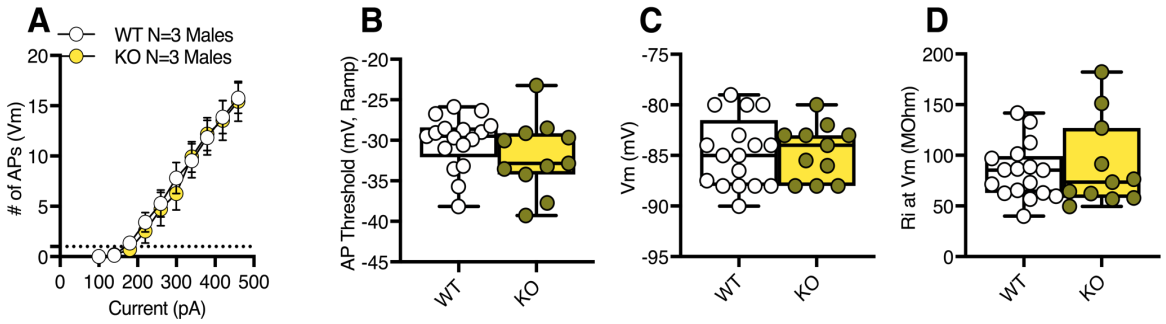

Figure 2.13 *Shank3B*$^{-/-}$ do not show changes in intrinsic neuronal properties in the NAc. A) *Shank3B*$^{-/-}$ (KO) do not show changes in intrinsic excitability as measured by the number of action potentials generated during successive current injections. *Shank3B*$^{-/-}$ exhibit **B)** a similar AP threshold, **C)** resting membrane potential (Vm) **D)** and input resistance (Ri) compared to WT animals; WT N=3, KO N=3 (A-D). Data analyzed via unpaired, two-tailed t-test. (B-D)

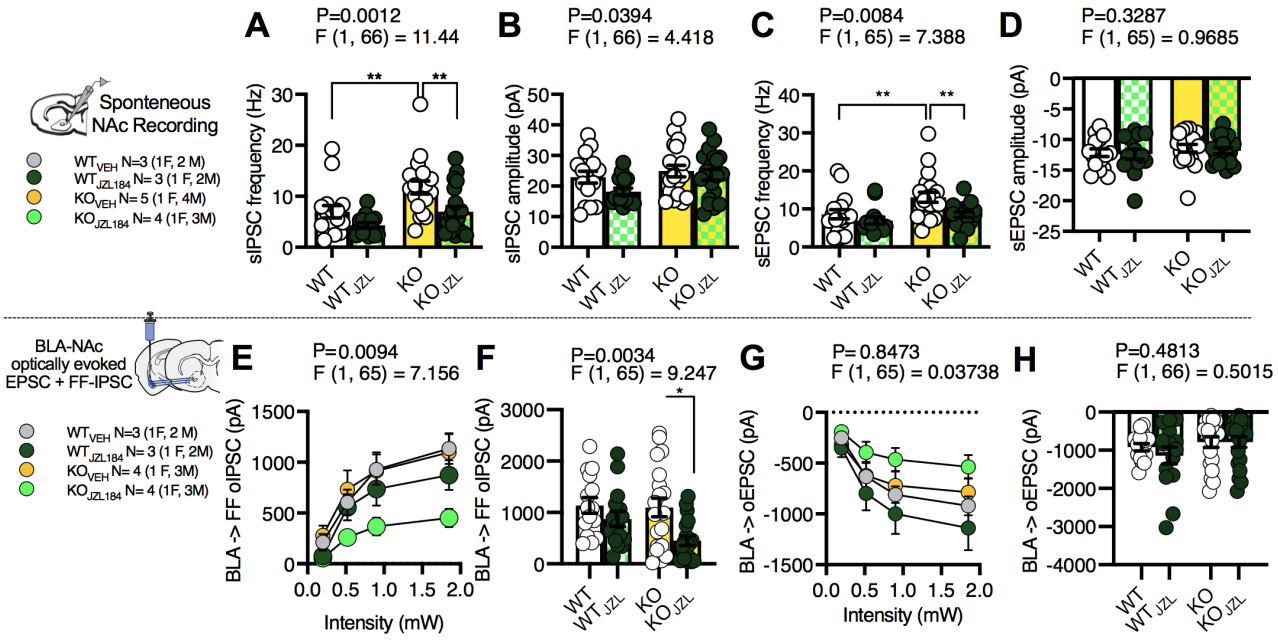

Figure 2.14 JZL184 significantly reduces sIPSC frequencies in the NAc and BLA-NAc feedforward inhibition in *Shank3B*$^{-/-}$ mice: A) sIPSC frequency on the NAc MSNs is significantly increased in *Shank3B*$^{-/-}$ compared to WT mice (**p = 0.0060) and is restored by JZL184 (**p = 0.0033). **B)** There is no effect of *Shank3B*$^{-/-}$ on sIPSC amplitude. **C)** sEPSC frequency is significantly increased in *Shank3B*$^{-/-}$ mice relative to WT animals (**p = 0.0084) and is restored by JZL184 (** p = 0.0060). **D)** There was no effect of genotype or drug on sEPSC amplitude; WT + VEH N=3, WT + JZL184 N=3, KO + VEH N=5, KO + JZL184 N=4 (A-D). **E)** There was no difference between WT and *Shank3B*$^{-/-}$ BLA feedforward (FF) oIPSCs onto NAc cells, However **F)** at maximal stimulation (1.85mW) JZL184 significantly reduces BLA FF oIPSCs onto NAc MSNs (*p=0.0101). **G-H)** There is no effect of JZL184 or genotype on BLA oEPSC in the NAc across intensities; WT + VEH N=3, WT + JZL184 N=3, KO + VEH N=4, KO + JZL184 N=4 (E-H). Data analyzed via Two-Way ANOVA with Sidak's multiple comparisons test (A-H), P and F values for drug effect shown in (A-H). M= males, F= females.

increased sEPSC frequency **(Figure 2.14 C)**, but not amplitude (**Figure 2.14 D**) in the NAc. Moreover, we observed that JZL184 significantly reduced sIPSC and sEPSC frequency in the NAc of *Shank3B*$^{-/-}$ mice **(Figure 2.14 A, C)**. In response to ex vivo BLA-NAc optogenetic stimulation, we observed no genotype-specific effects on either BLA-NAc oEPSCs or di-synaptic feed-forward (FF) oIPSCs **(Figure 2.14 E-H)**. However, JZL184 robustly decreased BLA-NAc feed-forward oIPSC amplitude in *Shank3B*$^{-/-}$ but not WT mice (**Figure 2.14 E-F**).

JZL184 did not affect BLA-NAc oEPSC amplitude in either *Shank3B*$^{-/-}$ or WT mice **(Figure 2.14 G-H)**. These data suggest 2-AG augmentation could normalize social function in *Shank3B*$^{-/-}$ mice via modulation of BLA-NAc-elicited FF inhibition (possibly mediated via local GABAergic interneurons), which could result ultimately in disinhibition of NAc MSNs **(Figure 2.15)**. This model could also explain increased sociability after BLA-NAc circuit inhibition in *Shank3B*$^{-/-}$ mice, as reduced BLA glutamatergic drive to local NAc GABAergic interneurons would also disinhibit MSNs **(Figure 2.15)**. How the balance of direct BLA excitation of NAc MSNs and local GABAergic interneurons are sculpted to ultimately direct optimal sociability remains to be determined.

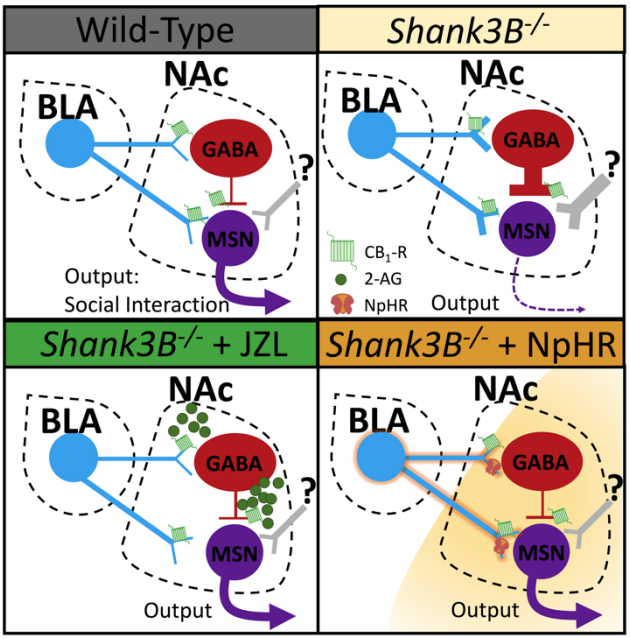

Figure 2.15 Working model of eCB-BLA-NAc interactions in *Shank3B*$^{-/-}$ mice. *Shank3B*$^{-/-}$ mice exhibit increased sEPSC and sIPSC frequency onto MSNs in the NAc relative to WT mice and exhibit social impairment. In *Shank3B*$^{-/-}$ mice treated with systemic or intra-NAc JZL184 to increase 2-AG levels, sEPSC and sIPSC frequency is normalized as is BLA-NAc FF-inhibition, resulting in a reduction in social deficits. *Shank3B*$^{-/-}$ mice with optogenetic inhibition of BLA-NAc circuit function are hypothesized to have similarly reduced FF-inhibition and reduced overall glutamatergic drive to GABA interneurons and MSNs, which also reduces social deficits.

Supplemental Figures

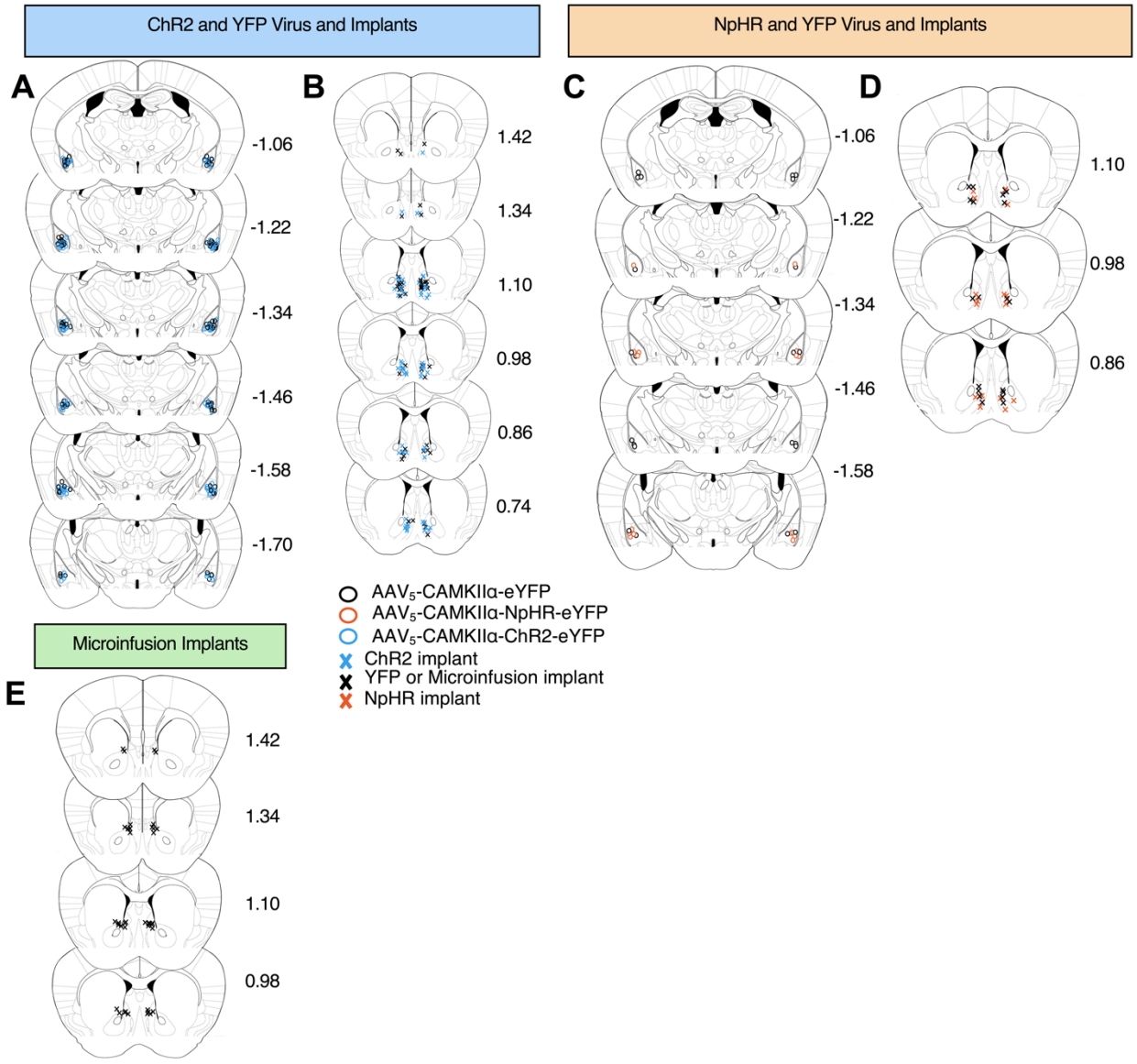

Figure 2.16. Histological verification of viral delivery and cannula placements. A) Location of ChR2 and YFP viral injections and **B)** unilateral fiber optic canula. **C)** Location of NpHR and YFP bilateral virus injections and **D)** bilateral fiber optic cannulas delivered to *Shank3B*$^{-/-}$ mice. **E)** Location of bilateral infusate cannulas in NAc of *Shank3B*$^{-/-}$ mice. Numbers represent Bregma coordinates in millimeters.

CHAPTER 3

METHODS

Animals

Mice were housed on a 12:12 light-dark cycle with lights on at 06:00. All experiments were conducted during the light phase. Food and water were available *ad libitum*. Male and female C57/BL6J mice were used for all experiments. Breeding cages were given access to 5LOD chow (PicoLab®, 28.7% Protein, 13.4% Fat, 57.9% Carbohydrate) to improve the viability of litters. Upon weaning at P21-28, experimental animals were switched to standard chow. Wild-type male and female C57/BL6J were ordered from JAX (stock #00064) at 5 weeks of age, target mice for social behavior were ordered at 3 weeks of age and used in experiments at 4 weeks unless otherwise noted. Male and female *Shank3B*$^{+/-}$ mice were ordered from JAX laboratories (Stock number: 017688) and bred in house. Male and Female transgenic BAC *Drd1a-tdTomato* and BAC Drd2-EGFP mice were obtained from JAX laboratories on a C57BL/6J background.

For all animals, viral delivery was performed within 3 weeks of arrival, and delivery of fiber optic implant occurred 4 weeks after viral delivery surgery. Behavior testing for optogenetic studies occurred at least 6 weeks following virus surgery *and* ex vivo recordings were performed at least 4 weeks after surgery. Following implantation

surgery, animals were single-housed. All experimental animals used were between 8-20 weeks old.

Drugs

JZL184 (8 mg kg^{-1}; AbCam, Cambridge, Massachusetts, USA) was prepared in dimethylsulfoxide (DMSO; Sigma-Aldrich, Milwaukee, WI, USA) and injected at a volume of 1 µl g^{-1} bodyweight. For microinfusion studies, JZL184 was prepared into 5 µg/µL DMSO. For electrophysiological recording, 2mM stock solution of JZL184 was prepared in DMSO and added to 0.05% w/v Bovine Serum Albumin (BSA, Sigma-Aldich, St. Louis, MO, USA) containing ACSF to a final 1 µM concentration. DO34 (50 mg kg^{-1}) was synthesized as previously described,[216] prepared in a 1:1:18 mixture of ethanol, kolliphor, and saline, and injected at a volume of 10 µl g^{-1} bodyweight. JZL184 was administered 1 hour before initiation of behavioral testing when combined with in vivo optogenetics **(Figure 2.8)**, while JZL184 and DO34 were administered 2 hours prior to behavior in naïve mice **(Figure 2.9)**. CP55,940 (Cayman Chemicals, Ann Arbor, Michigan, USA) and stocks were made at 10mM in DMSO and diluted 1:2000 (for a final concentration of 5µM) in ACSF with 0.05% w/v BSA to increase solubility. WIN55212-2 (Tocris Bio-Techne Corporation, Minneapolis, MN, USA) was dissolved in DMSO at 1mM and diluted into a final concentration of 1µM in ACSF. Ketoprofen, dexdomitodor, ketamine, and antisedan were obtained from Patterson Veterinary Supplies (Greeley, CO, USA).

Viruses

We used AAV5-CaMKIIa-hChR2(H134)-EYFP for optical excitation or AAV5-CaMKIIa-eNpHR3.0-EYFP for optical inhibition. AAV5-CaMKIIa-EYFP (250nL**,** UNC Vector Core, Chapel Hill, NC, USA) was used as a control in all studies.

Stereotaxic surgery

Male and female mice at 5–8 weeks old underwent unilateral or bilateral stereotaxic surgery, as indicated in the figures. Animals were anesthetized at 5% isoflurane, administered 10mg/kg ketoprofen (AlliVet, St. Hialeah, FL) as an analgesic before undergoing stereotaxic surgery. A motorized drill and 10uL microinjection syringe (Hamilton Co., Reno, NV) was guided via digital software (Neurostar Drill and Injection Robot, Tubingen, Germany) to each injection site. Animals were kept under constant 2.5% isoflurane anesthesia. For some ex vivo electrophysiology studies **(Figure 2.7 E-G)** mice were anesthetized using a cocktail of ketamine (75 mg/kg) and dexdomitidor (0.5 mg/kg) and were revived using 0.5 mg/kg antisedam.

Viruses were infused into the basolateral amygdala (BLA) (AP: −1.25, ML: ±3.25, DV: 5.05) at a rate of 100 nl min^{-1}. The syringe was first lowered (0.20 mm s^{-1}) to 0.5 μm deeper than the injection site, after 5 seconds, it was raised to the injection site where it paused for 10 seconds before injecting. After the virus was infused, the syringe remained in place for 600 seconds before retracting.

At least 4 weeks following viral injection, mice underwent unilateral or bilateral fiber optic cannula implantation. Cannula implants were lowered to the ipsilateral

nucleus accumbens (NAc) of the viral surgery or bilaterally (AP: 1.25, ML: ±0.55, DV: 4.10, +/- 10° tilt for bilateral implants) (0.20mms^{-1}) using an XCL Cannula Holder (Thor labs, Newton, NJ, USA). For microinfusion studies, bilateral, stainless-steel infusion guide cannulas (26 gauge, cut to 3mm length, 2mm center to center distance, C235GS-5-2.0/SPC- Plastics One, Roanoke VA) were placed above the NAc (AP: 1.35, ML: ±1.00, DV: 3.00) and fitted with a dummy cannula (C235DCS-5/SPC, Plastics One, Roanoke VA) and dust cap (303DC/1 Plastics One, Roanoke VA). A bone screw (Plastics One, Roanoke VA) was placed in the skull to anchor the weight of the implant. Metabond (Parkell, Edgewood, NY) was coated across the skull, screw, and implant and allowed to dry for at least 5 minutes. Next, FujiCEM dental cement (Instech, Plymouth Meeting, PA) was applied and allowed to dry for at least 5 minutes. The skin was sutured around the implant (Ny-Superion Havel's, Cincinnati, OH) and mice were single-housed. Animals were treated with 10mg/kg ketoprofen (AlliVet, St. Hialeah, FL) for up to 3 days following surgery as needed. Animals recovered for at least one week prior to any experimental manipulation.

Ex Vivo Electrophysiology

Mice were briefly anesthetized with isoflurane and transcardially perfused with ice-cold oxygenated (95% v/v O_2, 5% v/v CO_2) N-methyl-D-glucamine (NMDG) based ACSF{Ting, 2014 #26}[71](2) comprised of (in mM): 93 NMDG, 2.5 KCl, 1.2 NaH_2PO_4, 30 $NaHCO_3$, 20 HEPES, 25 glucose, 5 Na-ascorbate, 3 Na-pyruvate, 5 N-acetylcyctine, 0.5 $CaCl_2{\cdot}4H_2O$ and 10 $MgSO_4{\cdot}7H_2O$. The brain was quickly removed and 250 µm coronal or

parasagittal **(Figure 2.7 D-F)** slices of the NAc were cut using a Leica VT1000S vibratome (Leica Microsystems, Bannockburn, IL, USA) in the NMDG solution. Slices were incubated for 10-15 minutes at 32°C oxygenated NMDG-ACSF and stored at 24°C until recording in HEPES-based ACSF containing (in mM): 92 NaCl, 2.5 KCl, 1.2 NaH_2PO_4, 30 $NaHCO_3$, 20 HEPES, 25 glucose, 5 ascorbate, 3 Na-pyruvate, 5 N-acetylcyctine, 2 $CaCl_2 \cdot 4H_2O$ and 2 $MgSO_4 \cdot 7H_2O$. Recordings were performed in a submerged recording chamber during continuous perfusion of oxygenated ACSF containing (in mM): 113 NaCl, 2.5 KCl, 1.2 $MgSO_4 \cdot 7H2O$, 2.5 $CaCl_2 \cdot 2H2O$, 1 NaH_2PO_4, 26 $NaHCO_3$, 1 ascorbate, 3 Na-pyruvate and 20 glucose; at a flow rate of 2.5 - 3 ml/min. All drugs were dissolved in ACSF containing 1:2000 BSA (w/v) and ≤1:2000 DMSO (v/v). Slices were visualized using a Nikon microscope equipped with differential interference contrast video microscopy or Scientifica Slicescope Pro System **(Figure 2.7 D-F)**. Whole-cell current clamp recordings from NAc MSNs held at resting membrane potential were obtained under visual control using a 40x objective. 2 - 3 MΩ borosilicate glass pipettes were filled with high $[K^+]$ based solution containing (in mM): 125 K^+-gluconate, 4 NaCl, 10 HEPES, 4 Mg-ATP, 0.3 Na-GTP, and 10 Na-phosphocreatine. Whole-cell voltage clamp recordings were performed with the same internal solution in the experiments shown in **(Figure 2.7 A-C)** and **(Figure 2.3)**. Pipettes were filled with a Cs^+ internal solution (in mM: 120 CsMeSO3, 15 CsCl, 8 NaCl, 10 HEPES, 0.2 EGTA, 10 TEA-Cl, 4.0 Mg2-ATP, 0.3 Na2-GTP, 0.1 spermine, and 5.0 mM QX 314 bromide) for WIN-55 experiments **(Figure 2.7 D)**. Recording ACSF solution contained the $GABA_A$ receptor antagonist picrotoxin (50 μM; Abcam, Cambridge, MA) to pharmacologically isolate glutamatergic transmission. In the experiments where both

glutamatergic and GABAergic currents were assessed in each cell **(Figure 2.7 G-I and Figure 2.14)** a cesium based internal solution was used consisting of (in mM): 120 CsOH (50%), 120 D-gluconic acid (50%), 2.8 NaCl, 5 TEA-Cl, 20 HEPES, 2.5 Mg-ATP, 0.25 Na-GTP. Spontaneous and optically evoked EPSCs and IPSCs were measured at -70mV and +13mV, respectively. Only cells with access resistance <20 MΩ were included. *Shank3B*$^{-/-}$ and WT data **(Figure 2.7 G-I and Figure 2.14)** was carried out by using single housed (1 week+) mice similar to the behavioral experiments.

Optical stimulation as well as data collection was coordinated using pClamp 10 (Molecular Devices). Cell electrical properties were monitored using an Axopatch 500B Multiclamp amplifier and Axon Digidata 1550 low-noise data acquisition digitizer. Responses were filtered at 2 kHz and digitized at 10 kHz. Optical stimulation of ChR2-expressing BLA terminals was achieved using a Thorlab 480nm LED system **(Figure 2.7 A-C, 2.3)**, CoolLED pE-100 480nm LED excitation system (**Figure 2.7 D-F)** or a Mightex 455nm LED system **(Figure 2.14)**. 2ms light pulses were applied through a 40x objective to excite ChR2+ terminals at 0.1 – 0.2 Hz. Light intensity was adjusted to evoke stable responses. Depolarization induced suppression of excitation (DSE) was examined under voltage-clamp condition and was evoked by depolarizing patched MSNs to +30mV for 10 seconds. DSE was classified as the first EPSC following the depolarizing pulse. Electrophysiology experiments were analyzed using using Clampfit 10.4, Microsoft Excel, and Graphpad Prism v8.0.

Drug wash-on experiments were carried out after assessing a 7-10min stable baseline recording. Then, CP55,940 was applied during the entire session of the recordings, while

WIN55212-2 was only applied during the initial 10min to allow assessment of long-term depression (LTD).

BAC transgenic mice expressing td-Tomato under the D1 receptor promoter or GFP under the D2 receptor promoter were used to identify the two major populations of direct and indirect pathway neurons of the striatum, respectively (as depicted in figures). Putative D1 receptor or D2 receptor neurons were identified by the presence or absence of fluorophore expression, as previously reported[217] and neighboring neurons were patch-clamped at ≤60μm apart within the same depth and plane of the slice. Input/output curves were generated by increasing the intensity of the applied light pulses and the maximal oEPSC amplitude was used to compare the excitatory input ratios between D2+ and D2- neurons **(Figure 2.3)**. In the experiments assessing the asynchronous release probabilities of the BLA-NAc pathway on D1+ and D1- MSNs, the frequency and amplitude of aEPSCs were analyzed within the 50ms - 500ms time-window measured from the onset of the light stimulus **(Figure 2.7 B-C)**.

Cells were excluded from all analyses for any of the following reasons. 1: if the holding current dropped below -200 pA at any time during the recording. 2: if the access resistance was > 20 MΩ. 3: if the access resistance fluctuated by more than 20% throughout the recording. 4: There was no optogenetically-evoked response.

Histology and Imaging

After animals completed behavior experiments, brain tissue was collected in order to validate implant and viral placement. Mice were anesthetized using isoflurane (Abbott Labs, Chicago) and transcardially perfused with cold phosphate buffered saline (PBS, 10mL) followed by cold 4% paraformaldehyde in 0.1M phosphate buffer (PFA, 15-20mL). Brains were dissected and stored for at least two days at 4°C in 4% PFA and then transferred to a 30% sucrose solution for at least 2 days. Brain tissue was cut at 100uM using a Leica CM3050 S cryostat (Leica Microsytems, Weitzlar, Germany) and transferred to an antifreeze, ethylene-glycol solution and stored in a -20°C freezer.

For validation experiments, tissue was transferred to cell strainers in a bath of Tris-Buffered Saline for 10 minutes 6 times. Slices were then transferred to deionized water and mounted onto charged slides. Slides were mounted in VECTASHIELD + DAPI (Vector laboratories, Burlingame, CA, USA) and sealed with a clear nail polish. Images were collected using an upright Axio Imager M2 epifluorescent microscope at a 5x and 20x objective.

Behavior Testing

All behavioral experiments were recorded and analyzed using AnyMaze Behavioral tracking software (Stoelting, Wood Dale, IL).) with the exception of NAc microinfusion studies (**Figure 2.13**) in which Noldus EthoVision XT (Leesburg, VA USA). All animals for all experiments were single-housed, with the exception of the animals used in the grooming assay.

Cohorts:

We used 6 cohorts of animals in unilateral, WT, YFP/ChR2 experiments. With the exception of the bilateral social conditioned place preference (social CPP) assay, all animals were stimulated using unilateral stimulation at 20hz in a 5 seconds on 5 seconds off pattern at 10-13mW. Cohort 1 was sequentially tested in the 3-chamber SI (SI) test, elevated plus maze (EPM), and light-dark box (LD). Cohort 2 was sequentially tested in 3-chamber SI test using 20Hz stimulation, and the EPM. Cohort 3 was first test in the 3-chamber SI test, using 20hz stimulation, the EPM, juvenile reciprocal SI, and social CPP. Cohort 4 was first run through real-time place-preference (RT-PP), and second run through the JZL-184 pretreatment experiment with 3-chamber social interaction test. Cohort 5 was first run through the JZL pretreatment 3-chamber SI test, sequentially followed by the ensure 3-chamber task. Finally, cohort 6 animals were run through juvenile SI, social CPP, and the ensure 3-chamber task. Additionally, we used 2 YFP/NpHR WT cohorts. Both cohorts were first run through the 3-chamber SI task, and subsequently run through the EPM. For our *Shank3B*$^{-/-}$ NpHR studies, we used 2 cohorts. Both cohorts were run through the 3-chamber SI task with light ON and with light OFF following two days later. For all in vivo optogenetic studies, further testing was completed at a minimum of 72 hours following previous stimulation.

For JZL-184 studies, we used three cohorts of *Shank3B*$^{-/-}$ and WT littermate control animals. For the 3-chamber SI studies, animals were only run through the 3-chamber SI task once and sacrificed afterwards. For grooming studies, we used 3 cohorts of animals. In a

counter-balanced design, all animals were given either JZL-184 or VEH, tested, and then retested a minimum of 4-days later.

Finally, for our *Shank3B*$^{-/-}$ microinfusion experiments, we used 2 cohorts of animals. All animals were run through the 3-chamber SI task once and sacrificed for placement validation afterwards.

1) 3-chamber SI test: For in vivo optogenetic experiments, animals were first attached to a fiber optic cable. Mice were placed in the center chamber of a three-chamber arena, a 420mm x 565mm x 358mm box with 185mm x 420mm equal chambers made of 5mm thick, clear Plexiglas with two doors (120mm wide, 5mm thick, 358mm tall) connecting chambers from the middle (Vanderbilt Machine Shop, Nashville TN). Inside the chamber were two empty, wire pencil cups (Organize-it, Rochester Hills, MI) with clear, plastic cups (10oz, 7.5cm diameter 10.4cm tall) with approximately 6oz of water to anchor the cups and prevent the test animal from climbing on the pencil cup. Mice were given a 10-minute habituation period to the apparatus, after which mice were returned to the center and guillotine doors were shut to contain the mouse in the center. When *Shank3B*$^{-/-}$ animals were used, *Shank3B*$^{-/-}$ and WT littermate controls were given a 5-minute habituation while restricted only to the center chamber, as previously described.[143]

Next, a novel, sex-matched and juvenile (4-6 week-old) mouse was placed inside one pencil cup, and the doors were opened to begin the testing phase (5 minutes). *Shank3B*$^{-/-}$ and WT littermate controls were paired with age-matched, sex-matched targets. For in vivo optogenetic studies, stimulation was triggered to be delivered during the testing phase upon the opening of the doors, or prior to the habituation phase as indicated in the **(Figure**

2.2). Time spent in close interaction (5 cm. perimeter around inverted cups) with the mouse-containing and empty cups and time spent in social, empty, and center chambers, were assessed and compared between the test and control groups. Sociability is defined in this assay as having a significant preference for the mouse chamber compared to the empty chamber. All animals were tested in 80-130 lux. Videos were coded post-hoc for time investigating each cup by two, blinded coders using Anvil 6.0 video annotation software.[218] Time investigating represents time in which the test mouse is sniffing or interacting with the cup. Time investigating was averaged between two coders.

2) Ensure 3-Chamber Task: Animals were trained for 3 consecutive days in home cage to drink commercially available Ensure. 50mL conical tubes were filled with 30mL of Ensure, fitted with a sipper lid, and inserted into the home cage. Animals were exposed to the Ensure for 30 minutes. Animals that did not drink within 3 minutes on the third day were excluded from the study. On test day, animals were placed in the 3-chamber apparatus (as described above, in 80-130 lux) containing two inverted, wire, pencil cups with clear plastic cups filled with water anchoring on top. Animals were habituated for 10 minutes and returned to the center chamber and guillotine doors shut. The Ensure sipper was affixed to an inverted pencil cup so the animals could easily reach and drink from the sipper. Next, stimulation was turned on (20Hz 5s on 5s off ~10mW) and animals were permitted to freely explore the apparatus for 5-minutes. Time in each chamber and distance travelled was recorded. Videos were coded post-hoc for time drinking from Ensure sipper bottle and time investigating (sniffing or interacting with) the empty cup by two, blinded coders using Anvil 6.0 video annotation software (5). Time investigating was averaged between two coders.

3) Juvenile Reciprocal Social Interaction Test: Animals were placed in a clean, novel amber cage (32.5cm x 19.3cm x 14cm) concurrently with a novel, sex-matched juvenile mouse (4 weeks old). Animals were permitted to freely interact for 10-minutes. For in vivo optogenetic studies, the test mouse received light stimulation via the HELIOS wireless optogenetic system (Plexon, Dallas TX, USA) for the duration of the test. Videos were recorded during the interaction and analyzed post-hoc by two independent blinded coders for behavioral activity using Anvil 6.0 video annotation research tool software.[218] Videos were analyzed for the amount of time the test mouse was fleeing or withdrawing from target, sniffing target, self-grooming, following target, passively social, open exploring and immobility, as previously described.[219] Animals tested in 80-130 lux.

4) Light-dark box testing: Animals were placed in a three-chamber apparatus (two 30cm x 15cm x 38cm chambers connected by a 10cm x 7.5cm x 38cm hallway) made of opaque, white Plexiglas, fitted with two removable clear plexiglass inserts. (Vanderbilt University Machine Shop, Nashville, TN). The "light" side was lined with white construction paper behind the clear Plexiglas insert and brightly lit (>200lux) and the dark side was lined black construction paper and dimly lit (<20 lux). First, mice were attached to a fiber optic patch cable and placed in the center chamber, enclosed by two guillotine doors, and allowed to habituate for 5 minutes in the dark. Next, light for the light chamber was turned on and the doors to the light and dark sides were simultaneously lifted, triggering optogenetic stimulation and animals were tested for 5-minutes. Time spent in light, entries into the light side, and total distance traveled was quantified.

5) Elevated-plus maze: Animals were connected to a fiber optic patch cable and placed back into their home cage to habituate for 5 minutes in the dark (lux <10). Animals were then placed in the center of an elevated plus maze (San Diego Instruments, San Diego, CA, USA) and allowed to explore open arms (lux ~ 200) and closed arms (lux ~ 50). Stimulation was delivered through the entirety of the test. Time spent in open arms, entries into the open arms, and total distance traveled was quantified.

6) Social Conditioned Place Preference: We used a 3-chamber apparatus (two 30cm x 15cm x 38cm chambers connected by a 10cm x 7.5cm x 38cm hallway). One chamber was lined with dot-patterned construction paper, and the other outside chamber was lined with striped construction paper. Plastic floors with either a stippled pattern or a smooth pattern were inserted into the dots or smooth sides respectively. All chambers were lighted around 100 lux. First, animals were connected to a fiber optic patch cable and placed into the center chamber and allowed to habituate for 5 minutes in the dark, with doors enclosing the mouse in the center. The doors of both a side with a dot pattern and stippled floor and a side with a stripe pattern and smooth floor were simultaneously opened. The animals were given a 10-minute test period in order to exclude any bias preference for either side. Animals that had more than 65 percent bias (time in chamber/ (time in dot chamber plus stripe chamber) *100) for either chamber were excluded. The following day mice were assigned in a counter balanced, unbiased manner in either the dots or stripe chamber with a novel, juvenile sex-matched mouse for 10 minutes. Immediately following the social exposure phase, animals were placed on the opposite chamber alone for 10 minutes. This was repeated the following day with the isolation phase occurring first, and on the third day of testing animals were

exposed to the social stimuli first. Finally, on test day, animals were reconnected to the fiber optic cable and after 5-minute habituation in the center chamber, with doors closed to isolate the animal in the center. Next, in vivo optogenetic stimulation was turned on and the doors to social and empty chambers opened. Animals were able to freely move for 10 minutes. Data are recorded as CPP score (amount of time in social chamber in pretest minus the time in social chamber in post-test), amount of time in social chamber on post-test, and time in unassigned chamber on pre-test day.

7) Real-time place preference: We used the apparatus previously described in Social CPP. All chambers were lighted around 100 lux. First, a fiber optic patch-cable was attached, and animals were placed in the center chamber to habituate for 5 minutes in the dark (<10 lux) with doors enclosing the animal in the center. Next, the doors to the adjacent chambers were opened. When animals entered a randomly assigned chamber, light stimulation was delivered to the implant. Stimulation ended when animals left the stimulation chamber. Animals were tested for 5 minutes. Time in stimulation-assigned side and no stimulation side were quantified along with distance traveled in each chamber.

8) Grooming behavior assay: Animals were placed from home cage into separate clean, novel amber cages separated by dividers for 15 minutes. Videos were recorded during the interaction and analyzed post-hoc by two blinded coders for specified behavioral activity using Anvil 6.0 video annotation research tool software.[218] Coding began after a 5-minute habituation period. Videos were scored for time self-grooming and averaged between coders.

In vivo optogenetic stimulation:

Stimulation patterns were delivered from the PlexBright 4 Channel Optogenetic Controller and controlled by Radiant v2 Software (Plexon, Dallas TX). The optogenetics controller box was attached to the PlexBright Dual LED, rotatable commutator in which a blue (465 nm) or orange (620 nm) LED lights were affixed. PlexBright Optical Patch Cables (.5NA) were then attached to the commutator. Prior to studies, light power emitting from the patch cables was measured using the PlexBright Light Measurement Kit (Plexon, Dallas TX). For studies in which stimulation was triggered as a result of a distinct behavior (ie: RT-PP), we used the AnyMaze AMI2 box (AnyMaze Wood dale IL, USA) to trigger on and off stimulation. In blue-light stimulation studies, animals received 20Hz blue light stimulation (Plexon, Dallas, TX, USA) in a 5 second on 5 second off pattern at 10-13mW. For inhibition studies, animals received a constant orange light (~10mW). One week following implantation surgery, mice were habituated to dummy patch cables in 20- minute bins for 3 consecutive days. On test day, the patch cable was connected to fiber optic implants and animals were habituated for at least 5 minutes before the start of the test.

Microinfusion Studies:

After a 7-day surgery recovery period, animals were habituated for 3 consecutive days in which animals were restrained in increasing amounts (30s, 60s, 120s) and dummy cannula were replaced daily to prevent blocking and habituate animals to restraint. JZL184 was bilaterally infused into the NAc using a bilateral, 4mm cut length internal, infusion

cannula (C235IS-5/SPC, Plastics One, Roanoke VA) at a dose of 0 or 5 μg/μL and at a volume of 0.2μL per hemisphere over 1 min as previously described.[220] One additional minute was allowed for diffusion of drug into the brain tissue. 30 minutes following infusion, animals were placed into the 3-chamber SI task.

Exclusion Criteria:

For all viral and implant studies, animals were excluded based on *a priori* standards. The injection site of all viral injections was identified by the presence of GFP or eYFP fluorescent marker. For all fiber optic and microinfusion implantations, location was determined by implantation track. Animals were excluded from all data sets if the viral expression or implantation was not in the targeted regions. For all in vivo studies the location of the viral expression and implantation is displayed in **(Figure 2.16)**. *Shank3B*$^{-/-}$ and WT controls were genotyped following sacrifice for confirmation. In all data sets, data were analyzed using Grubbs' outlier test (alpha = 0.05) and removed accordingly. If animals were excluded from a behavioral test for outlying data points, all data collected from the animal in the experiment were removed.

Statistics:

Data represented as means +/- SEM, and individual plot points overlaid on a mean bar graph. Statistical analysis conducted using Prism 8 (Graphpad, La Jolla, CA). Statistical tests and parameters are indicated in figure legends. Significance set at alpha=0.05.

CHAPTER 4

DISCUSSION

A novel brain circuit for the regulation of social interaction behavior in an ASD model

In chapter 2 I provided significant data examining the role of the BLA-NAc circuit in social interaction behaviors in both WT and the *Shank3B*$^{-/-}$ mouse model of ASD. Through this work we establish a novel social circuit that bidirectionally regulates social behavior. We show that activation of the circuit decreases social behavior in WT mice, while inhibition of BLA terminals in the NAc significantly increases social behavior in the prominent ASD model, in which social behavior is normally deficient.

We began the investigation of the BLA-NAc circuit in part because of the role that the BLA has in anxiety and anxiety-like behaviors and the findings that social interaction deficits in ASD patient populations are exacerbated by stress and anxiety.[1,202,203] Specifically, I hypothesized that examining the role of the BLA circuitry may reveal a clear neurological mechanism for this compounding effects of anxiety and social interaction behavior. In support of this, previous groups have shown that BLA-Ventral Hippocampus (vHipp) and BLA- mPFC circuits both decrease social interaction behavior when activated and increase anxiety-like behavior in mice.[209,210,221] Contrary to this hypothesis however, we did not find that the BLA-NAc circuit had any effect on anxiety-like behavior as measured in multiple behavioral tests. We therefore concluded

that the BLA-NAc circuit regulates social interaction behavior in a manner that is independent or altered anxiety-like states.

Similarly, we found that the BLA-NAc does not have a role on anxiety-like behavior or repetitive behaviors in the *Shank3B*$^{-/-}$ mouse. At baseline, the *Shank3B*$^{-/-}$ animal shows significant increases in anxiety like behavior and excessive self-grooming.[144,222] However, here we demonstrated that inhibition of the BLA-NAc does not modify anxiety-like behavior in this *Shank3B*$^{-/-}$ mouse model **(Figure A.3)** as measured with the elevated plus maze. Moreover, self-grooming behavior was unaffected during BLA-NAc inhibition (data not shown). Collectively, these findings suggest the BLA-NAc exclusively regulates social interaction behavior, and does not contribute to other maladaptive behaviors in the *Shank3B*$^{-/-}$ animal. Further and more extensive investigation of the neuronal circuitry in the *Shank3B*$^{-/-}$ animal may provide more indication of how social interaction, anxiety, and excessive, repetitive behaviors arise in the *Shank3B*$^{-/-}$ animal model. Perhaps exploration of BLA circuits such as the BLA-vHIPP and the BLA-mPFC, which regulates anxiety and social behavior, in the *Shank3B*$^{-/-}$ animal may expand on the knowledge of how anxiety may drive decreases in social behavior as it is relevant to ASD. Studies of these anxiogenic circuits on excessive, repetitive behaviors such as self-grooming may also elucidate a mechanistic role of the anxiety-driven repetitive behaviors.

In addition to anxiety-like behavior, the BLA-NAc circuit is also widely implicated in reward-seeking behavior. Previous studies have shown that BLA-NAc stimulation is rewarding, in that animals will spend increased time in one side of a chamber to receive stimulation, or nose-poke to receive stimulation of the BLA-NAc

circuit.[122,196] It is therefore possible that the induced stimulation used in our experiments occludes social reward seeking. I therefore tested the animals in the 3-chamber social interaction task but replaced the social target with a palatable non-social reward, Ensure. However, we did not see any changes to non-social reward seeking in our animals during BLA-NAc stimulation in ChR2 compared to YFP-expressing animals. Interestingly and contrary to our studies, a recent study has shown that activation of the rostral BLA projections to the ventral lateral NAc circuit suppresses sucrose reward seeking, and that this circuit is active after sleep deprivation.[223] Our studies are limited to activation of the ventral medial NAc. Future studies focused on incorporating anatomically distinct regions of both the BLA and NAc need to be completed in order to explain the divergent results. Also, it will be interesting to investigate the role of the rostral BLA- ventral lateral NAc in social interaction and compare to our findings. Of note, sleep deprivation is also a common comorbidity in ASD[27,224,225] and further exploration of this circuit in reward seeking, sleep deprivation, and social interaction would improve our understanding of convergent neuronal networks in ASD across a multitude of behaviors.

One possible explanation for how BLA-NAc activation results in the social avoidance may relate to underlying BLA-NAc sub-circuits. Previous studies show that activation of D2-MSNs directly in the NAc, and *in vivo* optogenetic activation of the CCK-expressing BLA neurons that project to NAc D2-MSNs, significantly depresses time in the social interaction zones after social defeat stress.[122] In contrast, the reinforcing effects of BLA-NAc stimulation can be blocked by a D1 receptor antagonist,[196]

indicating BLA-NAc D1-MSN activation could underlie the rewarding effects of BLA-NAc circuit activation. Context-dependent differential engagement of these distinct subcircuits could explain parallel roles in reward and social avoidance observed after BLA-NAc circuit manipulations. Future studies directly examining and manipulating BLA-NAc subcircuit activity in social and non-social contexts may help clarify the neural mechanisms underlying BLA-NAc circuit effects on sociability and reward. Additionally, while previous studies have found distinctive roles of D1 and D2 circuitries in the dorsal striatum of *Shank3B*$^{-/-}$ animals, there are few investigations of the D1 and D2-MSN activities on maladaptive behavior in both the *Shank3B*$^{-/-}$ animal model or other ASD models. For instance, given our work and previous studies, perhaps the CCK subcircuits are overactive and cause heightened stress response and decreased social behavior in the *Shank3B*$^{-/-}$ animals. Future studies examining how and when these subcircuits are active, and how different projections onto these neuronal subtypes in ASD models would greatly improve our functional understanding of the role of D1 and D2 MSNs in regulating reward and social behavior in ASD.

While we show that activation of the BLA-NAc circuit is sufficient to reduce SI behavior, we also showed that activity is not necessary for the physiological expression of social behavior, as optogenetic inhibition of the circuit did not alter sociability under basal conditions. This finding differentiates the BLA-NAc circuit from other BLA circuits, such as the BLA-vHPC, which bi-directionally alter social behavior.[210] Although our data suggest BLA-NAc activity is not physiologically recruited to regulate sociability, it is possible that BLA-NAc circuit inhibition could increase or normalize sociability in mice with pre-existing

social impairment. Indeed, we found that inhibition of the BLA-NAc circuit robustly increased social behavior in the *Shank3B*$^{-/-}$ mouse, a model of ASD which has a well-established social deficit.[143,144,208] Consistent with our data, clinical reports have demonstrated that the amygdala is hyper-functional in ASD patients during anticipation of social cues, and that the NAc of ASD patients has increased functional connectivity relative to typically developing peers.[193,194] Continued research into the functional connectivity of the BLA-NAc circuit in ASD patients and additional preclinical mouse models of ASD is needed to fully understand the role the BLA-NAc circuit in ASD-associated social deficits.

Endocannabinoid augmentation as a potential thereaputic stragegy for ASD

First, given that BLA-NAc circuit activation reduces sociability, we sought to explore molecular mechanisms that reduce BLA-NAc circuit activity in an attempt to reveal therapeutic approaches to increase social behavior. Previous work has demonstrated that activation of the CB1 receptor by eCBs, including 2-AG, dampens glutamatergic activity[204] and has a functional role in social behavior via modulation of both NAc signaling and endogenous BLA-NAc activity.[68,76,122,211] Therefore, we investigated whether 2-AG signaling modulated BLA-NAc glutamatergic transmission. Indeed, we show that the CB1 receptor activation reduced glutamate release at BLA-NAc synapses and that enhancement of 2-AG signaling via MAGL inhibition by JZL184 reduced aEPSC frequency at BLA-NAc D1 and D2-MSNs. It is noteworthy that these results are in contrast to a recent study indicating cannabinoid signaling selectively modulates BLA-NAc D2-MSN synapses.[122] Consistent with the ability of CB1 activation and 2-AG augmentation to reduce optogenetically-elicited

glutamatergic signaling efficacy at BLA-NAc synapses ex vivo, we showed that systemic JZL184 administration prevented the decreased sociability elicited by BLA-NAc optogenetic stimulation in vivo. Our data suggest pharmacological 2-AG augmentation could serve as a therapeutic approach to increase sociability under pathological conditions associated with amygdala-NAc circuit hyperactivity.

Next we sought to test eCB regulation in a mouse model in which social interaction behavior is disrupted. Because we show that inhibition of the BLA-NAc circuit significantly increases social behavior in the *Shank3B*$^{-/-}$ mouse model, and that BLA-NAc overactivation-induced social deficits are restored by JZL184 we hypothesized that increased 2-AG in the NAc would restore social interaction behavior in the *Shank3B*$^{-/-}$ mouse. Indeed, we show that both systemic JZL184 and JZL184 directly administered into the NAc significantly increases social interaction behavior in this mouse model. We also showed that 2-AG augmentation via systemic JZL184 administration reverses both social and restricted, repetitive behavior deficits in *Shank3B*$^{-/-}$ mice. Taken together, these data add to the growing body of evidence suggesting pharmacological eCB augmentation could serve as a therapeutic approach for treating ASD and ASD-associated syndromes.[68,177,181,182,186] Currently there are no FDA-approved pharmacological treatments for ASD, and current medications to improve social deficits are limited. Given the recent advancement of MAGL inhibitors to early clinical trials,[212,213] our data could support examination of MAGL inhibitors for the treatment of social deficits in ASD, and other disorders characterized by social domain deficits.

Although we demonstrate that JZL184 was sufficient to increase social interaction behavior in *Shank3B*$^{-/-}$ animals, we had yet to show that JZL184 was indeed sufficient to increase 2-AG in the CNS of this model. Therefore, we performed several mass spectrometry experiments to characterize eCB levels after vehicle or JZL184 treatment in both WT and *Shank3B*$^{-/-}$ animals (**Figure A.2**). Indeed, we found that 2-AG levels were increased in the BLA, NAc and DS following JZL184 administration but surprisingly, we did not find that 2-AG levels were signficantly increased in the PFC. These results may be due to a loss of function of either DAGL, in which there is no synthesis of 2-AG in the PFC, or MAGL in which case there would not be a target for JZL184. The PFC is hypoactive in *Shank3B*$^{-/-}$ animals, and it is possible there are altered mechanics in the PFC that prevent release of 2-AG in order to prevent further dampening of glutamatergic activity. Although JZL184 appears to be non functioning in the PFC of this model, further supressing activity in the PFC by other eCB-agumentation approaches may be detrimental to behavior or function in this mouse model, and JZL184 may be a way to prevent these effects. Further investigation into why JZL184 is ineffectictive at increasing eCB levels would be valuble information to understand the role of eCBs in ASD.

Interestingly, our mass spectrometry investigations also reveal that at baseline, *Shank3B*$^{-/-}$ animals have highter 2-AG, AEA, and OG levels in the NAc. **(Figure A.2)** These findings are unexpected because increased eCBs would suggest a dampening of glutamatergic activity and yet our findgings show that inhibiting the glutamatergic BLA-NAc circuit and increasing 2-AG in the NAc increases social interaction behavior in the *Shank3B*$^{-/-}$ animal. Nevertheless, these data are supported by our electrophysiological

findings that there is an increased paired-pulse ratio (PPR) in the BLA-NAc circuit, and increased feedforward PPR in the *Shank3B*$^{-/-}$ animal relative to WT controls; suggesting there is decreased release probability onto glutamatergic and feedforward gabaergic circuitries in the NAc from the BLA **(Figure A.4)**. Taken together, these data suggest that the heightened eCBs do indeed dampen presynaptic release probability in the NAc in the *Shank3B*$^{-/-}$ animal compared to WT controls. Nevertheless, there are several hypotheses that could address these descrepancies. First, it is possible that in *Shank3B*$^{-/-}$ animals, heightened eCBs are a compensatory mechanism to counter hightened excitatory signaling during behaviors or stimuli that we are not captuing with our analyses. Second, there may be excessive glutamatergic activation from a different glutamatergic pathway, aside from the BLA, which is eliciting excessive 2-AG release at baseline. Our work is limited to the input from the BLA to the NAc, and perhaps a more thorough investigation of glutamatergic inputs into the NAc may reveal an explaination for these data. Indeed, further understanding the 2-AG mechanism of action, and the social circuits it regulates, will improve the understanding of whether 2-AG augmentation is an effective thereapy for ASD.

Elucidating the role of endocannabinoid regulation of the BLA-NAc circuit on social behavior

Because we found SI deficits were normalized by the BLA-NAc circuit inhibition in *Shank3B*$^{-/-}$ mice, we also analyzed the BLA-NAc circuit physiology in *Shank3B*$^{-/-}$ animals. Unexpectedly, we found no measurable differences in BLA input into the NAc in *Shank3B*$^{-}$

$^{-/-}$ mice compared to WT animals as oEPSC and feed-forward IPSC amplitudes were not different between genotypes; however, JZL184 was able to significantly reduce FF IPSC amplitude in *Shank3B*$^{-/-}$, but not WT, mice. This data seemingly contrasts with our finding showing inhibition of the BLA-NAc restores sociability behavior in *Shank3B*$^{-/-}$ animals as glutamatergic drive onto NAc neurons is not altered. However, it is possible that inhibition of GABAergic interneurons in the NAc of *Shank3B*$^{-/-}$ animals, by either NpHR-induced reductions in FF-inhibition or JZL184 application, is sufficient to restore social function. One possible way that JZL184 could improve SI is via inhibition of glutamatergic BLA synapses and GABAergic fast-spiking interneurons (FSIs) onto MSNs, both of which are regulated by CB1 receptors at the presynaptic level.[111,214] Increases in 2-AG may therefore inhibit activation of NAc-FSIs in response to BLA stimulation as well as inhibit GABAergic release from FSIs. Because FSIs in the NAc have been shown to gate impulsive behavior in mice,[215] we hypothesize that JZL184 inhibition of FSIs signaling could promote social interaction via increasing directed social behavior output in a similar manner. Additionally, reductions in FSI inhibition of NAc MSNs could allow for restoration of proper signaling from other NAc inputs such as the prefrontal cortex, which is be dysregulated in *Shank3B*$^{-/-}$ mice. Further investigation into the role of FSIs, GABAergic circuitry, and additional glutamatergic inputs to the NAc in the *Shank3B*$^{-/-}$ model, as they relate to social behavior, may uncover additional synaptic mechanism contributing to social deficits in ASD. In clinical research, there have been recent advances of GABA-mediated therapies for ASD, and perhaps understanding how eCBs regulate GABA signaling may solidify an eCB augmentation approach to treatment. Specifically,

a recent clinical study showed patients with ASD that are given with Riluzole, a $GABA_A$ positive allosteric modulator, show functional connectivity patterns that are similar to typically developing peers.[241] Moreover, a clinical trial is now recruiting for the testing of $GABA_A$ PAMs in ASD functional imaging outcomes.[242] Given the role we have established here of the potential of eCBs to regulate both GABA and glutamatergic activity in an ASD model, it is possible eCB modulation may also restore functional connectivity patterns in ASD patients.

Limitations

One major caveat to this study is the social isolation stress that each experimental animal was subjected to. Due to experimental and methodological limitations, all animals were single housed for a minimum of 7 days prior to any behavioral analysis or *in vivo* optogenetic manipulation. Previous studies have shown that after chronic social defeat stress, activation of the BLA-NAc decreases social interaction behavior.[122] Interestingly our data corroborate this finding, when the social isolation stress is also taken into account. However our data also show that YFP injected animals do not have a social interaction deficit at baseline indicating that the social isolation stress is not sufficient to decrease social interaction behavior in WT mice. Nevertheless, how social isolation stress may influence our findings on social behavior in both WT and *Shank3B*$^{-/-}$ animals has yet to be examined. It is therefore possible that the social interaction rescue of the BLA-NAc inactivation in *Shank3B*$^{-/-}$ animals may be influenced by stress. Future studies replicating our findings in group-housed animals are pertinent to fully understanding the role of the

BLA-NAc on social interaction behavior in naïve animals. These findings may also be necessary to understand the role of the BLA-NAc in cases of the many comorbidities of ASD, such as increased stress, and understanding how this circuit changes social behavior under chronic stress may reveal important details of the neurocircuitry of ASD.

An additional caveat to these experiments are the limited approaches for manipulating the BLA-NAc circuit. In Chapter 2 I rely solely on activating the BLA-NAc circuit using *in vivo* optogenetics. However, I also used Gq-DREADD to activate the circuit, and did not find any changes to social interaction behavior across multiple doses (**Figure A.1)**. One possible explanation, is that Gq-DREADDs elicit 2-AG release which counters any increased activity. This explanation may be indeed true, given that pretreatment of JZL184 blocks social interaction deficits caused by *in vivo* optogenetic activation. Nevertheless, exploring how GPCR activity versus channel-mediated activation differs in the circuit and in ASD would conclusively determine why these two approaches lead to different results.

As previously mentioned, there are several important brain regions and neuronal circuits in social interaction behavior as they relate to ASD, and our investigation is limited to one of these circuits. Interestingly, a recent study has shown that the anterior cingulate cortex (ACC) is hypoactive in *Shank3B*$^{-/-}$ mice. [208] It is worth considering how our findings outlined in chapter 2 may integrate with this recent study. On one hand, we proposed in our working model that the BLA regulates feed forward (FF) inhibiton of the NAc, and that inhibiton of the BLA-NAc circuit relieves excessive inhibition to allow for increased MSN output from the NAc. Further exploration of the GABAergic properties of

the PFC may reveal a smilar social circuitry mechanism in the *Shank3B*$^{-/-}$ animal. For instance, it is possible the excessive inhibitory current in the ACC and PFC may decrease overall neuronal activity and ultimately cause decreased social interaction behavior. Taken together, a multi-nodal exploration of social interaction behavior may be the most reliable way for understanding how neural circuitrs are interacting to regulate the social deficit in ASD mouse models. Although we show that inhibiton of the BLA-NAc circuit is sufficient to increase social interaction in an ASD model, it is not yet known how this circuit influences entire social brain networks. These future studies are critical for an in-depth understanding of social circuity in Shankopathies and ASD.

In addition, more expansive exploration the role of additional eCBs in the *Shank3B*$^{-/-}$ may reveal more novel therapeutic targets for ASD treatment. Particularly investigations have established a role of AEA in social behavior. In fact, there is an exciting study showing a link between AEA activity being released with oxytocin receptor activation in the NAc, which collectively drive social motivation behavior.[72] Oxytocin has been heavily investigated in the ASD field as a potential treatment for relief from social imapirment, but many of these studies have not yet advanced from clinical trials, and many trials have been discontinued.[226,228–232] Further understanding of the downstream signalling of oxytocin may therefore provide insight into a successful treatment for social beavior of ASD. Additionally, there is very limited investigation into several of the other lipid messengers in ASD, in spite of lipids regulating many ASD and ASD-associated symptoms and comborbidieis. First, PEA has been shown to have anti-inflammation and nocieptive effects and patients with ASD often reporter higher levels of pain and increased

inflammation.[233–235] Our mass spec data reveal there may be dysregulation of PEA in the PFC of *Shank3B*$^{-/-}$ animals, as vehicle-treated *Shank3B*$^{-/-}$ animals have levels of PEA compared to WT controls **(Figure A.2)**. Additionally, OEA has been shown to regulate food intake; ASD patients often exhibit gastrointestinal complications, including food consumption,[130,235–240] indicating a possible role for OEA regulation to aid in the treatment of these beaviors. Finally, OA may be a novel therapeutic target for the treatment of sleep behaviors in ASD. OA regulates sleep and sleep induction. ASD patients exhibit complications, sometimes extremely severe, in sleep behaviors and there may be a role of OA to treat these sleep abnormalities.[27,224,225] Taken together, future examinations of lipid messengers beyond the eCB 2-AG may reveal critical therapeutic targets that improve quality of life and decrease core behavioral deficits and commmon comorbidities in ASD.

One of the major limitations of this work is that we have only assessed the role of 2-AG in one genetic model of ASD. As previously mentioned, eCB enhancement has been studied in a multitude of ASD models. Further exploring the role of 2-AG enhancement across common genetic models would help to determine the efficacy of 2-AG enhancement as it pertains to the heterogeneous ASD population and not just patients with SHANK3 mutations.

Because eCBs have shown to have a precient role in regulating core behaviors of ASD in the CNS, studying eCBs in the periphery is crucial to understand their role in the disorder and the efficacy of their treatment *in vivo*. Studies have shown patients with ASD have signficantly decreased levels of peripheral eCBs and other lipid messengers compared to typically developing peers. Specifically, blood serum collected from patients

with ASD revealed low levles of AEA, OEA, and PEA but not 2-AG,[82] which contrasts our mass spectrometry findings in the CNS. Possibly there are different mechanicsms regulating eCBs of the peripherial systems compared to the CNS. It is not yet undersrood how eCBs in the periphery regulate behavior and how periphery eCBs contribute to ASD and ASD-associated symptoms. Additionally, how treatment of ASD by eCB modulating therapies, such as JZL184 suggested here, regulate peripherial eCBs is not yet known. These investigations are vital to understanding eCB regulation as a potential therapeutic target for ASD.

Conclusions

In summary, we show that BLA-NAc circuit activation reduces sociability and is highly regulated by 2-AG-mediated eCB signaling. We further show that systemic and NAc-specific 2-AG augmentation and optogenetic BLA-NAc circuit inhibition normalize social deficits in the *Shank3B*$^{-/-}$ model of ASD. We hypothesize that 2-AG augmentation reduces social deficits in *Shank3B*$^{-/-}$ mice via normalization of hyperactive GABAergic and glutamatergic signaling in the NAc and via reductions in BLA-elicited FF-inhibition onto NAc MSNs. Currently there are no FDA-approved medications for the treatment of ASD. Investigations into novel therapeutic targets are urgently needed to improve the quality of life in patients with ASD. The investigations presented in this work add a new therapeutic target of study for future drug development in ASD.

APPENDIX

Gq DREADD stimulation of the BLA-NAc does not affect social interaction behavior

In Chapter 2, I demonstrated that *in vivo* optogenetic activation of the BLA-NAc circuit significantly reduces social interaction behavior and increases social avoidance in WT mice **(Figure 2.1, 2.24**. I therefore wanted to test the hypothesis that a secondary approach to activation of the BLA-NAc circuit would also decrease social interaction behavior. I used a retrograde CRE virus delivered bilaterally to the NAc and a cre-activated Gq-DREADD bilaterally delivered to the BLA to localize Gq-DREADD to the BLA-NAc. After recovery, I tested WT animals on two separate doses of CNO, either 2mg/kg or 5mg/kg and assessed social behavior in the 3-chamber social interaction task. I found that neither 2mg/kg **(Figure A1 A-C)** nor 5mg/kg **(Figure A1 D-F)** altered social interaction behavior differently from vehicle (VEH) treatment. Interestingly, we do not see an effect of activation of BLA-NAc circuitry using this secondary approach. This may be the result of changed mechanics of activation, due to Gq activation being mediated through a signaling cascade leading to increased calcium release. These dynamics may not be sufficient to cause the same signaling that causes decreased social behavior. Additionally, activation of Gq also causes the release of DAG, which may lead to increased 2-AG release which may counteract the activation of the BLA-NAc. As I showed in chapter 2, increasing 2-AG levels blocks the effect of *in vivo* optogenetic activation of BLA-NAc-mediated social deficits.

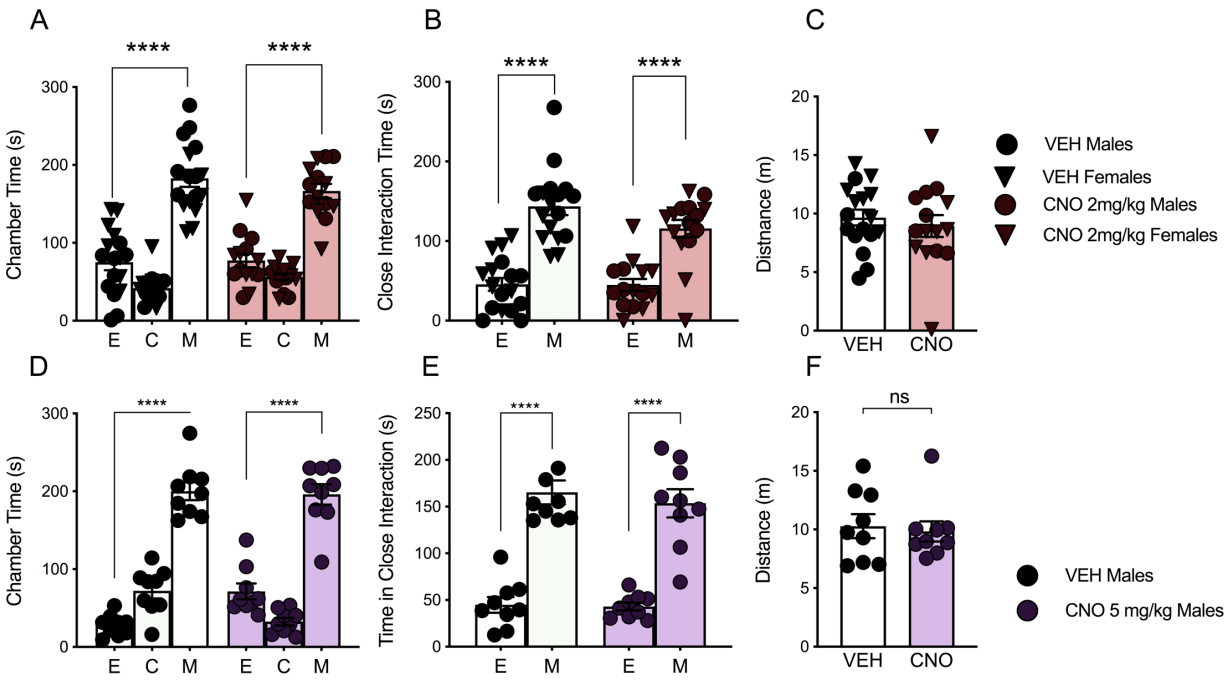

Figure A.1 Gq DREADD BLA- NAc Activation Does Not Reduce Social Interaction Behavior A) After viral placement of Gq DREADD selectively in the BLA-NAc pathway in WT animals, mice were treated VEH or various doses of CNO. Social interaction behavior was assessed by 3-chamber social interaction task. **A)** WT animals pretreated with both VEH and 2mg/kg CNO have a significant preference for the mouse chamber. **B)** Close interaction time and **C)** distance traveled are unaffected by 2mg/kg CNO drug treatment. **D)** Animals treated with VEH and 5mg/kg CNO have a preference for the mouse chamber, **E)** close interaction to the target mouse. **F)** Distance travelled was unaffected by drug treatment. Data analyzed via unpaired, two-tailed t-test (C, F) or Two-Way ANOVA with Sidak's multiple comparisons test (A-B, D-E). E= Empty, C= Center, M= Mouse

Mass spectrometry analysis reveals maladaptive changes in endocannabinoid levels in Shank3B$^{-/-}$ animals

Here, I have demonstrated that increasing 2-AG by JZL184, pharmacological treatment restored social interaction and decreased repetitive grooming activity in *Shank3B*$^{-/-}$ animals. We then wanted to demonstrate that JZL184 sufficiently increased 2-AG in the NAc, as well as other pertinent brain regions to social behavior. We also wanted to explore more of the underlying eCB mechanisms in the *Shank3B*$^{-/-}$ animals that may lead to dysregulated social and repetitive behaviors. Therefore, we ran mass spectrometry analysis to analyze levels of major eCBs including 2-AG, OG, AA, AEA, OEA, and PEA in the NAc, BLA, Dorsal striatum, and PFC **(Figure A.2)**. Interestingly, we found elevations of 2-AG and AEA in the NAc of *Shank3B*$^{-/-}$ mice compared to WT controls. Finally, we found that JZL184 was sufficient to increase 2-AG in the NAc, BLA, and dorsal striatum indicating no major loss of function of 2-AG signaling in these regions. However, in the PFC, we found that there was a significant interaction between drug and genotype effects, indicating there may be a change in all eCB machinery in this brain region.

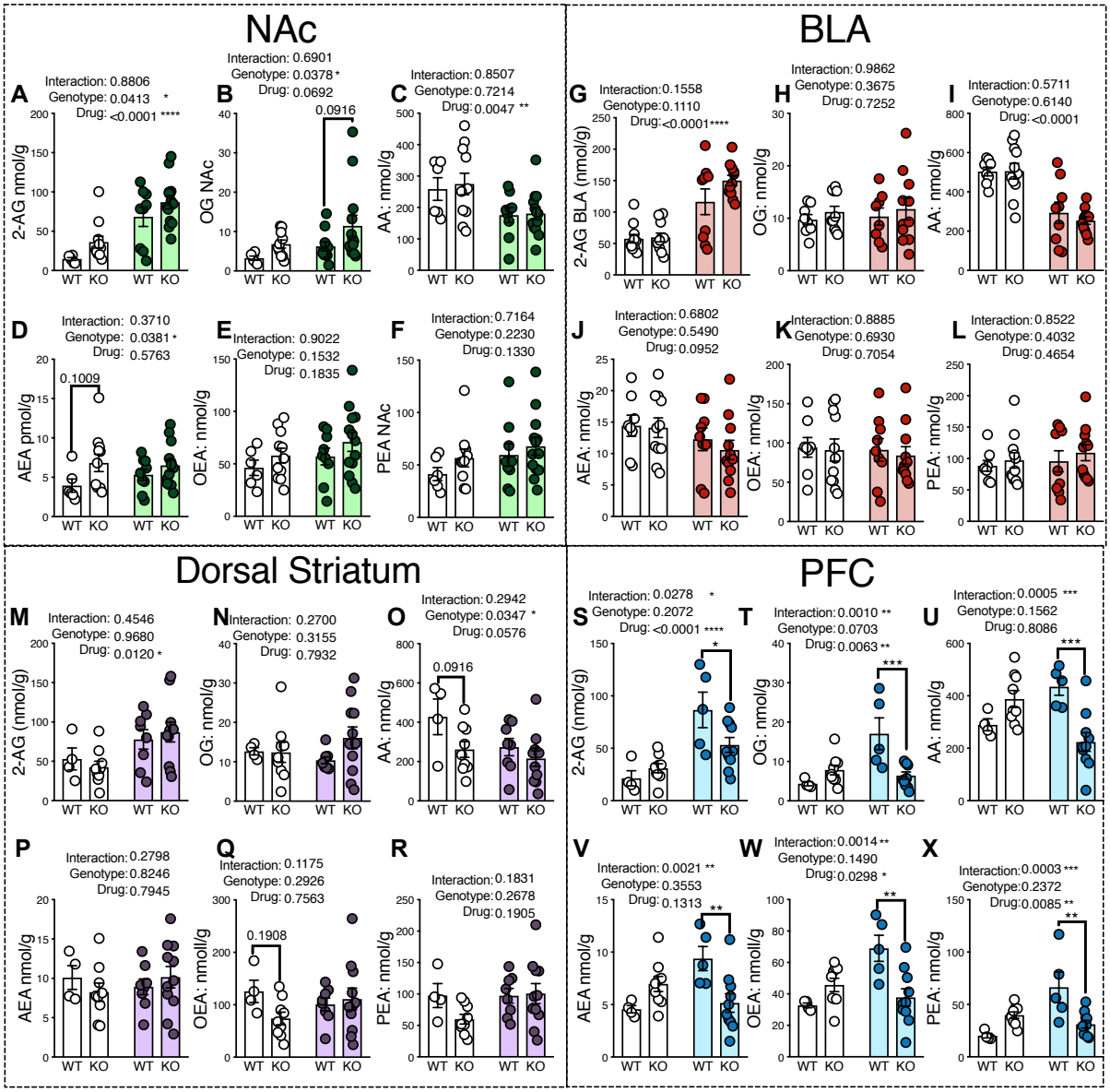

Figure A.2 Mass spectrometry of brain regions regulating social interaction reveal differential effects of JZL184 on *Shank3B*$^{-/-}$ animals compared to WT controls. A) There is significantly elevated 2-AG in the NAc of *Shank3B*$^{-/-}$ (KO) animals compared to WT controls, and JZL184 significantly increases 2-AG in both groups **B)** OG levels are heightened in KO animals. **C)** In both KO and WT animals, JZL184 reduces AA levels. **D)** There is a significant increase in AEA of the NAc of *Shank3B*$^{-/-}$ animals. There is no effect of JZL184 or genotype on neither **E)** OEA nor **F)** PEA levels. In the BLA, **G)** 2-AG levels are elevated after JZL184 treatment in WT and KO groups. **H)** JZL184 and genotype do not effect OG in the BLA. **I)** AA levels are significantly reduced in the BLA after JZL184 treatment in WT and KO groups. Neither **J)** AEA, **K)** OEA, **L)** nor PEA levels are affected by JZL184 or genotype in the BLA. **M)** Dorsal striatal 2-AG levels are heighted after JZL184 treatment in both WT and KO animals. **N)** OG levels are unaffected by genotype or drug treamtment in the dorsal striatum. **O)** AA levels are heightened in the dorsal striatum of KO mice, indicated by a significant effect of genotype. **P)** AEA, **Q)** OEA, and **R)** PEA are unaffected by genotype or drug treamtment in the dorsal striatum. **S)** There is a significant Interaction of genotype and drug in the PFC on 2-AG, **T)** OG, **U)** AA, **V)** AEA, **W)** OEA, and **X)** PEA, indicating a blunted reaction of endocannabinoids to JZL184 treatment in the PFC in KO animals. Data analyzed with a Two-Way ANOVA with Sidak's multiple comparisons test.

Silencing of the BLA-NAc circuit does not alter anxiety-like behavior in Shank3B$^{-/-}$ animals

In WT animals we found that the BLA-NAc *in vivo* optogenetic silencing has no effect on neither anxiety-like behavior nor social interaction behavior. However in the *Shank3B*$^{-/-}$ animals, inhibition of the circuit restores social interaction behavior from a baseline deficit. Previously, groups have shown that anxiety-levels are heightened in *Shank3B*$^{-/+}$ animals.[143,144] Therefore, I tested the hypothesis that BLA-NAc inhibition may restore anxiety-like behavior in *Shank3B*$^{-/-}$ animals. Interestingly, I did not find any effect of inhibition on behavioral output in the elevated plus maze **(Figure A.3)**. This result is anticipated given the results shown previously in chapter 2, indicating that activation of the BLA-NAc circuit in WT mice does not increase anxiety-like behavior **(Figure 2.6)**. It is noteworthy that these new data show that the social interaction deficit is corrected by a mechanism that does not affect anxiety like behavior in the *Shank3B*$^{-/-}$. These data further highlight that social interaction and anxiety-like behavior are regulated by different circuitries, even as it relates to ASD. Further research on the role of the anxiety circuitries as they regulate social interaction circuitries may reveal a neural network that further examines the heightened anxiety behavior in ASD patients and ASD mouse models.

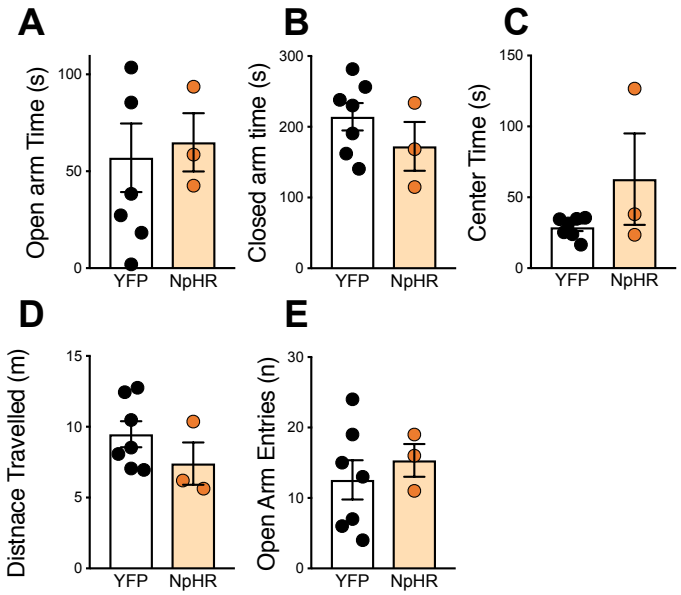

Figure A.3 Optogenetic silencing of the BLA-NAc in *Shank3B*$^{-/-}$ does not alter anxiety-like behavior in the elevated plus maze. A) Open arm time, **B)** closed arm time **C)** center time, **D)** distance travelled, and **E)** open arm entries are unaffected by NpHR expression (shown in orange) compared to YFP (shown in white) in *Shank3B*$^{-/-}$ animals. Data analyzed by two-tailed t-tests.

Shank3B$^{-/-}$ animals have decreased release probability in the BLA-NAc compared to WT controls

Thus far I have shown evidence that the BLA-NAc circuit is differentially regulated in the *Shank3B$^{-/-}$* animals compared to WT **(Figure 2.14).** We therefore wanted to expand upon our findings and investigate neurotransmitter release properties. Therefore, we analyzed the paired pulse ratio (PPR) of the BLA-NAc in WT and *Shank3B$^{-/-}$* animals with and without JZL184. We found that there is a significant effect of genotype on oPPR in the BLA-NAc circuit, with heightened levels in KO animals. Interestingly, we did not find an effect on oPPR with JZL184. Similarly, we found a significant effect on inhibitory PPR, and similarly no effect resulting from JZL184 on FF PPR.

These results appear to stand in stark contrast with our previous data outlined previously **(Figure 2.14)** in which we show increased sIPSC and sEPSC frequency in the NAc, and unchanged BLA-NAc oIPSC and EPSC in the *Shank3B$^{-/-}$* animals compared to WT littermates. Further information on the characteristics of this circuit would consolidate these two findings. For instance, it would be worth looking at the asynchronous firing properties of the BLA-NAc circuit to understand the BLA-NAc circuit properties in the *Shank3B$^{-/-}$* mouse model. Furthermore it would be interesting to study the *in vivo* mechanistic of the BLA-NAc in *Shank3B$^{-/-}$* animals. *In vivo* recording techniques, such as calcium imaging in the BLA-NAc circuit during social behavior would reveal the true properties of this circuit as they pertain to social interaction behavior.

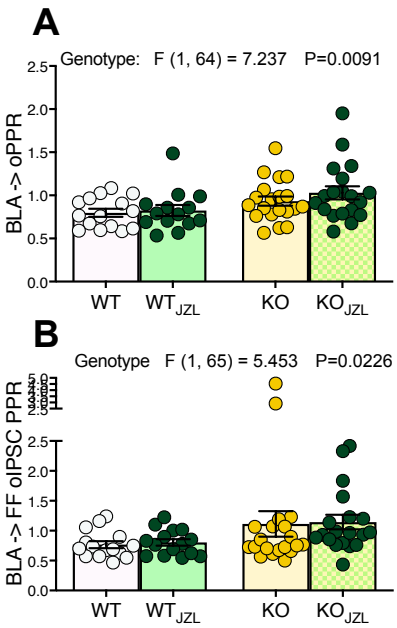

Figure A.4 Optical paired pulse ratio is significantly heightened in the BLA-NAc circuit of *Shank3B*$^{-/-}$ animals compared to WT animals A) In the BLA-NAc, there is a significant effect of genotype, while JZL184 had no effect on either WT or *Shank3B*$^{-/-}$ KO animals on both glutamatergic oPPR and **B)** GABAergic feedforward oIPSC PPR.

REFERENCES

1. American Psychiatric Association. *Diagnostic and Statistical Manual of Mental Disorders*. *Arlington* (2013). doi:10.1176/appi.books.9780890425596.744053
2. Qualls, L. R. & Corbett, B. A. Examining the relationship between social communication on the ADOS and real-world reciprocal social communication in children with ASD. *Res. Autism Spectr. Disord.* **33**, 1–9 (2017).
3. McCrimmon, A. & Rostad, K. Test Review: Autism Diagnostic Observation Schedule, Second Edition (ADOS-2) Manual (Part II): Toddler Module. *J. Psychoeduc. Assess.* (2014). doi:10.1177/0734282913490916
4. Mood, D. & Shield, A. Clinical Use of the autism diagnostic observation schedule-second edition with children who are deaf. *Semin. Speech Lang.* (2014). doi:10.1055/s-0034-1389101
5. Schopler, E., Reichler, R. J., DeVellis, R. F. & Daly, K. Toward objective classification of childhood autism: Childhood Autism Rating Scale (CARS). *J. Autism Dev. Disord.* (1980). doi:10.1007/BF02408436
6. Lord, C., Rutter, M. & Le Couteur, A. Autism Diagnostic Interview-Revised: A revised version of a diagnostic interview for caregivers of individuals with possible pervasive developmental disorders. *J. Autism Dev. Disord.* (1994). doi:10.1007/BF02172145
7. L., Z. *et al.* Studying the emergence of autism spectrum disorders in high-risk infants: Methodological and practical issues. *Journal of Autism and Developmental Disorders* (2007).

8. Yoder, P., Stone, W. L., Walden, T. & Malesa, E. Predicting social impairment and ASD diagnosis in younger siblings of children with autism spectrum disorder. *J. Autism Dev. Disord.* (2009). doi:10.1007/s10803-009-0753-0

9. Rogers, S. J. What are infant siblings teaching us about Autism in infancy? *Autism Research* (2009). doi:10.1002/aur.81

10. W.A., G., K.L., T., K., O. & M.A., S. Use of home videotapes to confirm parental reports of regression in autism. *J. Autism Dev. Disord.* (2008). doi:10.1007/s10803-007-0498-6 LK - http://vu.on.worldcat.org/atoztitles/link?sid=EMBASE&issn=01623257&id=doi:10.1007%2Fs10803-007-0498-6&atitle=Use+of+home+videotapes+to+confirm+parental+reports+of+regression+in+autism&stitle=J.+Autism+Dev.+Disord.&title=Journal+of+Autism+and+Developmental+Disorders&volume=38&issue=6&spage=1136&epage=1146&aulast=Goldberg&aufirst=Wendy+A.&auinit=W.A.&aufull=Goldberg+W.A.&coden=JADDD&isbn=&pages=1136-1146&date=2008&auinit1=W&auinitm=A

11. Luyster, R. *et al.* Early regression in social communication in autism spectrum disorders: A CPEA study. *Dev. Neuropsychol.* (2005). doi:10.1207/s15326942dn2703_2

12. Chawarska, K., Macari, S. & Shic, F. Decreased spontaneous attention to social scenes in 6-month-old infants later diagnosed with autism spectrum disorders. *Biol. Psychiatry* (2013). doi:10.1016/j.biopsych.2012.11.022

13. Elsabbagh, M. *et al.* Infant neural sensitivity to dynamic eye gaze is associated with

later emerging autism. *Curr. Biol.* (2012). doi:10.1016/j.cub.2011.12.056

14. McPartland, J. & Volkmar, F. R. Chapter 23 – Autism and related disorders. in *Handbook of Clinical Neurology* (2012). doi:10.1016/B978-0-444-52002-9.00023-1
15. Jones, E. J. H., Gliga, T., Bedford, R., Charman, T. & Johnson, M. H. Developmental pathways to autism: A review of prospective studies of infants at risk. *Neuroscience and Biobehavioral Reviews* (2014). doi:10.1016/j.neubiorev.2013.12.001
16. Wiśniowiecka-Kowalnik, B. & Nowakowska, B. A. Genetics and epigenetics of autism spectrum disorder—current evidence in the field. *Journal of Applied Genetics* (2019). doi:10.1007/s13353-018-00480-w
17. Rosenberg, R. E. *et al.* Characteristics and concordance of autism spectrum disorders among 277 twin pairs. *Arch. Pediatr. Adolesc. Med.* (2009). doi:10.1001/archpediatrics.2009.98
18. Hallmayer, J. *et al.* Genetic heritability and shared environmental factors among twin pairs with autism. *Arch. Gen. Psychiatry* (2011). doi:10.1001/archgenpsychiatry.2011.76
19. Ronald, A. & Hoekstra, R. Progress in understanding the causes of autism spectrum disorders and autistic traits: Twin studies from 1977 to the present day. in *Behavior Genetics of Psychopathology* (2014). doi:10.1007/978-1-4614-9509-3_2
20. Elsabbagh, M. *et al.* Global Prevalence of Autism and Other Pervasive Developmental Disorders. *Autism Res.* (2012). doi:10.1002/aur.239
21. Abrahams, B. S. & Geschwind, D. H. Advances in autism genetics: On the threshold of a new neurobiology. *Nature Reviews Genetics* **9**, 341–355 (2008).

22. Geschwind, D. H. Genetics of Autism Spectrum Disorders Autism genetics: a decade of progress. *Trends Cogn. Sci.* (2011). doi:10.1016/j.tics.2011.07.003

23. Farmer, C., Thurm, A. & Grant, P. Pharmacotherapy for the core symptoms in autistic disorder: Current status of the research. *Drugs* (2013). doi:10.1007/s40265-013-0021-7

24. Green, R. M., Travers, A. M., Howe, Y. & McDougle, C. J. Women and Autism Spectrum Disorder: Diagnosis and Implications for Treatment of Adolescents and Adults. *Current Psychiatry Reports* (2019). doi:10.1007/s11920-019-1006-3

25. Belpaeme, T., Kennedy, J., Ramachandran, A., Scassellati, B. & Tanaka, F. Social robots for education: A review. *Sci. Robot.* (2018). doi:10.1126/scirobotics.aat5954

26. Corbett, B. A., Blain, S. D., Ioannou, S. & Balser, M. Changes in anxiety following a randomized control trial of a theatre-based intervention for youth with autism spectrum disorder. *Autism* **21**, 333–343 (2017).

27. Malow, B. A. Sleep disorders, epilepsy, and autism. *Mental Retardation and Developmental Disabilities Research Reviews* (2004). doi:10.1002/mrdd.20023

28. Ung, D., Selles, R., Small, B. J. & Storch, E. A. A Systematic Review and Meta-Analysis of Cognitive-Behavioral Therapy for Anxiety in Youth with High-Functioning Autism Spectrum Disorders. *Child Psychiatry and Human Development* (2015). doi:10.1007/s10578-014-0494-y

29. Perihan, C. *et al.* Effects of Cognitive Behavioral Therapy for Reducing Anxiety in Children with High Functioning ASD: A Systematic Review and Meta-Analysis. *J. Autism Dev. Disord.* (2019). doi:10.1007/s10803-019-03949-7

30. Rapin, I. & Katzman, R. Neurobiology of autism. *Annals of Neurology* **43**, 7–14 (1998).

31. Adler, B. A. *et al*. Drug-refractory aggression, self-injurious behavior, and severe tantrums in autism spectrum disorders: A chart review study. *Autism* **19**, 102–106 (2015).

32. Broadstock, M., Doughty, C. & Eggleston, M. Systematic review of the effectiveness of pharmacological treatments for adolescents and adults with autism spectrum disorder. *Autism* **11**, 335–348 (2007).

33. Aman, M. G., Lam, K. S. L. & Collier-Crespin, A. Prevalence and Patterns of Use of Psychoactive Medicines among Individuals with Autism in the Autism Society of Ohio. *Journal of Autism and Developmental Disorders* (2003). doi:10.1023/A:1025883612879

34. Aman, M. *et al*. Tolerability, Safety, and Benefits of Risperidone in Children and Adolescents with Autism: 21-Month Follow-up After 8-Week Placebo-Controlled Trial. *J. Child Adolesc. Psychopharmacol.* (2015). doi:10.1089/cap.2015.0005

35. Yokoyama, H., Hirose, M., Haginoya, K., Munakata, M. & Iinuma, K. Treatment with fluvoxamine against self-injury and aggressive behavior in autistic children. in *No To Hattatsu* (2002).

36. McDougle, C. J. *et al*. A double-blind, placebo-controlled study of fluvoxamine in adults with autistic disorder. *Arch. Gen. Psychiatry* (1996). doi:10.1001/archpsyc.1996.01830110037005

37. Fukuda, T., Sugie, H., Ito, M. & Sugie, Y. Clinical evaluation of treatment with

fluvoxamine, a selective serotonin reuptake inhibitor, in children with autistic disorder. *No To Hattatsu* (2001).

38. Iadarola, S., Pérez-Ramos, J., Smith, T. & Dozier, A. Understanding stress in parents of children with autism spectrum disorder: a focus on under-represented families. *Int. J. Dev. Disabil.* **65**, 20–30 (2019).

39. Bargiela, S., Steward, R. & Mandy, W. The Experiences of Late-diagnosed Women with Autism Spectrum Conditions: An Investigation of the Female Autism Phenotype. *J. Autism Dev. Disord.* (2016). doi:10.1007/s10803-016-2872-8

40. Danielsson, U. E., Bengs, C., Samuelsson, E. & Johansson, E. E. My greatest dream is to be normal: The impact of gender on the depression narratives of young swedish men and women. *Qual. Health Res.* (2011). doi:10.1177/1049732310391272

41. Broderick, P. C. & Korteland, C. Coping style and depression in early adolescence: Relationships to gender, gender role, and implicit beliefs. *Sex Roles* (2002). doi:10.1023/A:1019946714220

42. Barrett, A. E. & White, H. R. Trajectories of Gender Role Orientations in Adolescence and Early Adulthood: A Prospective Study of the Mental Health Effects of Masculinity and Femininity. *J. Health Soc. Behav.* (2006). doi:10.2307/3090237

43. May, T., Cornish, K. & Rinehart, N. Does gender matter? A one year follow-up of autistic, attention and anxiety symptoms in high-functioning children with autism spectrum disorder. *J. Autism Dev. Disord.* (2014). doi:10.1007/s10803-013-1964-y

44. Mandy, W. *et al.* Sex differences in autism spectrum disorder: Evidence from a large sample of children and adolescents. *J. Autism Dev. Disord.* (2012).

doi:10.1007/s10803-011-1356-0

45. Solomon, M., Miller, M., Taylor, S. L., Hinshaw, S. P. & Carter, C. S. Autism symptoms and internalizing psychopathology in girls and boys with autism spectrum disorders. *J. Autism Dev. Disord.* (2012). doi:10.1007/s10803-011-1215-z

46. Hoch, E. *et al.* How effective and safe is medical cannabis as a treatment of mental disorders? A systematic review. *Eur. Arch. Psychiatry Clin. Neurosci.* (2019). doi:10.1007/s00406-019-00984-4

47. Howlett, A. C. *et al.* Cannabinoid physiology and pharmacology: 30 Years of progress. *Neuropharmacology* **47**, 345–358 (2004).

48. Yeh, M. L. & Levine, E. S. Perspectives on the Role of Endocannabinoids in Autism Spectrum Disorders. *OBM Neurobiol.* **1**, (2017).

49. Re, G., Barbero, R., Miolo, A. & Di Marzo, V. Palmitoylethanolamide, endocannabinoids and related cannabimimetic compounds in protection against tissue inflammation and pain: Potential use in companion animals. *Veterinary Journal* **173**, 21–30 (2007).

50. Naughton, S. S., Mathai, M. L., Hryciw, D. H. & McAinch, A. J. Fatty Acid Modulation of the Endocannabinoid System and the Effect on Food Intake and Metabolism. *Int. J. Endocrinol.* **2013**, 1–11 (2013).

51. Valastro, C. *et al.* Characterization of endocannabinoids and related acylethanolamides in the synovial fluid of dogs with osteoarthritis: A pilot study. *BMC Vet. Res.* **13**, (2017).

52. Mendelson, W. B. & Basile, A. S. The hypnotic actions of the fatty acid amide,

oleamide. *Neuropsychopharmacology* **25**, S36–S39 (2001).

53. Alger, B. E. & Kim, J. Supply and demand for endocannabinoids. *Trends in Neurosciences* **34**, 304–315 (2011).

54. Galante, M. Group I Metabotropic Glutamate Receptors Inhibit GABA Release at Interneuron-Purkinje Cell Synapses through Endocannabinoid Production. *J. Neurosci.* **24**, 4865–4874 (2004).

55. Jung, K. M. *et al.* Uncoupling of the endocannabinoid signalling complex in a mouse model of fragile X syndrome. *Nat. Commun.* **3**, (2012).

56. Pertwee, R. G. Targeting the endocannabinoid system with cannabinoid receptor agonists: Pharmacological strategies and therapeutic possibilities. *Philosophical Transactions of the Royal Society B: Biological Sciences* **367**, 3353–3363 (2012).

57. Gunduz-Cinar, O., Hill, M. N., McEwen, B. S. & Holmes, A. Amygdala FAAH and anandamide: Mediating protection and recovery from stress. *Trends in Pharmacological Sciences* **34**, 637–644 (2013).

58. Hill, M. N. *et al.* Suppression of Amygdalar Endocannabinoid Signaling by Stress Contributes to Activation of the Hypothalamic-Pituitary- Adrenal Axis HHS Public Access. *Neuropsychopharmacology* **34**, 2733–2745 (2009).

59. Haller, J. *et al.* Interactions between environmental aversiveness and the anxiolytic effects of enhanced cannabinoid signaling by FAAH inhibition in rats. *Psychopharmacology (Berl).* **204**, 607–616 (2009).

60. Busquets-Garcia, A. *et al.* Differential role of anandamide and 2-arachidonoylglycerol in memory and anxiety-like responses. *Biol. Psychiatry* **70**,

479–486 (2011).

61. Shonesy, B. C. *et al.* Genetic Disruption of 2-Arachidonoylglycerol Synthesis Reveals a Key Role for Endocannabinoid Signaling in Anxiety Modulation. *Cell Rep.* **9**, 1644–1654 (2014).

62. Hermanson, D. J., Gamble-George, J. C., Marnett, L. J. & Patel, S. Substrate-selective COX-2 inhibition as a novel strategy for therapeutic endocannabinoid augmentation. *Trends in Pharmacological Sciences* **35**, 358–367 (2014).

63. Gruber, A. J., Pope H.G., J. & Brown, M. E. Do patients use marijuana as an antidepressant? *Depression* **4**, 77–80 (1996).

64. Hyman, S. M. & Sinha, R. Stress-related factors in cannabis use and misuse: Implications for prevention and treatment. *J. Subst. Abuse Treat.* **36**, 400–413 (2009).

65. Gaetani, S., Cuomo, V. & Piomelli, D. Anandamide hydrolysis: A new target for anti-anxiety drugs? *Trends in Molecular Medicine* **9**, 474–478 (2003).

66. Kano, M., Ohno-Shosaku, T., Hashimotodani, Y., Uchigashima, M. & Watanabe, M. Endocannabinoid-mediated control of synaptic transmission. *Physiol. Rev.* **89**, 309–380 (2009).

67. Kano, M. Control of synaptic function by endocannabinoid-mediated retrograde signaling. *Proc. Jpn. Acad. Ser. B. Phys. Biol. Sci.* **90**, 235–50 (2014).

68. Wei, D. *et al.* A role for the endocannabinoid 2-arachidonoyl-sn-glycerol for social and high-fat food reward in male mice. *Psychopharmacology (Berl).* **233**, 1911–1919 (2016).

69. Jung, K.-M. *et al.* Uncoupling of the endocannabinoid signalling complex in a mouse model of fragile X syndrome. *Nat. Commun.* **3**, 1080 (2012).

70. Busquets-Garcia, A. *et al.* Targeting the endocannabinoid system in the treatment of fragile X syndrome. *Nat. Med.* **19**, 603–607 (2013).

71. Kerr, D. M., Downey, L., Conboy, M., Finn, D. P. & Roche, M. Alterations in the endocannabinoid system in the rat valproic acid model of autism. *Behav. Brain Res.* **249**, 124–132 (2013).

72. Wei, D. *et al.* Enhancement of Anandamide-Mediated Endocannabinoid Signaling Corrects Autism-Related Social Impairment. *Cannabis Cannabinoid Res.* **1**, 81–89 (2016).

73. Onaivi, E. S. *et al.* Consequences of cannabinoid and monoaminergic system disruption in a mouse model of autism spectrum disorders. *Curr. Neuropharmacol.* **9**, 209–14 (2011).

74. Siniscalco, D. Endocannabinoid System as Novel Therapeutic Target for Autism Treatment. *Autism. Open. Access* **04**, 1–8 (2014).

75. Jung, K. M. *et al.* 2-Arachidonoylglycerol signaling in forebrain regulates systemic energy metabolism. *Cell Metab.* **15**, 299–310 (2012).

76. Wei, D. *et al.* Endocannabinoid signaling mediates oxytocin-driven social reward. *Proc. Natl. Acad. Sci. U. S. A.* **112**, 14084–9 (2015).

77. Aliczki, M., Varga, Z. K., Balogh, Z. & Haller, J. Involvement of 2-arachidonoylglycerol signaling in social challenge responding of male CD1 mice. *Psychopharmacology (Berl).* **232**, 2157–2167 (2015).

78. Trezza, V. *et al.* Endocannabinoids in amygdala and nucleus accumbens mediate social play reward in adolescent rats. *J Neurosci* **32**, 14899–14908 (2012).

79. Salgado, C. A. & Castellanos, D. Autism Spectrum Disorder and Cannabidiol: Have We Seen This Movie Before? *Glob. Pediatr. Heal.* **5**, 2333794X1881541 (2018).

80. Karhson, D. S. *et al.* Plasma anandamide concentrations are lower in children with autism spectrum disorder. *Mol. Autism* **9**, (2018).

81. Bar-Lev Schleider, L., Mechoulam, R., Saban, N., Meiri, G. & Novack, V. Real life Experience of Medical Cannabis Treatment in Autism: Analysis of Safety and Efficacy. *Sci. Rep.* **9**, (2019).

82. Aran, A. *et al.* Lower circulating endocannabinoid levels in children with autism spectrum disorder. *Mol. Autism* (2019). doi:10.1186/s13229-019-0256-6

83. Chakrabarti, B., Kent, L., Suckling, J., Bullmore, E. & Baron-Cohen, S. Variations in the human cannabinoid receptor (CNR1) gene modulate striatal responses to happy faces. *Eur. J. Neurosci.* (2006). doi:10.1111/j.1460-9568.2006.04697.x

84. Geschwind, D. H. & Levitt, P. Autism spectrum disorders: developmental disconnection syndromes. *Current Opinion in Neurobiology* **17**, 103–111 (2007).

85. Shen, M. D. *et al.* Functional Connectivity of the Amygdala Is Disrupted in Preschool-Aged Children With Autism Spectrum Disorder. *J. Am. Acad. Child Adolesc. Psychiatry* **55**, 817–824 (2016).

86. Park, H. R. *et al.* A Short Review on the Current Understanding of Autism Spectrum Disorders. *Exp. Neurobiol.* **25**, 1 (2016).

87. Adolphs, R. What does the amygdala contribute to social cognition? *Annals of the*

New York Academy of Sciences (2010). doi:10.1111/j.1749-6632.2010.05445.x

88. Rosvold, H. E., Mirsky, A. F. & Pribram, K. H. Influence of amygdalectomy on social behavior in monkeys. *The Journal of Comparative and Physiological Psychology* **47**, 173–178 (1954).

89. Emery, N. J. *et al.* The effects of bilateral lesions of the amygdala on dyadic social interactions in rhesus monkeys (Macaca mulatta). *Behav. Neurosci.* (2001). doi:10.1037/0735-7044.115.3.515

90. Baron-Cohen, S. *et al.* The amygdala theory of autism. *Neurosci. Biobehav. Rev.* **24**, 355–364 (2000).

91. Hadjikhani, N. *et al.* Look me in the eyes: Constraining gaze in the eye-region provokes abnormally high subcortical activation in autism. *Sci. Rep.* **7**, (2017).

92. Hadjikhani, N. *et al.* Bumetanide for autism: More eye contact, less amygdala activation. *Sci. Rep.* **8**, (2018).

93. Park, H. R. *et al.* Nucleus accumbens deep brain stimulation for a patient with self-injurious behavior and autism spectrum disorder: functional and structural changes of the brain: report of a case and review of literature. *Acta Neurochir. (Wien).* **159**, 137–143 (2017).

94. Deisseroth, K. Optogenetics. *Nat. Methods* **8**, 26 (2010).

95. Mahmoudi, P., Veladi, H. & Pakdel, F. G. Optogenetics, Tools and Applications in Neurobiology. *J. Med. Signals Sens.* **7**, 71–79 (2017).

96. Zhang, F., Aravanis, A. M., Adamantidis, A., de Lecea, L. & Deisseroth, K. Circuit-breakers: optical technologies for probing neural signals and systems. *Nat. Rev.*

Neurosci. **8**, 577 (2007).

97. Zhang, F. *et al.* Multimodal fast optical interrogation of neural circuitry. *Nature* (2007). doi:10.1038/nature05744

98. Boyden, E. S., Zhang, F., Bamberg, E., Nagel, G. & Deisseroth, K. Millisecond-timescale, genetically targeted optical control of neural activity. *Nat. Neurosci.* (2005). doi:10.1038/nn1525

99. Fenno, L., Yizhar, O. & Deisseroth, K. The Development and Application of Optogenetics. *Annu. Rev. Neurosci.* (2011). doi:10.1146/annurev-neuro-061010-113817

100. Aravanis, A. M. *et al.* An optical neural interface: in vivo control of rodent motor cortex with integrated fiberoptic and optogenetic technology. *J. Neural Eng.* (2007). doi:10.1088/1741-2560/4/3/S02

101. Nagel, G. *et al.* Channelrhodopsin-1: A light-gated proton channel in green algae. *Science (80-.).* (2002). doi:10.1126/science.1072068

102. Williams, J. C. & Denison, T. From optogenetic technologies to neuromodulation therapies. *Science Translational Medicine* (2013). doi:10.1126/scitranslmed.3003100

103. Nagel, G. *et al.* Channelrhodopsin-2, a directly light-gated cation-selective membrane channel. *Proc. Natl. Acad. Sci.* (2003). doi:10.1073/pnas.1936192100

104. Lanyi, J. K. & Oesterhelt, D. Identification of the retinal-binding protein in halorhodopsin. *J. Biol. Chem.* (1982).

105. Roth, B. L. DREADDs for Neuroscientists. *Neuron* (2016).

doi:10.1016/j.neuron.2016.01.040

106. MacLaren, D. A. A. *et al.* Clozapine N-oxide administration produces behavioral effects in long-evans rats: Implications for designing DREADD experiments. *eNeuro* (2016). doi:10.1523/ENEURO.0219-16.2016

107. Owen, S. F., Liu, M. H. & Kreitzer, A. C. Thermal constraints on in vivo optogenetic manipulations. *Nat. Neurosci.* (2019). doi:10.1038/s41593-019-0422-3

108. Ambroggi, F., Ishikawa, A., Fields, H. L. & Nicola, S. M. Basolateral Amygdala Neurons Facilitate Reward-Seeking Behavior by Exciting Nucleus Accumbens Neurons. *Neuron* **59**, 648–661 (2008).

109. Namburi, P. *et al.* A circuit mechanism for differentiating positive and negative associations. *Nature* **520**, 675–678 (2015).

110. Stuber, G. D. *et al.* Excitatory transmission from the amygdala to nucleus accumbens facilitates reward seeking. *Nature* **475**, 377–80 (2011).

111. Yu, J. *et al.* Nucleus accumbens feedforward inhibition circuit promotes cocaine self-administration. *Proc. Natl. Acad. Sci.* **114**, E8750 LP-E8759 (2017).

112. Beyeler, A. *et al.* Divergent Routing of Positive and Negative Information from the Amygdala during Memory Retrieval. *Neuron* (2016). doi:10.1016/j.neuron.2016.03.004

113. Beyeler, A. *et al.* Organization of Valence-Encoding and Projection-Defined Neurons in the Basolateral Amygdala. *Cell Rep.* **22**, 905–918 (2018).

114. Millan, E. Z., Kim, H. A. & Janak, P. H. Optogenetic activation of amygdala projections to nucleus accumbens can arrest conditioned and unconditioned

alcohol consummatory behavior. *Neuroscience* **360**, 106–117 (2017).

115. Bercovici, D. A., Princz-Lebel, O., Tse, M. T., Moorman, D. E. & Floresco, S. B. Optogenetic Dissection of Temporal Dynamics of Amygdala-Striatal Interplay during Risk/Reward Decision Making. *eneuro* (2018). doi:10.1523/eneuro.0422-18.2018

116. Cardinal, R. N. & Howes, N. J. Effects of lesions of the nucleus accumbens core on choice between small certain rewards and large uncertain rewards in rats. *BMC Neurosci.* (2005). doi:10.1186/1471-2202-6-37

117. Ghods-Sharifi, S., St. Onge, J. R. & Floresco, S. B. Fundamental Contribution by the Basolateral Amygdala to Different Forms of Decision Making. *J. Neurosci.* (2009). doi:10.1523/jneurosci.0315-09.2009

118. Stopper, C. M. & Floresco, S. B. Contributions of the nucleus accumbens and its subregions to different aspects of risk-based decision making. *Cogn. Affect. Behav. Neurosci.* (2011). doi:10.3758/s13415-010-0015-9

119. St. Onge, J. R., Stopper, C. M., Zahm, D. S. & Floresco, S. B. Separate Prefrontal-Subcortical Circuits Mediate Different Components of Risk-Based Decision Making. *J. Neurosci.* **32**, 2886–2899 (2012).

120. Piantadosi, P. T., Yeates, D. C. M., Wilkins, M. & Floresco, S. B. Contributions of basolateral amygdala and nucleus accumbens subregions to mediating motivational conflict during punished reward-seeking. *Neurobiol. Learn. Mem.* (2017). doi:10.1016/j.nlm.2017.02.017

121. Cisneros-Franco, J. M. & de Villers-Sidani, E. Bidirectional Control of Risk-Seeking

Behavior by the Basolateral Amygdala. *eneuro* **5**, ENEURO.0168-18.2018 (2018).

122. Shen, C. J. *et al.* Cannabinoid CB 1 receptors in the amygdalar cholecystokinin glutamatergic afferents to nucleus accumbens modulate depressive-like behavior. *Nat. Med.* (2019). doi:10.1038/s41591-018-0299-9

123. Moessner, R. *et al.* Contribution of SHANK3 mutations to autism spectrum disorder. *Am. J. Hum. Genet.* **81**, 1289–1297 (2007).

124. Leblond, C. S. *et al.* Meta-analysis of SHANK Mutations in Autism Spectrum Disorders: A Gradient of Severity in Cognitive Impairments. *PLoS Genet.* (2014). doi:10.1371/journal.pgen.1004580

125. Gauthier, J. *et al.* Novel de novo SHANK3 mutation in autistic patients. *Am. J. Med. Genet. Part B Neuropsychiatr. Genet.* (2009). doi:10.1002/ajmg.b.30822

126. Monteiro, P. & Feng, G. SHANK proteins: Roles at the synapse and in autism spectrum disorder. *Nature Reviews Neuroscience* (2017). doi:10.1038/nrn.2016.183

127. Durand, C. M. *et al.* Mutations in the gene encoding the synaptic scaffolding protein SHANK3 are associated with autism spectrum disorders. *Nat. Genet.* **39**, 25–27 (2007).

128. Boeckers, T. M., Bockmann, J., Kreutz, M. R. & Gundelfinger, E. D. ProSAP/Shank proteins - A family of higher order organizing molecules of the postsynaptic density with an emerging role in human neurological disease. *Journal of Neurochemistry* (2002). doi:10.1046/j.1471-4159.2002.00931.x

129. Sala, C., Vicidomini, C., Bigi, I., Mossa, A. & Verpelli, C. Shank synaptic scaffold proteins: Keys to understanding the pathogenesis of autism and other synaptic

disorders. *Journal of Neurochemistry* (2015). doi:10.1111/jnc.13232

130. Kolevzon, A. *et al.* Phelan-McDermid syndrome: A review of the literature and practice parameters for medical assessment and monitoring. *Journal of Neurodevelopmental Disorders* (2014). doi:10.1186/1866-1955-6-39

131. Phelan, K. & McDermid, H. E. The 22q13.3 Deletion Syndrome (Phelan-McDermid Syndrome). *Mol. Syndromol.* 186–201 (2011). doi:10.1159/000334260

132. Kazdoba, T. M., Leach, P. T. & Crawley, J. N. Behavioral phenotypes of genetic mouse models of autism. *Genes, Brain and Behavior* (2016). doi:10.1111/gbb.12256

133. Bonaglia, M. C. *et al.* Disruption of the ProSAP2 Gene in a t(12;22)(q24.1;q13.3) Is Associated with the 22q13.3 Deletion Syndrome. *Am. J. Hum. Genet.* (2001). doi:10.1086/321293

134. Bonaglia, M. C. *et al.* Identification of a recurrent breakpoint within the SHANK3 gene in the 22q13.3 deletion syndrome. *J. Med. Genet.* (2006). doi:10.1136/jmg.2005.038604

135. Wilson, H. L. Molecular characterisation of the 22q13 deletion syndrome supports the role of haploinsufficiency of SHANK3/PROSAP2 in the major neurological symptoms. *J. Med. Genet.* (2003). doi:10.1136/jmg.40.8.575

136. Wilson, H. L. *et al.* Interstitial 22q13 deletions: Genes other than SHANK3 have major effects on cognitive and language development. *Eur. J. Hum. Genet.* (2008). doi:10.1038/ejhg.2008.107

137. Cusmano-Ozog, K., Manning, M. A. & Hoyme, H. E. 22q13.3 deletion syndrome: A

recognizable malformation syndrome associated with marked speech and language delay. *Am. J. Med. Genet. Part C Semin. Med. Genet.* (2007). doi:10.1002/ajmg.c.30155

138. Roussignol, G. Shank Expression Is Sufficient to Induce Functional Dendritic Spine Synapses in Aspiny Neurons. *J. Neurosci.* (2005). doi:10.1523/jneurosci.4354-04.2005

139. Baron, M. K. *et al.* An architectural framework that may lie at the core of the postsynaptic density. *Science (80-.).* (2006). doi:10.1126/science.1118995

140. Kim, E. & Sheng, M. PDZ domain proteins of synapses. *Nature Reviews Neuroscience* (2004). doi:10.1038/nrn1517

141. Lim, S. *et al.* Characterization of the Shank family of synaptic proteins. Multiple genes, alternative splicing, and differential expression in brain and development. *J. Biol. Chem.* (1999). doi:10.1074/jbc.274.41.29510

142. Qualmann, B. Linkage of the Actin Cytoskeleton to the Postsynaptic Density via Direct Interactions of Abp1 with the ProSAP/Shank Family. *J. Neurosci.* (2004). doi:10.1523/jneurosci.5479-03.2004

143. Peça, J. *et al.* Shank3 mutant mice display autistic-like behaviours and striatal dysfunction. *Nature* (2011). doi:10.1038/nature09965

144. Mei, Y. *et al.* Adult restoration of Shank3 expression rescues selective autistic-like phenotypes. *Nature* (2016). doi:10.1038/nature16971

145. Hung, A. Y. *et al.* Smaller Dendritic Spines, Weaker Synaptic Transmission, but Enhanced Spatial Learning in Mice Lacking Shank1. *J. Neurosci.* (2008).

doi:10.1523/jneurosci.3032-07.2008

146. Silverman, J. L. *et al.* Sociability and motor functions in Shank1 mutant mice. *Brain Res.* (2011). doi:10.1016/j.brainres.2010.09.026

147. Sungur, A. Ö., Vörckel, K. J., Schwarting, R. K. W. & Wöhr, M. Repetitive behaviors in the Shank1 knockout mouse model for autism spectrum disorder: Developmental aspects and effects of social context. *J. Neurosci. Methods* (2014). doi:10.1016/j.jneumeth.2014.05.003

148. Beri, S. *et al.* DNA methylation regulates tissue-speci.c expression of Shank3. *J. Neurochem.* (2007). doi:10.1111/j.1471-4159.2007.04539.x

149. Ching, T. T. *et al.* Epigenome analyses using BAG microarrays identify evolutionary conservation of tissue-specific methylation of SHANK3. *Nat. Genet.* (2005). doi:10.1038/ng1563

150. Maunakea, A. K. *et al.* Conserved role of intragenic DNA methylation in regulating alternative promoters. *Nature* (2010). doi:10.1038/nature09165

151. Tu, J. C. *et al.* Coupling of mGluR/Homer and PSD-95 complexes by the Shank family of postsynaptic density proteins. *Neuron* (1999). doi:10.1016/S0896-6273(00)80810-7

152. Hayashi, M. K. *et al.* The Postsynaptic Density Proteins Homer and Shank Form a Polymeric Network Structure. *Cell* (2009). doi:10.1016/j.cell.2009.01.050

153. Boeckers, T. M. *et al.* C-terminal synaptic targeting elements for postsynaptic density proteins ProSAP1/Shank2 and ProSAP2/Shank3. *J. Neurochem.* (2005). doi:10.1111/j.1471-4159.2004.02910.x

154. Wang, X., Xu, Q., Bey, A. L., Lee, Y. & Jiang, Y. H. Transcriptional and functional complexity of Shank3 provides a molecular framework to understand the phenotypic heterogeneity of SHANK3 causing autism and Shank3 mutant mice. *Mol. Autism* (2014). doi:10.1186/2040-2392-5-30

155. Wang, X. *et al.* Synaptic dysfunction and abnormal behaviors in mice lacking major isoforms of Shank3. *Hum. Mol. Genet.* **20**, 3093–3108 (2011).

156. Bozdagi, O. *et al.* Haploinsufficiency of the autism-associated Shank3 gene leads to deficits in synaptic function, social interaction, and social communication. *Mol. Autism* (2010). doi:10.1186/2040-2392-1-15

157. Yang, M. *et al.* Reduced Excitatory Neurotransmission and Mild Autism-Relevant Phenotypes in Adolescent Shank3 Null Mutant Mice. *J. Neurosci.* **32**, 6525–6541 (2012).

158. Wang, X. *et al.* Altered mGluR5-Homer scaffolds and corticostriatal connectivity in a Shank3 complete knockout model of autism. *Nat. Commun.* (2016). doi:10.1038/ncomms11459

159. Wang, X. *et al.* Synaptic dysfunction and abnormal behaviors in mice lacking major isoforms of Shank3. *Hum. Mol. Genet.* **20**, 3093–3108 (2011).

160. Sung, K.-W., Choi, S. & Lovinger, D. M. Activation of Group I mGluRs Is Necessary for Induction of Long-Term Depression at Striatal Synapses. *J. Neurophysiol.* (2017). doi:10.1152/jn.2001.86.5.2405

161. Keown, C. L. *et al.* Local functional overconnectivity in posterior brain regions is associated with symptom severity in autism spectrum disorders. *Cell Rep.* (2013).

doi:10.1016/j.celrep.2013.10.003

162. Supekar, K. *et al*. Brain Hyperconnectivity in Children with Autism and its Links to Social Deficits. *Cell Rep*. (2013). doi:10.1016/j.celrep.2013.10.001

163. Khan, S. *et al*. Local and long-range functional connectivity is reduced in concert in autism spectrum disorders. *Proc. Natl. Acad. Sci*. (2013). doi:10.1073/pnas.1214533110

164. Di Martino, A. *et al*. The autism brain imaging data exchange: Towards a large-scale evaluation of the intrinsic brain architecture in autism. *Mol. Psychiatry* (2014). doi:10.1038/mp.2013.78

165. Langen, M., Durston, S., Kas, M. J. H., van Engeland, H. & Staal, W. G. The neurobiology of repetitive behavior: ...and men. *Neuroscience and Biobehavioral Reviews* **35**, 356–365 (2011).

166. Ronesi, J. A. *et al*. Disrupted Homer scaffolds mediate abnormal mGluR5 function in a mouse model of fragile X syndrome. *Nat. Neurosci*. (2012). doi:10.1038/nn.3033

167. Giuffrida, R. A Reduced Number of Metabotropic Glutamate Subtype 5 Receptors Are Associated with Constitutive Homer Proteins in a Mouse Model of Fragile X Syndrome. *J. Neurosci*. (2005). doi:10.1523/jneurosci.0932-05.2005

168. Padgett, C. L. *et al*. Methamphetamine-Evoked Depression of GABAB Receptor Signaling in GABA Neurons of the VTA. *Neuron* **73**, 978–989 (2012).

169. Gauthier, J. *et al*. De novo mutations in the gene encoding the synaptic scaffolding protein SHANK3 in patients ascertained for schizophrenia . *Proc. Natl. Acad. Sci*. (2010). doi:10.1073/pnas.0906232107

170. Boccuto, L. *et al*. Prevalence of SHANK3 variants in patients with different subtypes of autism spectrum disorders. *Eur. J. Hum. Genet.* (2013). doi:10.1038/ejhg.2012.175

171. Cai, G. *et al*. Brain mGluR5 in Shank3B –/– Mice Studied with in vivo [18 F]FPEB PET Imaging and ex vivo Immunoblotting. *Front. Psychiatry* (2019). doi:10.3389/fpsyt.2019.00038

172. Peixoto, R. T., Wang, W., Croney, D. M., Kozorovitskiy, Y. & Sabatini, B. L. Early hyperactivity and precocious maturation of corticostriatal circuits in Shank3B â ′/â ′ mice. *Nat. Neurosci.* (2016). doi:10.1038/nn.4260

173. Garber, K. B., Warren, S. T. & Visootsak, J. Fragile X syndrome and X-linked intellectual disability. in *Emery and Rimoin's Principles and Practice of Medical Genetics* (2013). doi:10.1016/B978-0-12-383834-6.00112-9

174. Zamberletti, E., Gabaglio, M. & Parolaro, D. The endocannabinoid system and autism spectrum disorders: Insights from animal models. *International Journal of Molecular Sciences* **18**, (2017).

175. Kazdoba, T. M., Leach, P. T., Silverman, J. L. & Crawley, J. N. Modeling fragile X syndrome in the Fmr1 knockout mouse. *Intractable Rare Dis. Res.* (2014). doi:10.5582/irdr.2014.01024

176. Gomis-González, M., Matute, C., Maldonado, R., Mato, S. & Ozaita, A. Possible therapeutic doses of cannabinoid type 1 receptor antagonist reverses key alterations in fragile X syndrome mouse model. *Genes (Basel)*. (2016). doi:10.3390/genes7090056

177. Qin, M. *et al*. Endocannabinoid-mediated improvement on a test of aversive memory in a mouse model of fragile X syndrome. *Behav. Brain Res.* (2015). doi:10.1016/j.bbr.2015.05.003

178. McFarlane, H. G. *et al*. Autism-like behavioral phenotypes in BTBR T+tf/J mice. *Genes, Brain Behav*. (2008). doi:10.1111/j.1601-183X.2007.00330.x

179. Silverman, J. L., Tolu, S. S., Barkan, C. L. & Crawley, J. N. Repetitive self-grooming behavior in the BTBR mouse model of autism is blocked by the mGluR5 antagonist MPEP. *Neuropsychopharmacology* (2010). doi:10.1038/npp.2009.201

180. Benno, R., Smirnova, Y., Vera, S., Liggett, A. & Schanz, N. Exaggerated responses to stress in the BTBR T+tf/J mouse: An unusual behavioral phenotype. *Behav. Brain Res.* (2009). doi:10.1016/j.bbr.2008.09.041

181. Kerr, D. M., Gilmartin, A. & Roche, M. Pharmacological inhibition of fatty acid amide hydrolase attenuates social behavioural deficits in male rats prenatally exposed to valproic acid. *Pharmacol. Res.* (2016). doi:10.1016/j.phrs.2016.08.033

182. Servadio, M. *et al*. Targeting anandamide metabolism rescues core and associated autistic-like symptoms in rats prenatally exposed to valproic acid. *Transl. Psychiatry* (2016). doi:10.1038/tp.2016.182

183. Ornoy, A., Weinstein-Fudim, L. & Ergaz, Z. Prenatal factors associated with autism spectrum disorder (ASD). *Reproductive Toxicology* (2015). doi:10.1016/j.reprotox.2015.05.007

184. Smith, S. E. P., Li, J., Garbett, K., Mirnics, K. & Patterson, P. H. Maternal Immune Activation Alters Fetal Brain Development through Interleukin-6. *J. Neurosci.*

(2007). doi:10.1523/jneurosci.2178-07.2007

185. Hsiao, E. Y. & Patterson, P. H. Activation of the maternal immune system induces endocrine changes in the placenta via IL-6. *Brain. Behav. Immun.* (2011). doi:10.1016/j.bbi.2010.12.017

186. Doenni, V. M. *et al.* Deficient adolescent social behavior following early-life inflammation is ameliorated by augmentation of anandamide signaling. *Brain. Behav. Immun.* (2016). doi:10.1016/j.bbi.2016.07.152

187. Wang, W. *et al.* Striatopallidal dysfunction underlies repetitive behavior in Shank3-deficient model of autism. *J. Clin. Invest.* (2017). doi:10.1172/JCI87997

188. Shyn, S. I. *et al.* Novel loci for major depression identified by geno... [Mol Psychiatry. 2009] - PubMed result. *Mol. Psychiatry* (2009). doi:10.1038/mp.2009.125

189. Aragona, B. J. *et al.* Nucleus accumbens dopamine differentially mediates the formation and maintenance of monogamous pair bonds. *Nat Neurosci* **9**, 133–139 (2006).

190. Francis, T. C. *et al.* Nucleus accumbens medium spiny neuron subtypes mediate depression-related outcomes to social defeat stress. *Biol. Psychiatry* **77**, 212–222 (2015).

191. Gunaydin, L. A. *et al.* Natural neural projection dynamics underlying social behavior. *Cell* **157**, 1535–1551 (2014).

192. Van Der Kooij, M. A. *et al.* Diazepam actions in the VTA enhance social dominance and mitochondrial function in the nucleus accumbens by activation of dopamine

D1 receptors. *Mol. Psychiatry* (2018). doi:10.1038/mp.2017.135

193. Di Martino, A. *et al.* Aberrant striatal functional connectivity in children with autism. *Biol. Psychiatry* (2011). doi:10.1016/j.biopsych.2010.10.029

194. Dichter, G. S. *et al.* Reward circuitry function in autism spectrum disorders. *Soc. Cogn. Affect. Neurosci.* (2012). doi:10.1093/scan/nsq095

195. Varghese, M. *et al.* Autism spectrum disorder: neuropathology and animal models. *Acta Neuropathologica* **134**, 537–566 (2017).

196. Stuber, G. D. *et al.* Excitatory transmission from the amygdala to nucleus accumbens facilitates reward seeking. *Nature* **475**, 377–382 (2011).

197. Phelan, K. & McDermid, H. E. The 22q13.3 deletion syndrome (Phelan-McDermid syndrome). *Mol. Syndromol.* (2012). doi:10.1159/000334260

198. Vorstman, J. a S. *et al.* Identification of novel autism candidate regions through analysis of reported cytogenetic abnormalities associated with autism. *Mol. Psychiatry* **11**, 1, 18–28 (2006).

199. Naisbitt, S. *et al.* Shank, a novel family of postsynaptic density proteins that binds to the NMDA receptor/PSD-95/GKAP complex and cortactin. *Neuron* **23**, 569–82 (1999).

200. Zhou, Y. *et al.* Atypical behaviour and connectivity in SHANK3-mutant macaques. *Nature* (2019). doi:10.1038/s41586-019-1278-0

201. Stamatakis, A. M. *et al.* Simultaneous optogenetics and cellular resolution calcium imaging during active behavior using a miniaturized microscope. *Front. Neurosci.* (2018). doi:10.3389/fnins.2018.00496

202. Sukhodolsky, D. G. *et al.* Parent-rated anxiety symptoms in children with pervasive developmental disorders: Frequency and association with core autism symptoms and cognitive functioning. *J. Abnorm. Child Psychol.* (2008). doi:10.1007/s10802-007-9165-9

203. Allsop, S. a., Vander Weele, C. M., Wichmann, R. & Tye, K. M. Optogenetic insights on the relationship between anxiety-related behaviors and social deficits. *Front. Behav. Neurosci.* **8**, 241 (2014).

204. Araque, A., Castillo, P. E., Manzoni, O. J. & Tonini, R. Synaptic functions of endocannabinoid signaling in health and disease. *Neuropharmacology* (2017). doi:10.1016/j.neuropharm.2017.06.017

205. Trusel, M. *et al.* Coordinated Regulation of Synaptic Plasticity at Striatopallidal and Striatonigral Neurons Orchestrates Motor Control. *Cell Rep.* (2015). doi:10.1016/j.celrep.2015.10.009

206. Grueter, B. A., Brasnjo, G. & Malenka, R. C. Postsynaptic TRPV1 triggers cell type-specific long-term depression in the nucleus accumbens. *Nat. Neurosci.* (2010). doi:10.1038/nn.2685

207. Kreitzer, A. C. & Malenka, R. C. Striatal Plasticity and Basal Ganglia Circuit Function. *Neuron* (2008). doi:10.1016/j.neuron.2008.11.005

208. Guo, B. *et al.* Anterior cingulate cortex dysfunction underlies social deficits in Shank3 mutant mice. *Nat. Neurosci.* (2019). doi:10.1038/s41593-019-0445-9

209. Felix-Ortiz, A. C., Burgos-Robles, A., Bhagat, N. D., Leppla, C. A. & Tye, K. M. Bidirectional modulation of anxiety-related and social behaviors by amygdala

projections to the medial prefrontal cortex. *Neuroscience* **321**, 197–209 (2016).

210. Felix-Ortiz, A. C. & Tye, K. M. Amygdala inputs to the ventral hippocampus bidirectionally modulate social behavior. *J. Neurosci.* **34**, 586–595 (2014).

211. Manduca, A. *et al.* Dopaminergic Neurotransmission in the Nucleus Accumbens Modulates Social Play Behavior in Rats. *Neuropsychopharmacology* **41**, 1–9 (2016).

212. Granchi, C., Caligiuri, I., Minutolo, F., Rizzolio, F. & Tuccinardi, T. A patent review of Monoacylglycerol Lipase (MAGL) inhibitors (2013-2017). *Expert Opinion on Therapeutic Patents* (2017). doi:10.1080/13543776.2018.1389899

213. Clapper, J. R. *et al.* Monoacylglycerol Lipase Inhibition in Human and Rodent Systems Supports Clinical Evaluation of Endocannabinoid Modulators. *J. Pharmacol. Exp. Ther.* **367**, 494–508 (2018).

214. Manz, K. M., Baxley, A. G., Zurawski, Z., Hamm, H. E. & Grueter, B. A. Heterosynaptic GABA B receptor function within feedforward microcircuits gates glutamatergic transmission in the nucleus accumbens core . *J. Neurosci.* (2019). doi:10.1523/jneurosci.1395-19.2019

215. Pisansky, M. T. *et al.* Nucleus Accumbens Fast-Spiking Interneurons Constrain Impulsive Action. *Biol. Psychiatry* (2019). doi:10.1016/j.biopsych.2019.07.002

216. Ogasawara, D. *et al.* Rapid and profound rewiring of brain lipid signaling networks by acute diacylglycerol lipase inhibition. *Proc. Natl. Acad. Sci.* **113**, 201522364 (2015).

217. Turner, B. D., Rook, J. M., Lindsley, C. W., Conn, P. J. & Grueter, B. A. mGlu 1 and mGlu 5 modulate distinct excitatory inputs to the nucleus accumbens shell.

Neuropsychopharmacology (2018). doi:10.1038/s41386-018-0049-1

218. Kipp, M. ANVIL: The Video Annotation Research Tool. in *Handbook of Corpus Phonology* (2014).

219. Füzesi, T., Daviu, N., Wamsteeker Cusulin, J. I., Bonin, R. P. & Bains, J. S. ARTICLE Hypothalamic CRH neurons orchestrate complex behaviours after stress. (2016). doi:10.1038/ncomms11937

220. Hartley, N. D. *et al.* 2-arachidonoylglycerol signaling impairs short-term fear extinction. *Transl. Psychiatry* **6**, e749 (2016).

221. Felix-Ortiz, A. C. *et al.* BLA to vHPC inputs modulate anxiety-related behaviors. *Neuron* **79**, 658–664 (2013).

222. Peça, J. *et al.* Shank3 mutant mice display autistic-like behaviours and striatal dysfunction. *Nature* **472**, 437–42 (2011).

223. Wang, Y. *et al.* A Critical Role of Basolateral Amygdala to Nucleus Accumbens Projection in Sleep Regulation of Reward Seeking. *Biol. Psychiatry* (2019). doi:10.1016/j.biopsych.2019.10.027

224. Reynolds, A. M. & Malow, B. A. Sleep and Autism Spectrum Disorders. *Pediatric Clinics of North America* (2011). doi:10.1016/j.pcl.2011.03.009

225. Souders, M. C. *et al.* Sleep behaviors and sleep quality in children with autism spectrum disorders. *Sleep* (2009). doi:10.1093/sleep/32.12.1566

226. Stavropoulos, K. K. M. & Carver, L. J. Research Review: Social motivation and oxytocin in autism - Implications for joint attention development and intervention. *Journal of Child Psychology and Psychiatry and Allied Disciplines* (2013).

doi:10.1111/jcpp.12061

227. Chevallier, C., Kohls, G., Troiani, V., Brodkin, E. S. & Schultz, R. T. The social motivation theory of autism. *Trends in Cognitive Sciences* **16**, 231–238 (2012).

228. Young, L. J. & Barrett, C. E. Can oxytocin treat autism? *Science (80-.).* (2015). doi:10.1126/science.aaa8120

229. Hollander, E. *et al.* Oxytocin infusion reduces repetitive behaviors in adults with autistic and asperger's disorders. *Neuropsychopharmacology* (2003). doi:10.1038/sj.npp.1300021

230. Yamasue, H. Promising evidence and remaining issues regarding the clinical application of oxytocin in autism spectrum disorders. *Psychiatry Clin. Neurosci.* (2016). doi:10.1111/pcn.12364

231. Parker, K. J. *et al.* Intranasal oxytocin treatment for social deficits and biomarkers of response in children with autism. *Proc. Natl. Acad. Sci. U. S. A.* (2017). doi:10.1073/pnas.1705521114

232. Elissar Andari,University, E. Autism Oxytocin Brain Project. *clinicaltrials.gov* (2017). Available at: https://clinicaltrials.gov/ct2/show/study/NCT03033784.

233. Siniscalco, D., Schultz, S., Brigida, A. L. & Antonucci, N. Inflammation and neuro-immune dysregulations in autism spectrum disorders. *Pharmaceuticals* (2018). doi:10.3390/ph11020056

234. Tonhajzerova, I. *et al.* Inflammatory activity in autism spectrum disorder. *Adv. Exp. Med. Biol.* (2015). doi:10.1007/5584_2015_145

235. Mangiola, F. *et al.* Gut microbiota in autism and mood disorders. *World Journal of*

Gastroenterology (2016). doi:10.3748/wjg.v22.i1.361

236. Hsiao, E. Y. Gastrointestinal issues in autism spectrum disorder. *Harvard Review of Psychiatry* (2014). doi:10.1097/HRP.0000000000000029

237. Vuong, H. E. & Hsiao, E. Y. Emerging Roles for the Gut Microbiome in Autism Spectrum Disorder. *Biological Psychiatry* (2017). doi:10.1016/j.biopsych.2016.08.024

238. Bandini, L. G. *et al.* Food selectivity in children with autism spectrum disorders and typically developing children. *J. Pediatr.* (2010). doi:10.1016/j.jpeds.2010.02.013

239. Ledford, J. R. & Gast, D. L. Feeding Problems in Children With Autism Spectrum Disorders: A Review. *Focus Autism Other Dev. Disabl.* (2006). doi:10.1177/10883576060210030401

240. Cermak, S. A., Curtin, C. & Bandini, L. G. Food Selectivity and Sensory Sensitivity in Children with Autism Spectrum Disorders. *J. Am. Diet. Assoc.* (2010). doi:10.1016/j.jada.2009.10.032

241. Ajram, L. A. *et al.* Shifting brain inhibitory balance and connectivity of the prefrontal cortex of adults with autism spectrum disorder. *Transl. Psychiatry* (2017). doi:10.1038/tp.2017.104

242. Dr Grainne McAlonan, K. C. L. GABA Pathways in Autism Spectrum Disorder (ASD). *clinicaltrials.gov* (2018).

243. Sheng, M. & Kim, E. The postsynaptic organization of synapses. *Cold Spring Harb. Perspect. Biol.* (2011). doi:10.1101/cshperspect.a005678

244. Costales, J. L. & Kolevzon, A. Phelan–McDermid Syndrome and SHANK3:

Implications for Treatment. *Neurotherapeutics* (2015). doi:10.1007/s13311-015-0352-z